A Fibre Optic Oxygen Sensor based on the Fluorescence Quenching of Ruthenium Compounds

submitted for the degree of

Master of Science

presented to

Dublin City University

by

Adrian Kieran Geissel B.Sc.

The School of Physical Sciences

Dublin City University

Research Supervisor

Dr. Brian Lawless M.Sc. Ph.D.

August 1991

Declaration

I declare that the work documented in this thesis is original and my own

This thesis is dedicated to my parents, Helga and Hermann, for their total support throughout all of my third level education

Table of Contents

Chapter II: Background experimental work

Chapter III: Ru $(bpy)_3^{2+}$ probe characterisation:

Chapter IV: Ru $(phen)_3^{2+}$ probe characterisation:

Abstract

Oxygen quenching of long lifetime fluorescent dyes takes place when the excited state of the fluorescent dye decays non-radiatively to the ground state by energy transfer to the oxygen Thus, by monitoring the intensity of fluorescence, the oxygen dependence is seen as a decrease in intensity for an increase in oxygen concentration The Ruthenium based fluorescent dyes used in this work have lifetimes of the order of 0 7μs which allows them to be oxygen sensitive, and two such dyes, Ru $(bpy)_3^{2+}$ and Ru $(phen)_3^{2+}$, were extensively tested for use in a fibre optic oxygen sensor

The oxygen sensitive dyes were incorporated into a fibre optic system which was used to transmit the 488nm light from an Ar ion laser to the sensor tip and also to carry the fluorescence signal back to the detector The fibres from a 4 - port coupler were used in this sensor as follows 1) for the launching of excitation hght, 2) for housing the sensing probe tip, 3) for the return of fluorescence signal to the detector and 4) for monitoring the stability of the Ar ion excitation source The oxygen sensing dye is immobilised in Nafion ion exchange resin with which a cavity etched into the fibre end was coated A method was developed for securely attaching the Nafion polymer to the fibre surface

The final probe was found to respond to changes in dissolved oxygen partial pressure of 0 053 bar, while the spatial resolution was estimated at 50μm which corresponds to the core diameter of the fibre used in the work The sensor was found to operate equally well in both aqueous and gaseous environments without requiring separate manufacturing procedures

The etching of graded index glass optical fibres in conc HF acid was also investigated The resultant cavity was found to develop in a manner not predicted by the current etching models An etching model was developed to account for the development of the etched cavity which was observed using both optical and electron microscope techniques The etching process was also modelled on a computer

List of Tables

List of Figures

Glossary

$Ru(bpy)_3^{2+}$	tris(2,2'-bipyridyl) Ruthemum(II) (22,475-8)†
$Ru(phen)_3^{2+}$	tris(1,10-phenanthroline) Ruthenium(II)
$Os(bpy)_3^{2+}$	tris(2,2'-bipyridyl) Osmium(II)
bpy	2,2'-bipyridyl
phen	1,10-phenanthroline
bdt	5,5'-bis, 2,2'-dimethyl-1,3,4-thiadiazole
FITC	fluorescein isothiocyanate
HOPSA	hydroxypyrene trisulphomc acid
PIM	patient interface module
PTFE	polytetrafluoroethylene
quantum yield	ratio of emitted to absorbed photons
lifetime	excited state lifetime of fluorescent molecule
Stern - Volmer equation	$I_0 = I(1 + K_D[Q])$
K_D	Stern - Volmer quenching constant
Nafion	fluorocarbon based ion exchange resin (27,470-4)
AA	acryl amide
HF	hydrofluoric acid
Buf HF	buffered hydrofluoric acid (1 9 40%NH_4F 48%HF)
APTS	3-aminopropyltriethoxy silane (11,339-5)
DMF	n,n-dimethyl formamide (15,481-4)
HNO_3	nitric acid
NaOH	sodium hydroxide
Al_2O_5	aluminium oxide
Intensity decay constant	percentage signal decay per μW per minute
P_2O_5	phosphorous pentoxide (23,481-8)
GeO_2	germanium dioxide
OVD	outside vapour deposition (fibre manufacture)
SEM	scanning electron microscope

† Numbers in brackets represent Aldrich Chemicals identification codes

Chapter I: Introduction

A) Introduction to fibre optic chemical sensors

Optical fibre based sensors have been developed over the last two decades as fast, sensitive, durable and safe sensors with a potentially large range of applications The common characteristics of such sensors are that they respond to a change in the environment so that light can be used to carry information about that change This information is passed from the sensing site to the analysis center by means of an optical fibre, or bundle of optical fibres

There are two classes of optical fibre sensors, intrinsic and extrinsic sensors Intrinsic optical fibre sensors sense changes in the properties of the fibre material, for example transmission loss, polarisation, etc Examples of intrinsic fibre optic sensors are the fibre optic gyroscope based on the Mach Zehnder interferometer and fibre optic pressure transducers using losses induced due to microbending of fibres Extrinsic sensors, however, use an external material having the required optical properties as the sensor, with the waveguide acting as mformation transmission medium only For extrinsic sensors, the sensing material is chosen to interact with the property being monitored in a predictable and reproducible manner and so that a minimum of other external changes influence the optical characteristics of the sensing material If this is not possible, then several sensors with different responses can be used together to isolate many different and separate properties

Extrinsic chemical sensors have been designed to measure or just detect species like CO_2 (Zhujun and Seitz, 1984), O_2 (Peterson *et al*, 1984), pH (Kirkbright *et al,* 1984), glucose (Parker and Cox, 1986), Halothane (Wolfbeis *et al,* 1985), as well as many other chemicals

I A(1) The pH sensor

The fibre optic pH sensors that have been developed to date are based on four basic principles These involve using pH indicators that change colour with pH (Seitz, 1984), usmg a change m the fluorescence signal of a pH sensitive dye (Kawabata *et al*, 1986), measuring the absorbance change in certain dyes, such as Phenol Red (Peterson and Vurek, 1984) or measuring a change in reflectance of a pH sensitive surface (Kirkbright *et al*, 1986)

The probe described by Seitz (1984) shown in Figure I 1 is composed of a set of optical fibres which pass to and from a vessel containing the pH sensitive dye The end of the cavity is sealed with a H^+ ion selective membrane so that only H^+ ions can influence the dye The optical fibre

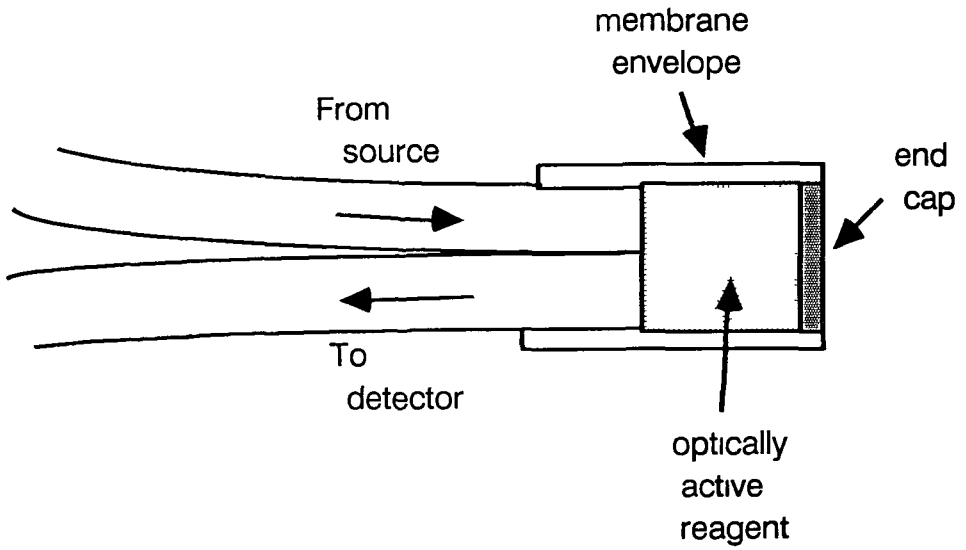

Figure I 1 Typical fibre optic pH probe
(Seitz, 1984)

carrying light from the sensor feeds into signal processing equipment This usually comprises a monochromator and photomultiplier tube, or another filter system with possibly a photodiode The signal from the detector is then passed to an amplifier and finally to an output device In principle, this design can be used for any kind of chemical sensor and the only variables which need to change are the sensing dye and the selective membrane Some common dyes used for measuring pH are given in Table I 1 The light source is chosen so that its spectral output matches the absorbance of the dye being used, while not overlapping with the emission of the dye Typical light sources are lasers, filtered white light sources and light emitting diodes

Table I 1 Common pH sensing dyes

Dye name:	**Method used.**	**Reference:**
Bromothymol blue	absorption	Sheggi *et al*, 1986
Bromothymol blue	reflectance	Kirkbright *et al*, 1984
		Bacci *et al*, 1986
FITC	fluorescence	Kawabata *et al*, 1986
Fluoresceinamine	fluorescence	Saari *et al*, 1982
HOPSA	fluorescence	Seitz, 1984
		Zhujun *et al*, 1984
		Sheggi *et al*, 1986

I A(2) The CO_2 sensor

The CO_2 sensor is a variation on the pH sensor theme It is known that the change in acidity of a carbonate solution is a direct function of the concentration of the CO_2 in solution and it is this characteristic that is used in the fibre optic CO_2 sensor Thus if a small cavity containing carbonate is placed in front of the pH sensing cavity, then the pH sensor is configured for use as a CO_2 sensor Such a system was designed by Zhujun and Seitz (1984) They modified a fluorescence based pH sensor by placing it in contact with a dilute Calcium carbonate solution and enclosing the probe in a CO_2 selective membrane Here the pH sensitive material is the fluorescent dye HOPSA This dye in the absence of H^+ ions dissociates to give H^+ and $OPSA^-$ The $OPSA^-$ component is also fluorescent but at a different wavelength and by comparing the ratio of HOPSA fluorescence to that of $OPSA^-$, the pH of the solution can be determined CO_2 in solution forms carbonic acid H_2CO_3, which dissociates to give H^+ and HCO_3^-

$$H_2O + CO_2 \longleftrightarrow H_2CO_3 \longleftrightarrow H^+ + HCO_3^-$$

Consequently, as the CO_2 concentration in solution changes, then the concentration of hydrogen ions in the third part of the equation changes The change in the final stage is recorded as a change in pH, which can be measured using the pH probe

CO_2 sensors have also been made from other types of pH sensors, for example one based on absorption of phenol red (Peterson *et al*, 1984) Such CO_2 sensors have biomedical applications where they are used to measure the concentration of CO_2 in the blood Sometimes, the fibre optic CO_2 sensor has been coupled with a pH sensor and an O_2 sensor to give a blood analysis unit in the form of a catheter type probe (Miller *et al*, 1987, Tusa *et al*, 1986) This allows the monitoring of the important variables in the blood using the one probe head There has been a development toward a disposable fibre optic probe containing the sensing elements of pH, CO_2 and O_2 sensors, which can be disposed of after use Such a plug-in system has been described by Gehrich *et al* (1986) which uses a probe connected to the analyser via a patient interface module (PIM) The latter is a device that would form part of the equipment surrounding the patient in intensive care The PIM should be small so as not to overcrowd the patient and to take up valuable floor space from other instruments The analytical unit, including light source and detector, can then be located in a remote location, with all interaction of the medical staff and the instrument taking place through the PIM The probe plugs into the PIM by means of an optical multiplexer which activates each of the three sensing units in turn

B) Advantages of fibre optic sensors

I:B(1) Size

The small diameter of the optical fibres used in sensors is most likely to be the greatest advantage of this type of sensor. Typically, the size of the optical fibres range from 100μm to 300μm in diameter. This means that if the sensing area is limited to the size of the fibre, then quite high spatial resolution can be attained. The small size of a sensor probe affects the response time of the sensor greatly, which as a result can be minimised.

This small size is of great advantage when dealing within restricted environments. The fibre optic sensor can then be placed in normally inaccessible regions. This is especially true when considering the field of biomedical sensors. It is possible to insert sensors based on fibre optics into the blood vessels of patients and to take measurements *in vivo* (Gehrich *et al*, 1986). The sensing probe is normally inserted via a catheter and can be directed along any major blood vessel. The fibres used in these cases are usually plastic fibres, as glass fibres are very difficult to recover in case of breakage.

I:B(2) Cost

The cost of producing large quantities of commercial optical fibres has been reduced dramatically over recent times, and is set to fall even more as production techniques are established. This means that the cost of the short lengths of fibre used in fibre optic sensors becomes almost negligible. The volume of chemicals used in the probe element is so small (eg. $7.8\text{x}10^{-3}\text{mm}^3$ for 200μm fibre diameter with 250μm deep dye cavity) that the quantities required are very small.

The main production costs are those of the instrument associated with the light source and detector system. The standard light sources are lasers, but these may be replaced by appropriate light emitting diodes, or filtered white light sources. The detector often consists of a monochromator and photomultiplier system, although these can be replaced by a filter and photodiode. The optics are also a significant factor. The light from the source must be launched into the fibre at constant intensity, while the returned light from the sensor must be separated and passed to the detector. In some sensor designs, a fibre cross coupler may be used, but these are expensive. The cost of these couplers is offset by the fact that complex beam splitting and focussing systems are no longer needed and so improves the general performance of the sensor.

The sensor can be designed so that the probe becomes disposable. Such a design would require that the light source, alignment optics and detector be fixed and that the sensing tip be located

on a length of optical fibre that can be replaced easily This is of great importance in biomedicine as the probe can be kept in sterile packing until required by the doctor, at which point it is attached to the main unit by means of a standard connector The probe element can be safely disposed of after the measurements have been taken, minimising the risk of cross contamination between patients

I B(3) Simplicity

After development of a fibre optic sensor, the number of manufacturing stages can be kept to a minimum Such stages may include fibre preparation (removal of protective coating, cleaving, possible surface treatment for bonding), manufacture of the vessel for containing the sensing material, placing the sensing material in the container and fixing it to the fibre A selective membrane may be placed over the probe to retain the sensing dye and allow passage of the analyte The fibre must also be connected to the source / detector configuration

The number of manufacturing stages for a fibre optic sensor compare quite favourably with those for a state of the art polarographic sensor, for example The probe shown in Figure I 4 (Baumgartl and Lubbers, 1983) has approximately 40 stages in the manufacturing process which are quite complicated and require very tight control

The simpler that each manufacturing stage is kept, the lower the manufacturing cost of the final product and the more it is suited for mass production

I B(4) Safety

Because the carrier of information for fibre optic sensors is light, such sensors are intrinsically safe At low power levels (less than 100mW in single mode fibre for 13% hydrogen in air using 40μm coal particles (Hills, 1990)), visible light does not initiate chemical reactions in cases where such reactions would be disastrous, for example in the storage of flamable gases A low intensity beam of visible light will not ignite the gas, even in the presence of oxygen An electronic sensor may, however, produce a spark, or overheat unless the design and construction procedures used in intrinsically safe equipment are applied

The low attenuation of optical fibres allows the light source and detector to be housed at a safe distance from the probe head, reducing the risk even further

I:B(5) Speed

There are two aspects to sensor speed. Firstly, the actual measurement of the result: Fibre optic sensors have been developed with short respone times, often of the order of 10 seconds. This usually allows any changes in the environment to be detected as they happen, and therefore allows a temporal picture of the change to be built up.

Secondly, most fibre optic sensors are capable of making realtime measurements in a biomedical system. For example, consider methods for monitoring a patients' blood gas levels. With conventional methods, a blood sample is taken and sent to a remote laboratory for processing. The time lag between sampling and results can range between 10 minutes and 3 hours. In the case of a fibre optic sensor located in the patient, these measurements can be made continuously.

I:B(6) Environmental isolation

Most fibre optic based sensors remain isolated from the environment in which they are placed. With the exception of sensors based on immunological systems (antibody - antigen competitive binding), they do not alter the status of the analyte. This is important, for example, in fibre optic oxygen sensors. Solid state oxygen probes (e.g. the polarographic probe shown in Figure I.4; Baumgartl and Lubbers, 1983) consume oxygen to generate a current that is measured. This has the effect of changing the localised oxygen concentration which is not so with optical oxygen sensors such as the one described in this work since the sensor relies on energy interactions between the excited state fluorophore molecules and the oxygen.

In optical based sensing systems, the only interaction with the environment is due to the light used to illuminate the probe. Because of the small diameter of the core in optical fibres, the intensity of the light emerging from the probe can be quite high. In practice, most fibre optic sensors tend to operate below the ignition limit.

I:B(7) Portability

With correct design of a fibre optic sensor, it is possible to make the probe portable although the light source and detectors are still sizable units.

This section has outlined some advantages of fibre optic sensors. It shows that fibre optic sensors are potentially superior to comparable electronic sensors that are currently being used. However, some work remains to be done on the reliability and size of the optical fibre sensor systems. This is especially true for sensors designed for use in the field of biomedicine. Since fibre optic sensors

can be developed for most analytes, often with only a minor change in probe design, it is possible that in the future, a faster analysis of a patient's condition can be made

The fibre optic sensors can also be applied to other areas, for example in research An application requiring high spatial resolution is the measurement of the radial oxygen concentration across Calcium Alginate pellets which are used in bioreactors to culture microorganisms in the manufacture of drugs, etc These pellets are approximately 4mm in diameter, although pellets with diameters of 10mm are possible, and as a result require a spatial resolution of at least 0 1mm if the sensor is to generate a reasonable data set Such resolution can be achieved by the fibre optic probe described in this project A polarographic sensor would not be suitable here due to its consumption of oxygen during the measurement process

Further possibilities exist for designing sensor units capable of measuring different analytes only by exchanging the probe head This is possible since the different probes are based on the same principle, for example fluorescence quenching, etc

C) The history of oxygen sensors

I C(1) History of non-fibre optic O_2 sensor

Traditionally, dissolved oxygen concentrations were measured using titration methods The most common method was the Winkler titration (Skoog, 1956) The sample under investigation is treated with an excess of manganese(II), potassium iodide and sodium hydroxide Manganese(II) hydroxide is quickly formed and reacts with the dissolved oxygen to give manganese(III) hydroxide When acidified, the manganese(III) oxidises iodide to iodine The liberated iodine can be titrated in the usual manner using 0 025*N* $Na_2S_2O_3$

$$4Mn(OH)_2 + O_2 + 2H_2O \longrightarrow 4Mn(OH)_3$$
$$2Mn(OH)_3 + 2I^- + 6H^+ \longrightarrow I_2 + 6H_2O + 2Mn^{2+}$$

This method will only work under certain conditions The first is that the concentration of oxygen in the sample remains constant for the duration of the titration It is obvious that if this concentration changes, then the result is inaccurate The major problem is that the procedure is quite lengthy The sample should also be free of any solutes that will interact with iodine, either oxidising or reducing, as either will result in a change in the concentration of free iodine in the solution

The Winkler titration is an accurate method for determining the amount of oxygen in solution, but is slow and prone to misuse In 1956, L C Clark described an electrode that could measure the partial pressure of oxygen in solution by measuring the current flow between electrodes The Clark cell is constructed with the cathode embedded in a block of electrical insulator, such as glass A thin membrane (5 - 50 μm thick) is stretched over the insulator block face, within which a thin layer of electrolyte is held The membrane can be made of rubber, or of some polymer, such as PTFE, polythene, etc The electrolyte can be supported in the roughness of the block surface, in paper tissue or in another matrix If the cathode is polarised, then the current flow depends on two factors The first is the rate at which oxygen can diffuse across the membrane to accept electrons from the cathode which in turn depends on the material used in the membrane The second factor is the partial pressure of O_2 at the electrode and it is this quantity that is measured by the device

The major problem with the Clark electrode is the use of an electrolyte layer between the electrode and membrane If this layer is too thin, then the electrolyte will evaporate and render the instrument inoperative If the layer is too thick, then the response time of the sensor will be

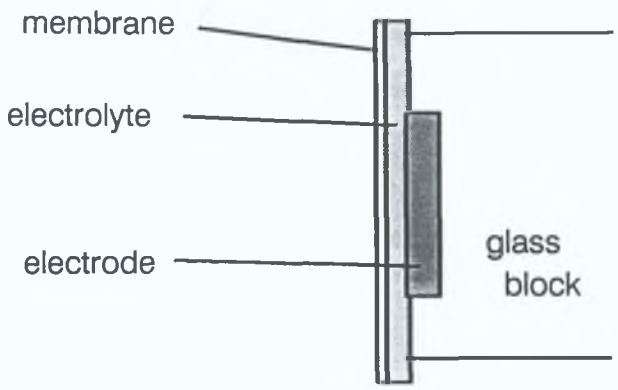

Figure I.2: Clark Electode

very long. As the thickness of the electrolyte layer changes, the response time and readings from the Clark cell also change. The thickness of this layer is very difficult to control since it varies with atmospheric pressure and because the surface of the insulator block may not be uniform. The sensor must also be mounted rigidly as sudden mechanical shocks may cause oxygen rich electrolyte to come in contact with the electrode, giving erroneous readings. The Clark cell was often configured so that the layer of electrolyte was relatively thick, which resulted in the major disadvantage of having a very slow response time, often of the order of 30 minutes.

To overcome the limitations associated with the electrolyte in the Clark cell, Bergman (1968) developed an electrode that did not depend as strongly on the electrolyte layer between the membrane and cathode. In this sensor, a polymer which was permeable to oxygen, but electrically non-conductive, for example PTFE, was coated with a thin porous metal film on the electrolyte side to make contact with an electrode. An area of the metallised surface was then exposed to the electrolyte, and a corresponding area on the opposite side of the membrane was exposed to the atmosphere. Often a dialysis membrane was added for mechanical strength. The oxygen concentration is measured between the metallised layer and the membrane and the electrolyte serves to remove the hydroxyl ions formed at the cathode. By changing the metal used on the membrane, the sensor could be adapted to measure hydrogen ion concentrations, while a change in the electrolyte solution could further adapt this sensor for measuring CO_2. Again the major drawback is the long time constant, which does not allow any real-time monitoring to take place.

In 1968, Bergman also developed an oxygen sensor based on fluorescence quenching of long lifetime fluorescent compounds by singlet oxygen. The quenching of fluorescence is the process by which a fluorophor molecule is de-excited by collision, or other means, resulting in non-radiative decay of the excited state (Chapter I:E Quenching of fluorescence.). For long excited state lifetime fluorescent compounds, the probability of an encounter that will result in quenching

is much higher than for one with a short lifetime. Long lifetimes are considered in this instance to be of the order of microseconds. Bergman used the polycyclic aromatic compound fluoranthene which is quenched quite strongly by atmospheric concentrations of oxygen (to 41% of its maximum intensity). The dye was immobilised in a polyethylene matrix which is 25-50μm thick. This immobilisation greatly enhances the response time of the sensing unit. A problem occurs when the polymer dries out causing the fluorescent dye molecules to be restricted in terms of vibrational modes resulting in reduced quantum fluorescence yield. This is also coupled with a decrease in diffusion of oxygen within the sensor. This problem was overcome by using Vycor porous glass as the matrix for retaining the dye. The glass is cast as a disk which is placed between a UV light source and a detector, with the appropriate filters in place. This arrangement was used to measure oxygen partial pressures, but because of its design, has limited applications.

The quenching of fluorescence is used quite extensively in measuring oxygen concentrations in biological systems. The dyes used are non-toxic over short term and do not interfere with the biosystem. A common fluorescent dye used is pyrene butyric acid (PBA), which is quenched by oxygen. This dye has been incorporated into intracellular spaces (Knopp and Langmuir, 1972; Mitnick and Jobsis, 1976), as well as in living cells (Kohen *et al*, 1974; Benson *et al*, 1980; Podgorski *et al*, 1981). The localised oxygen partial pressures were reflected in the intensity of fluorescence of PBA at that location. The fluorescence was monitored using a camera attached to a microscope, using UV excitation and filters. Since the observed intensity reflects the oxygen concentration, a series of such photographs can be used to analyse the diffusion of oxygen under different conditions.

When the fluorescent dye is used in this way, the sensing process is termed 'Molecular Fluorescence Sensing' because the dye is added to the analyte solution directly, rather than housed in a portable instrument. The molecular fluorescence sensing system has spatial resolution dependent on the distribution of the dye within the solution and is generally quite high, although the temporal resolution is determined by the speed of image analysis of the monitoring system.

A probe based on the use of fluorescence quenching was developed by Kroneis and Marsoner (1983) that could measure the oxygen concentration in bioreactors (Figure I.3). The sensing element was composed of a rigid transparent plastic plate to which a membrane matrix containing the fluorophor was attached. There was also an optically isolating membrane which minimises light picked up externally. Sometimes, a protective Teflon (PTFE) membrane was added for long term stability. The probe was constructed of two channels, one of which passed the excitation light and the other the return signal from the sensing element. With an appropriate filter system,

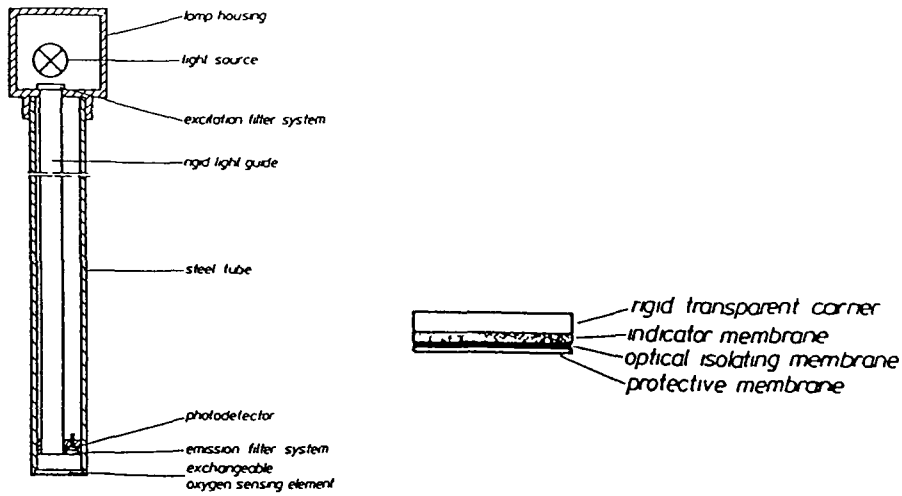

Figure I 3 Bioreactor oxygen monitoring probe
(Kroneis *et al* , 1983)

the concentration of oxygen was calculated from the intensity of fluorescence The probe was used in a bioreactor and could easily be sterilised for use in other environments. The large size of the probe and the long response-time make the instrument impractical for most other applications

Polarographic (solid state) oxygen sensors have been developed with high spatial resolutions, which allow the oxygen concentrations to be measured over a wide range of applications. Such a sensor has been described by Baumgartl and Lubbers (1983) In principle, it measures the current due to oxygen in solution

$$O_2 + 2H_2O + 4e^- \longrightarrow 4\,OH^-$$

The electrons are supplied from the cathode and this current can be measured The above reaction will only proceed under alkaline or neutral conditions This, however, is not a disadvantage, as most living systems usually have pH within this range

The polarographic oxygen sensing probe (Figure I 4) is extremely complex in both theory and manufacture From beginning to end, there are ~ 40 manufacturing stages including glass cleaning and drawing, platinum etching, insertion of the platinum tip, fusion of the tip, reference electrode sputtering, electro-chemical polishing, coating with gold, polymer application, annealing and calibration There are other problems associated with the sensor, which are mainly concerned with stability The sensor is sensitive to both light and temperature There is approximately a 2 1% change in signal per degree kelvin The changes with temperature are non-linear with respect to temperature and also vary from sensor to sensor This requires the calibration of each sensor at the desired temperature before precise measurements can be taken

Baumgartl and Lubbers (1983) reported that the sensor was sensitive to certain wavelengths of light. When illuminated from the side by a microscope lamp, the observed signal increased and when the light source was removed, the signal decreased by the same amount. Re-illumination caused the same increase in the measured signal as before.

The polarographic oxygen sensor is also prone to signal drift, as well as genuine instability. This was observed over a 30 day test period at constant pH and air saturation.

From examples of conventional oxygen sensors which were described above, there are none which satisfy the need for a long term stable, high resolution (both spatial and concentration) and fast response time. The development of fibre optic probes is an attempt to combine these properties, with possibly some additional enhancements such as a simpler manufacturing cycle and simpler user interface.

I:C(2) History of fibre-optic O_2 sensors.

In 1980, Peterson *et al* described a fiber optic oxygen sensor for measuring concentrations of oxygen *in vivo*. This sensor was based on fluorescence quenching of perylene dibutyrate by singlet oxygen. The excitation and emission light signals were carried to and from the probe head using

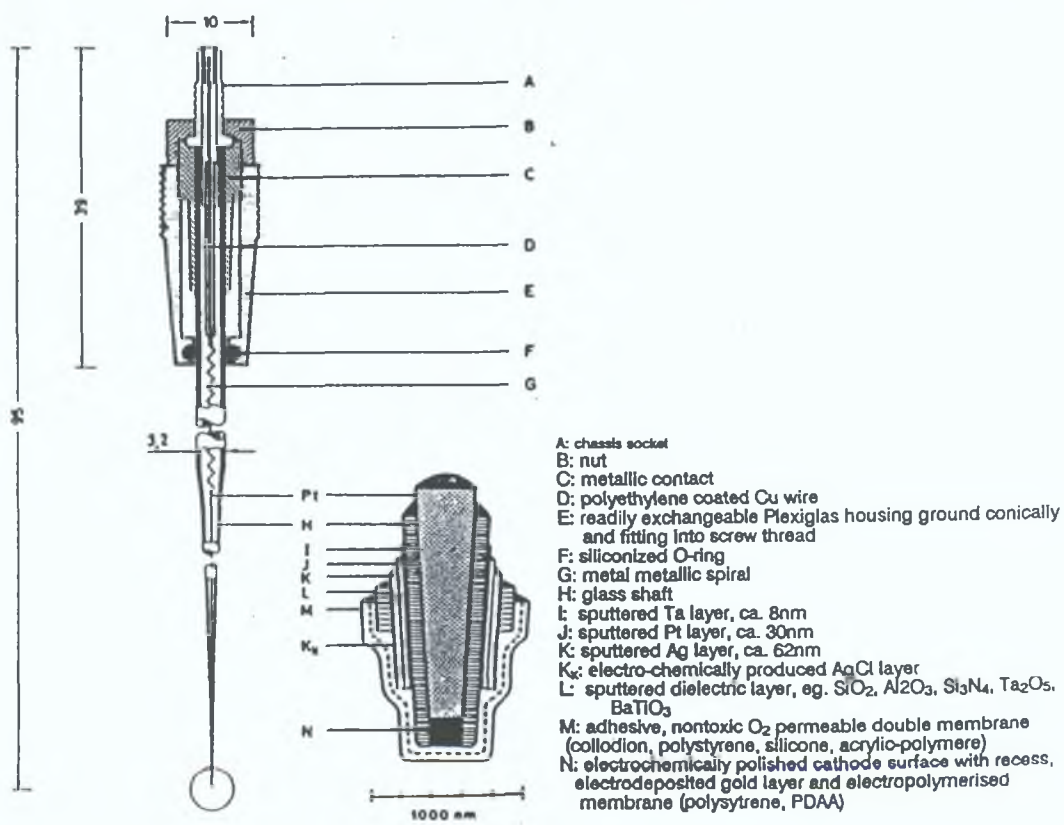

Figure I.4: Polarographic Oxygen Sensor
(Baumgartl, 1983)

plastic optical waveguides (with 250μm core diameter) The probe end consisted of a section of porous polymer approx 3 mm long and 0 6 mm in diameter The fluorescent dye was enclosed within the tubing and immobilised on an absorptive support The support used was amberhte XAD4 that allowed the dye to be sensitive to oxygen, while remaining insensitive to water (the dye is moisture sensitive and the amberlite is hydrophobic) The polymer tubing composed of polypropylene, which is highly gas permeable, but hydrophobic

The light source used was a 60W deuterium lamp with two filters The first was a heat reflecting filter, which removed the red portion of the spectrum The second was a short pass interference filter with a nominal cutoff at 480 nm The small luminous spot of the deuterium lamp allows relatively easy launching of the light into an optical fibre using a lens

The return signal was measured by two photomultiplier tubes, one operated with a blue filter and the other with a green filter The signal from the blue filter was used as reference, while the green filter passed the fluorescence signal The two voltages were then ratioed and the result was then corrected so that the final output corresponded to a value for the concentration of oxygen according to the Stern - Volmer equation (Chapter I E Quenching of fluorescence)

This sensor was extensively tested in the blood stream of a living ewe The readings taken by the fibre optic probe were compared to readings taken from blood samples taken from the sheep The probe performed quite well, although the probe was subject to clotting at the sensing end and a good correlation was found between the *in vivo* readings and the blood samples taken During *in vitro* tests, the sensor showed a response time of 0 5 minutes for a 63% change in the response after a step change in oxygen concentration The sensitivity of the probe was found to decrease at a rate of 0 1% per day, with the probe stored in water, while a 3% loss per day was reported if the probe was stored in air

One of the major drawbacks of the sensor was its sensitivity to other gases Nitrous oxide gave a change of approx 2% of corresponding oxygen concentration, while Halothane had a much more serious effect It adsorbed onto the support for the dye and the effect was cumulative and depended on concentration and exposure time The reaction reversed if exposure was not too long The effect of halothane on the readings given by the sensor were reflected both in a zero offset and a change in sensitivity

This sensor was shown to be suitable for use *in vivo* in conditions where halo-carbon anaesthetics are not used

Wolfbeis *et al* (1985) described a sensor for measuring both oxygen and Halothane The principle of operation was that of a two dye sensor system in which a halothane sensitive fluorescent dye was used to determine Halothane concentrations by the quenching method A second dye was used that was quenchable by oxygen, as well as Halothane The Halothane sensitive dye, a polycyclic aromatic hydrocarbon, was incorporated into a fibre optic sensor with a similar design to that described by Peterson *et al* The second oxygen/ Halothane sensitive dye was incorporated in a second sensor of the same design The Stern-Volmer equation that describes the effects of quencher concentrations on the intensity of fluorescence, was then modified for the two quencher system The final concentrations of both halothane and oxygen were calculated from

$$[H] = \frac{(\alpha {}^{0}K_b - \beta {}^{0}K_a)}{({}^{H}K_a {}^{0}K_b - {}^{0}K_a {}^{H}K_b)}$$

$$[O_2] = \frac{({}^{H}K_a - {}^{H}K_b)}{({}^{H}K_a {}^{0}K_b - {}^{0}K_a {}^{H}K_b)}$$

Where

$\alpha = (I_{a0}/I_a) - 1$ for the halothane sensor, $\beta = (I_{b0}/I_b) - 1$ for the oxygen/halothane sensor

${}^{0}K_a$ is the oxygen quenching constant for the halothane sensor calculated from calibrations

${}^{0}K_b$ is the oxygen quenching constant for the oxygen sensor calculated from calibrations

Likewise, ${}^{H}K_a$ and ${}^{H}K_b$ are the halothane quench constants for the two sensors

I_{a0} and I_{b0} are the intensities of the two sensors at 0% oxygen

These equations can be simplified if the sensors are designed so that the quenching constant for each gas is the same in both This can be achieved if the same fluorescent dye is used in both, but one sensor is coated with an oxygen selective membrane, such as PTFE The above equations then simplify to give the following

$$[H] = (\alpha - \beta) / {}^{H}K_a$$

$$[O_2] = \beta / {}^{H}K_b$$

These equations have been used in a successful sensor for both oxygen and Halothane and give a good example of a dual quenching environment The response times of the final sensors were found to be 10 - 15 seconds for the oxygen sensor and 15 - 20 seconds for the halothane sensor The range of applications envisaged included *in vivo* , as well as *in vitro* measurements and also breath gas analysis

Gehrich *et al* (1986) described an intravascular blood gas probe composed of pH, CO_2 and oxygen fibre optic sensors The three sensors were contained within a polymer matrix to form a catheter-like probe A thermocouple was also included for completeness The oxygen sensor was

based on the fluorescence quenching of a proprietary long lifetime fluorescent dye The dye was immobilised in a silicone matrix, which allows the diffusion of oxygen The whole sensor was manufactured so that the sensing probes could be easily removed from the excitation light sources and the electronics A new probe is attached for use with the next patient The oxygen probe was found to have an accuracy of 15% during *in vivo* tests (Tusa *et al*, 1986) when compared to the concentrations of oxygen found by taking blood samples and analysmg them separately

Lippitsch *et al* (1988) described a system where the fluorescence lifetime was used to determine the oxygen concentration in solution The system that they used was based on a blue emitting LED as the light source modulated at 455kHz exciting immobilised Ru $(bpy)_3^{2+}$ m Kiesel gel The optical system used involved a bifurcated fibre optic bundle, with the excitation and emission signals carried in separate fibres The detector used was a photomultiplier tube operating with a red filter The lifetime was derived from the phase shift between the excitation and emission modulation and was electronically calculated

There are several advantages associated with this sensor given as follows
There is no need for a reference system as the life time is independent, firstly, of the concentration of the dye at low concentrations where self quenching is not significant, secondly, of the intensity of the excitation source and thirdly, of the efficiency of the detector system This removes the need for a reference system in which, for example, a second dye is used The second advantage is that the cost of the sensor is significantly reduced because they use an LED as opposed to a laser, which also makes the instrument portable The major disadvantage of this sensor is that its spatial resolution is very poor, but this is balanced by its stability, which was quoted at three weeks minimum

These sensors outline the development of the fibre optic oxygen sensor to date and set a target for the present project The major disadvantage of these sensors is their spatial resolution The main aim of the present work is to improve the spatial resolution When this resolution is coupled with good response time, good sensitivity and long stability, a sensor is developed that can have many potential applications and is not limited to the biomedical fields A specific application in which the fibre optic sensor will be used is in measuring the radial oxygen concentration gradient within calcium alginate pellets of 4mm diameter This type of measurement requires a high resolution, of the order of 0 1mm to allow the gradient to be plotted.

D) Review of fluorscent dyes used

I D(1) Photochemistry of Ru $(bpy)_3^{2+}$

The transition metal complex Ru $(bpy)_3^{2+}$ is classed as a bidentate heterocyclic complex (Note. bpy = 2,2'-bipyridyl) The three dimensional structure is shown in Figure I.5 The absorption spectrum has maxima at 454, 428, 345, 323, 285, 250 nm and the fluorescence emission peaks at 608nm in water (§ Figure 1 6) The fluorescence is due to the decay of an excited metal - ligand charge transfer (MLCT) complex which occurs between the central Ruthenium ion and the surrounding bipyridyl ligands The MLCT state is where a π_M electron is promoted a π_L^* ligand orbital This MLCT state is quite long lived giving the fluorophor the characteristic long lifetime of 580ns in water It is this long lifetime of the excited state which makes the dye oxygen sensitive (§ Chapter I E Quenching of Fluorescence) The quantum yields of fluorescence for Ru $(bpy)_3^{2+}$ are given as 0 062 in aerated solution and 0 1 in degassed solution (Durham *et al,* 1982) The quantum yield is given as the proportion of photons emitted to those absorbed. The Ru $(bpy)_3^{2+}$ is easily immobilised into Nafion cation exchange resin, as the central ion has a 2+ charge associated with it when in solution The Nafion resin (§ Chapter I.F Immobilisation techniques) will concentrate the dye from a millimolar solution to a concentration of approximately 0 5M within the polar regions of the polymer matrix (Wilkinson *et al,* 1983)

The fluorescence intensity of Ru $(bpy)_3^{2+}$ decreases to ~40% of its maximum intensity in oxygen saturated aqueous solution and displays 70% I_{max} at atmospheric levels (21% O_2) This allows an oxygen sensor based on Ru $(bpy)_3^{2+}$ to have a large operating range for determining dissolved oxygen concentrations

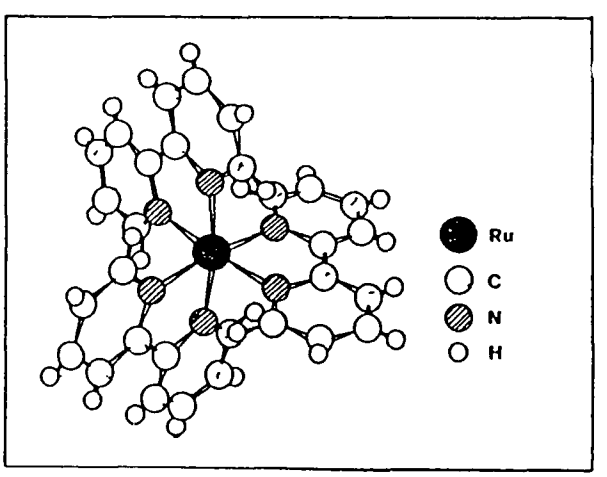

Figure I 5 3-D structure of $Ru(bpy)_3^{2+}$

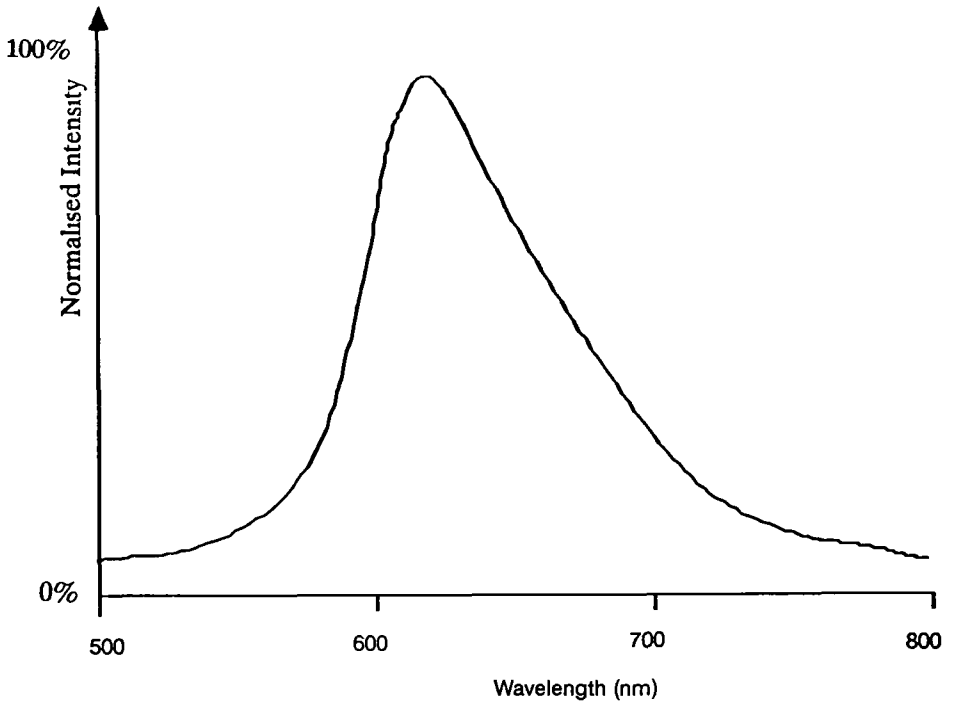

Figure I 6 Emission Spectrum of $Ru(bpy)_3^{2+}$

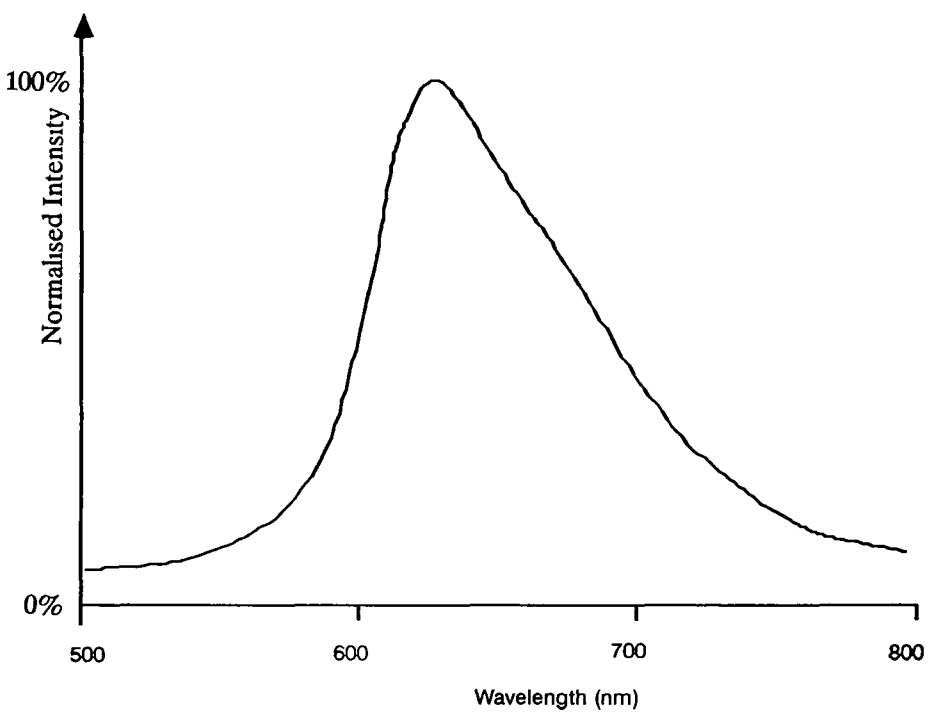

Figure I 7 Emission Spectrum of $Ru(phen)_3^{2+}$

A disadvantage of the Ru $(bpy)_3^{2+}$ system is that the excited state is chemically active (Durham *et al*, 1982). Since the excited state is easily oxidised into Ru $(bpy)_3^{3+}$, it will easily form intermediary compounds which change the photophysical properties of the molecule. The oxidised Ru $(bpy)_3^{3+}$ is also an efficient quencher of Ru $(bpy)_3^{2+}$ by the same quenching process (Wilkinson *et al*, eds., 1983) as O_2 and as such can be mistaken for oxygen in a probe designed with $Ru(bpy)_3^{2+}$.

The Ru $(bpy)_3^{2+}$ excited state is also easily reduced to Ru $(bpy)_3^{+}$ and this leads to another alternative path for non-radiative energy loss. These oxidation / reduction reactions have been extensively studied, namely for the photochemically induced splitting of water, but in this sensor, are not desired. A further problem with this compound is its susceptibility to photo- dissociation when illuminated. This is due to the relatively weak π-bonding of the bipyridyl groups which may cause detachment of one or more such groups from the molecule when excited.

The excited state of Ru $(bpy)_3^{2+}$ is quenched only by a limited number of chemical species. The important ones are Ru $(bpy)_3^{3+}$ (the triple-ionised state), oxygen and Halothane (an anaestethic gas). If the oxidation of Ru $(bpy)_3^{2+}$ is kept to a minimum (by removing oxidising agents) and the sensor is designed with an oxygen permeable membrane, then the response of the probe is only due to oxygen interactions.

I:D(2) Photochemistry of Ru $(phen)_3^{2+}$

The Ru $(phen)_3^{2+}$ molecule is quite similar in structure to that of Ru $(bpy)_3^{2+}$, differing only by the type of ligand (Note: phen = 1,10-phenanthroline). As a result, the photo-chemical characteristics are also quite similar. The Ru $(phen)_3^{2+}$ has absorption peaks at 446, 417, 263, 224 nm . The fluorescence peaks at 608nm (§ Figure 1.7) as for Ru $(bpy)_3^{2+}$ and the lifetime of the excited state is 850ns at room temperature. The quantum yields are given as 0.0086 in aerated solution and 0.014 in degassed solution (Durham *et al*, 1982).

The Ru $(phen)_3^{2+}$ is easily absorbed by the Nafion ion exchange resin and behave quite similarly to the Ru $(bpy)_3^{2+}$. The excited Ru $(phen)_3^{2+}$ species is much less photoreactive as compared to Ru $(bpy)_3^{2+}$ (Wilkinson *et al*, eds.) and so leads to a more stable sensing dye which is less susceptable to photo induced decay with high light intensities at the sensor tip. The excited state lifetime for Ru $(phen)_3^{2+}$ is about 30% longer than that for Ru $(bpy)_3^{2+}$ (850ns, 580ns resp.) and as a result has a potentially greater sensitivity to collisional quenching by oxygen. The increase in stability coupled with the greater oxygen response makes the Ru $(phen)_3^{2+}$ a more suitable

fluorescent dye for use in a dynamic quenching based oxygen detector

I D(3) Photochemistry of Os $(bpy)_3^{2+}$

The structure of Os $(bpy)_3^{2+}$ is the same as that for Ru $(bpy)_3^{2+}$, except for the central bound transition metal The absorption characteristics for Os $(bpy)_3^{2+}$ are similar to those for Ru $(bpy)_3^{2+}$, being dominated in the visible region by a large MLCT complex. The peaks for absorption for Os $(bpy)_3^{2+}$ are 590, 480, 435, 385, 367, 330, 290, 245 nm (Creutz *et al*, 1980) The major differences between the two species are the wavelength of maximum fluorescence and the lifetime of the excited state

The lifetime of the Os $(bpy)_3^{2+}$ complex is much shorter than that for Ru $(bpy)_3^{2+}$ and is given as 19ns in aqueous solution (Creutz *et al*, 1980) This is short enough to render the excited state of Os $(bpy)_3^{2+}$ effectively insensitive to oxygen by collisional quenching, which leaves the intensity of fluorescence constant at different oxygen concentrations

The second difference between the Ru $(bpy)_3^{2+}$ and the Os $(bpy)_3^{2+}$ is the wavelength of maximum fluorescence which for Os $(bpy)_3^{2+}$ lies at 715nm (§ Figure 1 8) compared to 608nm for Ru $(bpy)_3^{2}$ This allows easy differentiation between the respective fluorescence signals from

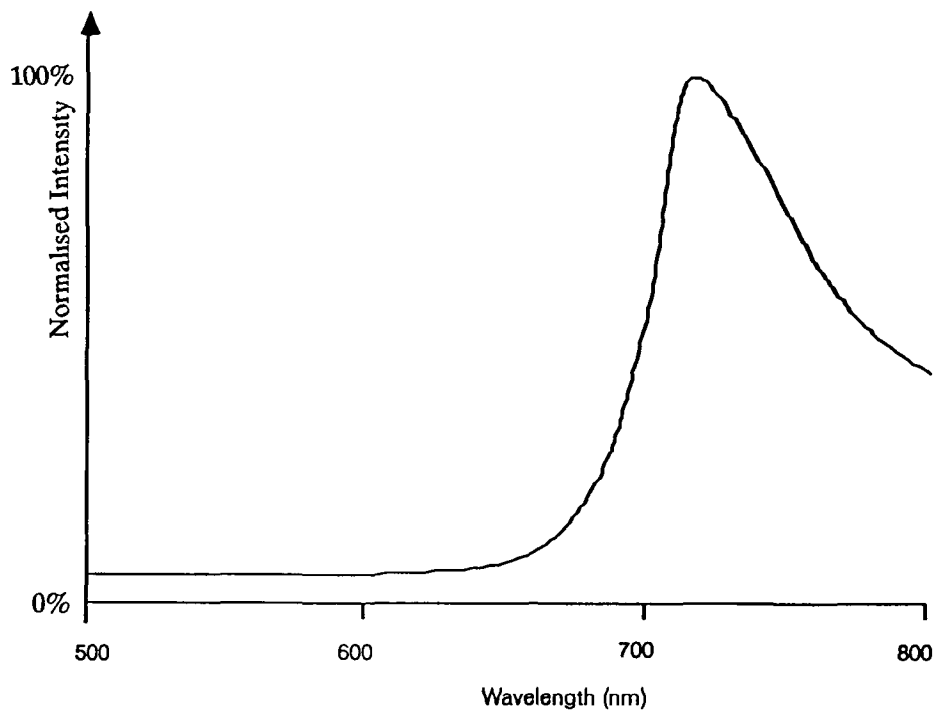

Figure I 8 Emission Spectrum of $Os(bpy)_3^{2+}$

a solution containing a mixture of the two dyes

The ion exchange resin Nafion easily allows the uptake of Os $(bpy)_3^{2+}$ from aqueous solution as it is also a cation in solution This allows a possible system where both the Ru $(bpy)_3^{2+}$ and Os $(bpy)_3^{2+}$ are placed together in the same Nafion polymer probe and where the intensity from the Ru $(bpy)_3^{2+}$ is monitored for oxygen concentration while the fluorescence from the Os $(bpy)_3^{2+}$ is used as a reference for the system

E) Quenching of fluorescence

Fluorescence is the emission of a photon of light from a molecule which has been placed in the excited state by the absorption of another photon The emitted photon is of a lower energy than that of the absorbed photon due to energy loss encountered during inter electromc level crossover events Fluorescence quenching is any process which depopulates the excited state without the emission of a photon (Lakowicz, 1983) There are two forms of fluorescence quenching, namely static and dynamic quenching Static quenching is where the absorbed energy is transferred to the surface to which the fluorophor is bound The degree of static quenching is dependent on the degree of mteraction between the excited molecule and the substrate and is not a rate dependent process

Dynamic quenchmg occurs when a free molecule interacts with the excited fluorophor resultmg m the transfer of energy This process is very much rate dependent and is mathematically described by the Stern-Volmer equantion The degree of dynamic quenching is dependent on the concentration of the quenching molecule and on the mobility or rate at which the quencher can diffuse to the excited molecule

The lifetime of the excited molecule is dependent on the quantum lifetime, which is governed by the depopulation rates for the excited energy states, the static quenchmg constant, and the dynamic quenchmg rate coupled with the quencher concentration The lifetime of an excited molecule decreases with increasing quencher concentrations, as does the intensity The Stern-Volmer equation describes how these factors interact mathematically and can be derived as follows The intensity of fluorescence is proportional to the concentration of excited flourophor molecules (F*) in a given volume Under continuous illumination, a constant population of F* is estabhshed so that

$$\frac{d(F^*)}{dt} = 0 \qquad (1)$$

In the absence of quenching species, the rate of population of the excited state equals the rate of

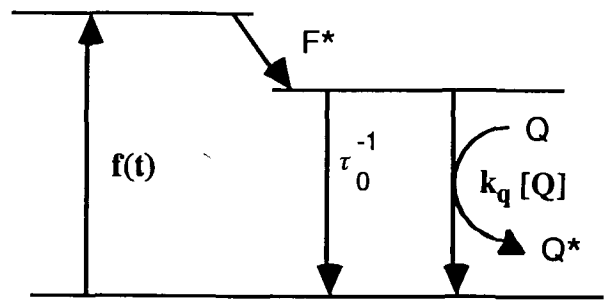

Figure I 9 Quenching Process

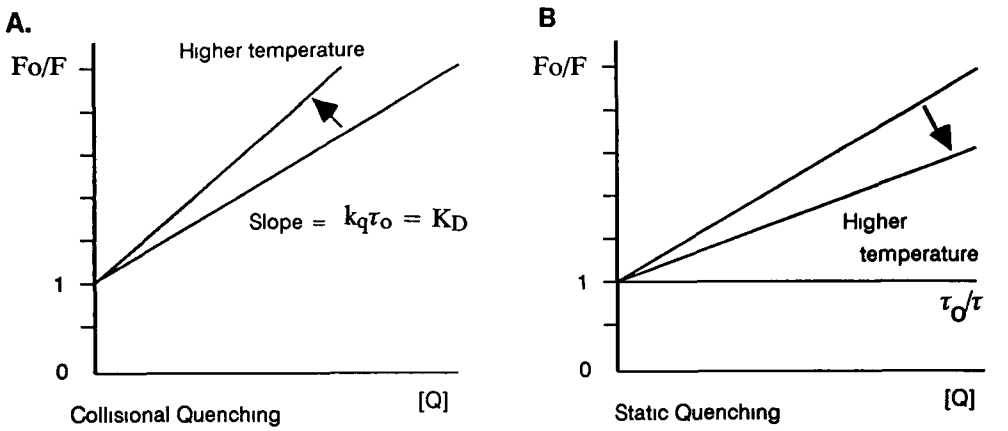

Figure I 10 Theorethical Stern - Volmer plots

decay

$$\frac{d(F^*)}{dt} = f(t) - \Gamma F^*_0 = 0 \qquad (2)$$

f(t) is the population function for the production of the excited state Γ is the decay rate of the excited fluorophor in the absence of quencher ($\Gamma = \tau^{-1}$)

Similarly, when there is quencher present, an additional term is inserted to account for the alternative decay process Equation (2) becomes

$$\frac{d(F^*)}{dt} = f(t) - (\Gamma + k_q[Q])F^* = 0 \qquad (3)$$

The terms f(t) cancel, giving

$$\frac{F_0^*}{F^*} = \frac{\Gamma + k_q[Q]}{\Gamma} = 1 + k_q\tau[Q] \qquad (4)$$

The equation is known as the Stern-Volmer relation which describes the process of dynamic quenching An alternative derivation uses the fact that the collisional quenching process is a rate dependent process leading to the depopulation of the excited state The excited state lifetime in the absence of a quenching species is given by

$$\tau = \Gamma^{-1} \qquad (5)$$

where Γ is the decay rate of the excited level In the presence of quencher, an additional depopulation process is present This gives

$$\tau = (\Gamma + k_q[Q])^{-1} \qquad (6)$$

This leads to the ratio

$$\frac{\tau_0}{\tau} = \frac{\Gamma^{-1}}{(\Gamma + k_q[Q])^{-1}} = 1 + k_q\tau_0[Q] \qquad (7)$$

which is again the Stern-Volmer relation. This leads to an important observation

$$\frac{F_0}{F} = \frac{\tau_0}{\tau} = 1 + K_D[Q] \quad \text{... (8)}$$

The constants $k_q\tau_0$ are often rewritten as K_D which is the Stern-Volmer quenching constant. If the ratio of the quencher free intensity to intensity at a given quencher concentration is plotted against the quencher concentration, a linear plot is obtained which passes through the point (0,1) on the intensity axis (§ Figure 1.10). The slope of this line is K_D and is intrinsic for a given fluorescent dye / quencher combination.

An important concept associated with dynamic quenching is the volume around the fluorophor which can actively influence the quenching of the excited molecule (Lakowitz, 1983). This is a sphere of volume V with radius Z_x given by

$$Z_x^2 = 2D\tau \quad \text{...(9)}$$

where D is the diffusion coefficient of the quencher around the fluorophors and τ is the lifetime of the excited molecules.

The value for Z_x is approximately $5x10^{-6}$cm taking D as $2.5x10^{-5}$ cm^2s^{-1} (for oxygen in water at 25°C) and the lifetime of the dye as 0.58μs. If a quencher molecule is contained within this sphere, it may quench the excited molecule if a collision event occurs. All quencher molecules outside this sphere will have essentially zero probability of interaction with the molecule centered within this sphere, as the excited state will have emitted a photon by the time that an interaction may occur. This concept is important when defining the spatial resolution of a sensor based on collision quenching.

Temperature effect on fluorescence quenching.

For dynamic quenching, an increase in temperature implies that the quencher molecule has greater energy and thus has a greater probability of collisional encounter. This means that the quenching process is more efficient at higher temperatures. At higher temperatures, other effects also come into play, such as the effect of solvent quenching, for similar reasons. For static quenching, the reverse is true. Because static quenching occurs due to the restricted vibration of the excited fluorophor, as the temperature is increased, the molecule has more freedom and so the effect of static quenching is reduced. These effects can be seen on a Stern- Volmer plot as an increase in slope for dynamic quenching and a decrease in slope for static quenching. The closer the slope of the Stern-Volmer plot is to zero, the less the effect of the quencher.

F) Immobilisation techniques

Several different techniques for immobilisation of fluorescent dyes onto the surface of optical fibres have been reported in the literature. Such methods include immobilisation of the dye directly onto the glass surface of the fibre, use of a polymer matrix to support the dye or use of a bound ion exchange resin to retain the dye.

The first method of dye immobilising the dye directly onto the surface is by means of a coupling agent such as a silane derivitive which bridges the gap between the fluorescent dye molecule and the glass surface. When a fluorescent dye is directly bonded onto a glass surface, a number of problems occur. The first is that the intensity of fluorescence that will be launched into the fibre for sensing is extremely low due to the low concentration of dye on the surface. The fact that the dye molecules are bound presents another problem due to static quenching, where the energy of the excited state is transfered to the support surface, rather than resulting in the emission of a photon to be used for sensing. The final problem is that the chemistry of dye and surface preparation is quite complex in nature and is not always understood. Usually the surface is prepared by silanising the glass and ensuring that the sidechains of the silane groups are free to interact with the dye molecules.

A second process for dye immobilisation is the use of a polymer matrix that is used to support the dye without binding the molecules of the fluorophor. This allows the dye molecules to vibrate freely reducing the static quenching factor. One example is acryl amide polymer bound to the glass surface or more recently a Sol-gel (porous soluble silica polymer) on the glass surface giving a rigid matrix. In either case, it is usually necessary to encase the polymer and dye with a membrane which retains the sensing material while allowing the analyte through to the sensor. The main disadvantage of this method of immobilisation is that the number of active dye molecules which contribute to the observed signal is quite low unless very large quantities of dye are used. This requires sensitive detection equipment, often in the form of a photon counting system, to detect the fluorescence. The compromise is to use a larger sensing volume which decreases the spatial resolution.

A third possible option for dye immobilisation is to use an ion exchange resin bound to the glass surface of the fibre. Such a polymer will electrostatically retain the charged dye molecules and also concentrate these ions out of solution. An example of such a resin is Nafion®, developed by du Pont de Nemours Chemical Company Inc. Nafion will retain cations within the cavities of its structure and will concentrate the ions from a millimolar solution to approximately 0.1 - 0.5 molar

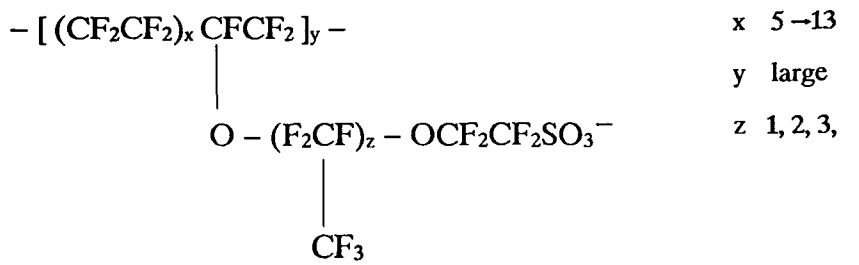

Figure I 11 Repeating unit of Nafion polymer

within the matrix. This concentrating effect has both an advantage and disadvantage The advantage comes from the relatively large quantities of dye which can be packed into a small volume, potentially reducing the size of the sensor The disadvantage in having such high concentrations is that self quenching processes come into effect, where the energy of excited molecules is passed to other dye molecules without emission of a photon

The chemistry and physics of Nafion ion exchange resin.

Nafion is a cation exchange resin composed of copolymers of tetrafluoroethylene and monomers such as perfluoro-3,6-dioxa-4- methyl-7-octensulphonic acid This gives the basic repetitive unit of the Nafion polymer with the structure shown in Figure I 11 The polymer is formed by the inter-linking of the long CF_2 based chains as the solution dries out for solution cast membranes. The polymer has two distinct regions associated with it (Yeo and Eisenberg, 1977) The two regions are the hydrophobic matrix and the hydrophilic cavities lined with the SO_3^- tails of the sulfonate chains These cavities are linked by tunnels of hydrophilic regons which results in a network effect (Lee *et al*, 1980) as shown in Figure I 12 The cavities behave like reverse micelles in a continuous

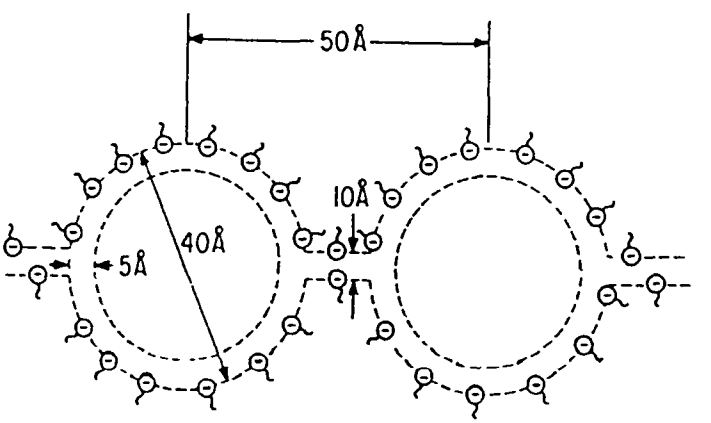

Figure I 12 Cavity Structure of Nafion
(Lee *et al*, 1980)

phase of the fluorocarbon backbone (Lee and Rogers, 1984). Gierke (1978) developed a thermodynamic model which showed that this network of linked cavities was possible and was also constantly evolving with old tunnels collapsing and new ones forming. The matrix of the polymer is held together by the crystallinity of the polymer fibres and/or by van der Waals forces (Yeo, 1980).

The thickness of the Nafion film seems quite important. Films produced by multiple layers of thin coatings have a lower stability than a single thick film (Krishnan *et al*, 1984) and tend to develop cracks. It was found that the Nafion films soaked in water are twice as thick as dry films (Rubinstein and Bard, 1981). This means that if the thin films are considered as separate entities, then the swelling process causes the outer most layers to be streched resulting in the cracking. The optimum configuration would seem to be a thin film that would minimise the stress on soaking.

Nafion was developed for use in electrochemical processes, like the recovery of precious metals from spent etch solutions (Grot, 1980). Another application is as a separator in electrolytic cells (Grot, 1978). The application of Nafion films on electrodes with large organic complexes incorporated into the film have become quite popular (Rubinstein and Bard, 1980; Martin *et al*, 1982; Elliot and Redpenning, 1984; Krishnan *et al*, 1984). In these cases, the electrodes are modified to enhance their sensitivity or selectivity or to make the electrodes photo-sensitive. One of the most popular complexes to be incorporated into the Nafion structure is $Ru(bpy)_3^{2+}$. This fluorescent dye is normally chosen because it is active in the visible and because it is easily reduced / oxidised either electrically or chemically (Rubinstein and Bard, 1981; Buttry and Anson, 1982). A typical procedure adopted for coating the electrodes with Nafion was described by Buttry and Anson (1982). The electrode was dipped into a ~2% Nafion solution in propanol/water (5:1) and allowed to dry for 5 minutes. The electrode was then left soaking in 1mM $Ru(bpy)_3^{2+}$ solution for 30 minutes and then washed with purified water. This left the electrode coated with a characteristic red layer of $Ru(bpy)_3^{2+}$. The absorption and emission spectra of $Ru(bpy)_3^{2+}$ in Nafion change slightly as compared to those in water. The absoption maxima are blue shifted by 3nm and the emission spectrum by 5nm (Lee and Meisel, 1980). The $Ru(bpy)_3^{2+}$ was found to be concentrated in the outer layers of the membrane directly after soaking (Binh Cirlot *et al*, 1989). The distribution was found to equalise when left soaking in water at approximately 40°C overnight. This made concentration effects less pronounced and improved contact of the $Ru(bpy)_3^{2+}$ with the electrodes. The tripley ionised excited state $Ru(bpy)_3^{3+}$ is retained very poorly by the Nafion (Wilkinson *et al*, 1983) and so its formation should be avoided since this would result in a net loss of dye within the polymer.

The bulk polymer is a very inert and stable entity Martin *et al* (1982) described a procedure for dissolving the bulk membrane which involved placing the polymer in an ethanol/water mixture (1 1) at 250°C under high pressure These membranes can then be recast by the evaporation of the solvent The solution cast films, however, were found not to be as stable as the original film. Elliot and Redpenning (1984) reported that recast films dissolved in non-aqueous solvents suitable for electrochemistry Szentirmay *et al* (1986) also described that such solution cast Nafion films were soluble in warm water and a variety of other polar organic solvents such as ethanol, propanol, CH_3CN and N,N-DMF Gebel *et al* (1987) suggested that the use of a high boiling point cosolvent in the formation of Nafion films from solution increased the likeness to the bulk membrane when annealed at high temperature (200°C) The annealing temperature of 200°C is an effective limit as the Nafion changes character at 250°C An annealing time of over 3 hours has little effect on the quality of the polymer They suggested that the annealing process in the presence of residual solvent increases the size of the lamellar crystalites, improving their internal order and causes a long range order to develop The annealing temperature depends on the solvent used in the Nafion solution (Moore and Martin, 1988) When N,N-dimethylformamide is used, a minimum temperature of 130°C is required while dimethylsulfoxide requires 160°C and ethylene glycol 190°C

The suitability of the Nafion as an immobilisation polymer in this work depends on the oxygen diffusion through the polymer Some reports suggest that the diffusion rate for oxygen in Nafion is lower than that in water (Lee and Meisel, 1985) Other reports, however, suggest that the diffusion rates in Nafion are superior to those in water (Gottesfeld *et al*, 1987, Lawson *et al*, 1988) Work performed here has found no evidence to suggest that oxygen diffusion is retarded in Nafion Anyhow, it would seem unlikely, as the oxygen could diffuse through either the water in the micelles (Figure I 12), or through the fluorocarbon matrix (which has a better diffusion rate than water)

When Nafion coated electrodes were left to dry in air and then returned to the storage solution, the signal from the electrode was found to decrease sharply or disappear altogether (Rubinstein and Bard, 1980) This suggests that the Nafion is not bound to the surface of the electrode, but only retained Much work was done in preparation of the glass surface (the elecrodes are usually glassy carbon in a silica glass insulator) to facilitate the binding of the Nafion (Szentirmay *et al*, 1986). The glass was treated with a silane derivitive with a positively charged side group which then interacted with the negative SO_3^- species of the Nafion to give a stable Nafion-glass bond This bonding of Nafion to glass was found to be best in a 1M HCl solution and worst in 1M NaOH where the Nafion was removed from the surface The binding of the film in water was found to

be very good and the major problem was found to be the dissolution of the Nafion film in the solvent The removal of the Nafion by the NaOH was caused by the hydrolysis of the bonds between the surface of the substrate and the coupling agent

Nafion has been used in an ion sensor based on the fluoresence quenching of Rhodamine 6G by various ions (Bright *et al*, 1988) The Rhodamine 6G was immobilised in Nafion on HF treated microscope cover slides The slide was illuminated by light from an arc lamp passed through an optical fibre and the fluorescence monitored with a detector mounted on the end of a second fibre

The Nafion ion exchange polymer is useful for immobilisation of cations on electrodes or other glassy substrates This holds true since the problems associated with solution cast membranes which are outlined previously are kept in mind when designing the system to take the Nafion

G) Fibres used in this work

During the development of this fibre optic oxygen sensor, two sizes of optical fibres were used with the 4-port coupler, namely 50μm and 100μm diameter core, each with 125μm outer diameter The couplers were supplied by Canstar and have model numbers PC-4-C-050 and PC-4-C-100 respectively A standard 50μm diameter core graded index phosphorous oxide doped silica glass fibre was used in the investigation of the etching process and the bonding of Nafion polymer to glass This fibre has cladding diameter of 125μm and was supplied by Optical Fibres, Deeside, Clwyd, Wales

All three fibres were found to etch in concentrated HF to give conical cavities, although the etch rates differed somewhat Procedures which worked for the single fibre were found to be transferable to the fibre in the coupler without loss in result This made the inexpensive Deeside fibre invaluable for testing and perfecting procedures during the development of the fibre optic oxygen sensor The etching of optical fibres is described in more detail m Chapter VI.

Chapter II: Background experimental work

A) Introduction

The experimental work carried out on the development of the fibre optic oxygen sensor is described in this chapter This chapter is composed of several sections that are concerned with specific individual aspects of the sensor Section B details with the selection of the optical configuration used in the sensor A number of configurations were tested and the 4-port coupler was found to be that best suited to the device The design of a filter unit for the detector is also described in this section, which was later used in preference to the monochromator

Section C contains a listing of the quenching properties of the different dyes tested for use in the oxygen sensor The choice of the Ruthenium based dyes was made based on their excitation and emission properties, since they are excited and emit in the visible with a large Stokes shift, although other dyes were investigated These are listed in Table II 1 and a more detailed account of the dyes used can be found in Chapter I D

Two main methods were investigated for immobilising the dye for use in the oxygen sensor Section D describes the methods for dye entrapment that were considered for use with the sensor The first method described using polyacryl amide was not used because the second using Nafion ion exchange resin was found to be more suited to the single fibre concept as the Nafion could be formed in thinner membranes and because it concentrated the dye out of solution, thus increasing the signal and time response of the probe

B) Optical configurations

II B(1) Single fibre systems

The 50μm core graded index multimode glass fibre was tested to see if it was possible to observe fluorescence through the fibre Using a high pressure mercury vapour discharge lamp with a 452nm interference filter, a drop of Rhodamine 6G in aqueous solution was illuminated while suspended in front of the optical fibre (§ Figure II 1) The fibre was then passed to a monochromator with a photomultiplier tube as detector The output from the PMT was observed on an oscilloscope By scanning the monochromator from 500-700nm, the fluorescence of the Rhodamine was clearly seen

The same apparatus was used for a drop of pyrene butyric acid, but no comparable signal was observed on the oscilloscope This is attributed to the very much greater quantum fluorescence efficiency of the Rhodamine dye (0 35 compared to 0 09 for PBA and 0 10 for Ru $(bpy)_3^{2+}$)

Light from the mercury vapour lamp was focussed into a cuvette containing Ru $(bpy)_3^{2+}$ An optical fibre was placed so that the illuminated region in the cuvette was under the cleaved face of the fibre (§ Figure II 2) The light collected by the fibre in this way was passed to a monochromator and therefore to a PMT The signal from the PMT was viewed on an oscilloscope and showed 100Hz mains modulation Fluorescence was detected for Ru $(bpy)_3^{2+}$ when a large diameter 200μm plastic clad silica (PCS) fibre was used

Several beam splitting devices were investigated to see if it was possible to pass both the excitation and emission light down the same fibre Two similar cases were investigated where a microscope covershde was coated with aluminium to make a front silvered mirror In the first instance, a transparent hole approximately 4mm in diameter was masked while making the mirror This device was used as in Figure II 3a A length of 50μm multimode glass fibre was used in this experiment The fibre was immersed in a Rhodamine 6G solution and the fluorescence signal was observed quite strongly The fluorescence was still visible when the fibre was removed from the bulk solution, as some dye had become adsorbed on the surface of the fibre The same set-up was used to try to observe fluorscence of Ru $(bpy)_3^{2+}$ in aqueous solution, but no significant signal was seen

The second beam splitting device consisted of a spot of aluminium on a microscope covershde The positions of the light source and monochromator were reversed as compared to the last configuration (§ Figure II 3b) No appreciable fluorescence signal was observed for either

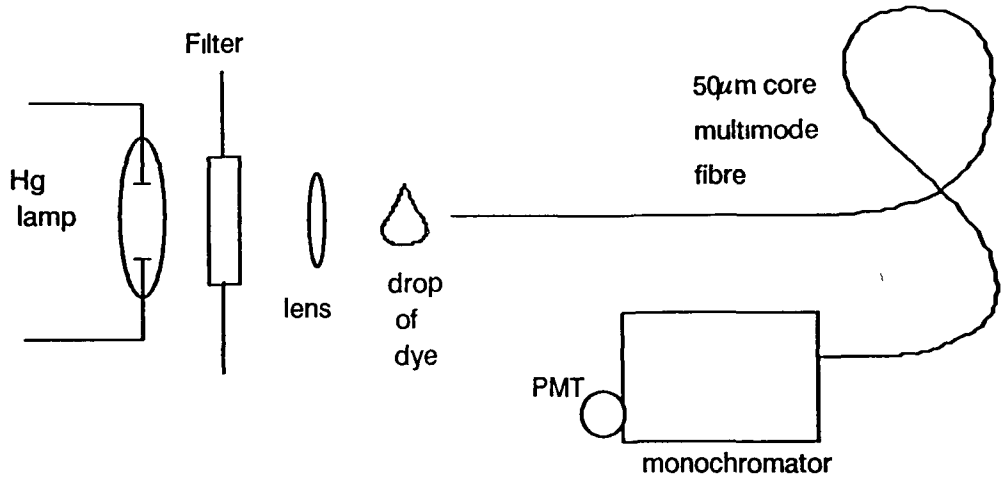

Figure II 1 Experimental configuration for dye drop held in front of a multimode fibre during launching

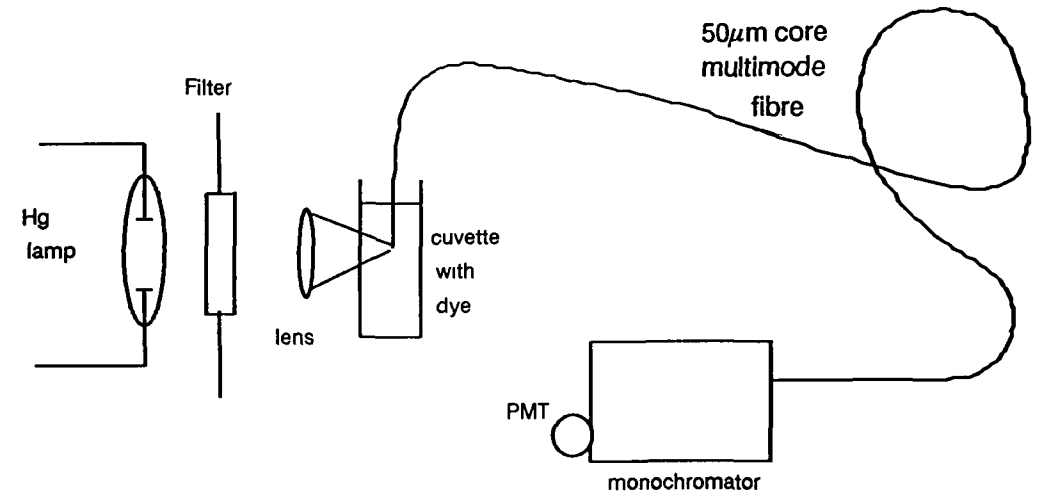

Figure II 2 Experimental configuration for side illuminated cuvette used with multimode fibre

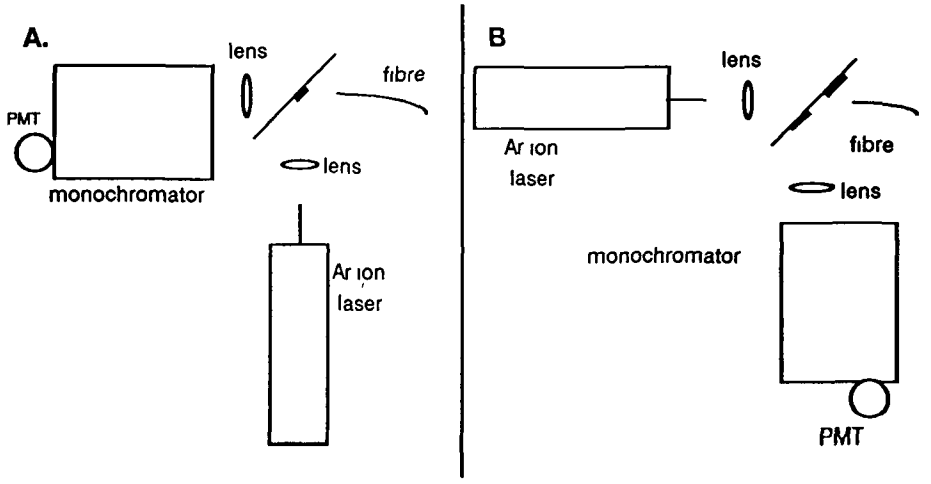

Figure II 3 Detector and laser configurations for two types of beam splitter tested

Rhodamine or Ru $(bpy)_3^{2+}$

An attempt was made to couple Ar ion laser light into the multimode glass fibre by focussing the laser beam onto the cleaved face of the fibre at an angle close to the critical angle (~20°) (§ Figure II 4) As a result, the return light signal can pass unhindered to the monochromator, without obstruction by the launching optics Neither Rhodamine or Ru $(bpy)_3^{2+}$ were observed using this setup

II B(2) Two fibre system

A two fibre system was set up by taping some 200μm core diameter PCS fibre beside some large diameter plastic fibre Chopped light was launched from an argon ion laser into the plastic fibre as m Figure II 5 The two fibre end was placed mto a solution of Ru $(bpy)_3^{2+}$ in water The signal from the 200μm PCS fibre was passed through a monochromator to a PMT The signal from the detector was viewed on an oscilloscope A response to different oxygen concentrations was observed by a change in signal on the scope When nitrogen was passed through the solution, the signal was found to increase, while a decrease was noted when air was passed

The same set of tests was repeated using the 50μm multimode glass fibre in place of the 200μm PCS fibre Both fluorescence and quenching were observed for this fibre configuration

II B(3) Fibre optic 4-port coupler system

To avoid the necessity for elaborate beam splitting devices in a single fibre system, a fibre optic cross coupler was used This device has two fibres that allow light to pass from one to the other due to the proximity of their respective cores at a certain point This is usually achieved by heating and twisting the fibres over a region where the cladding has either been removed, or reduced to a minimum In practice, it is possible to make devices with many ports, but in this instance a four port device, Canstar PC-4-C-050, was used The rated coupling loss between fibres is given as 4db in the forward direction and 40db in the reverse direction This gives an even spht between the two arms emerging from either side of the device irrespective of which arm carries the source light

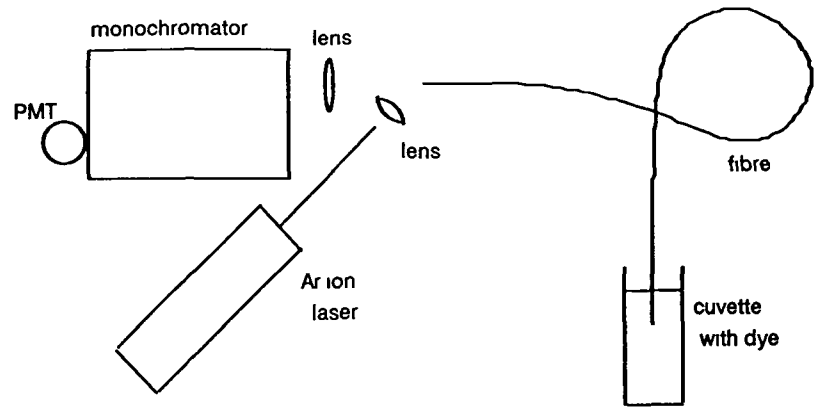

Figure II 4 Acute angle launching configuration

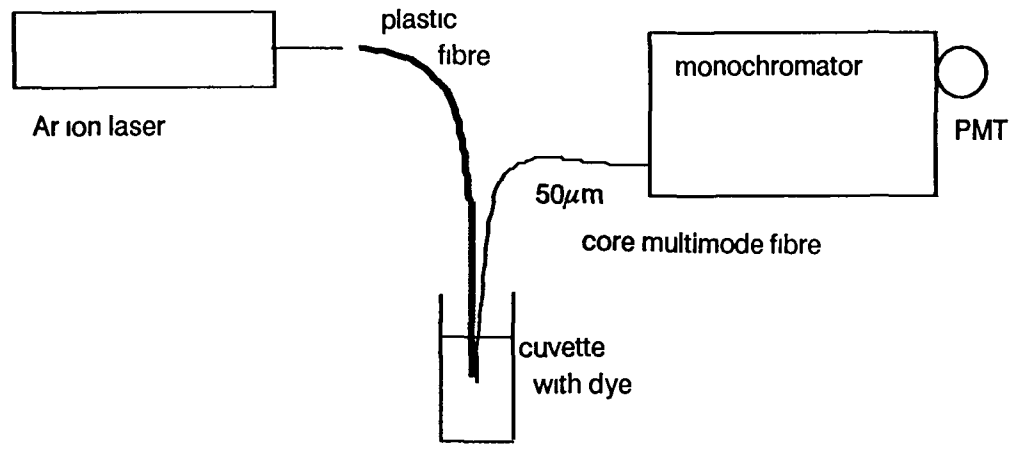

Figure II 5 Two fibre configuration

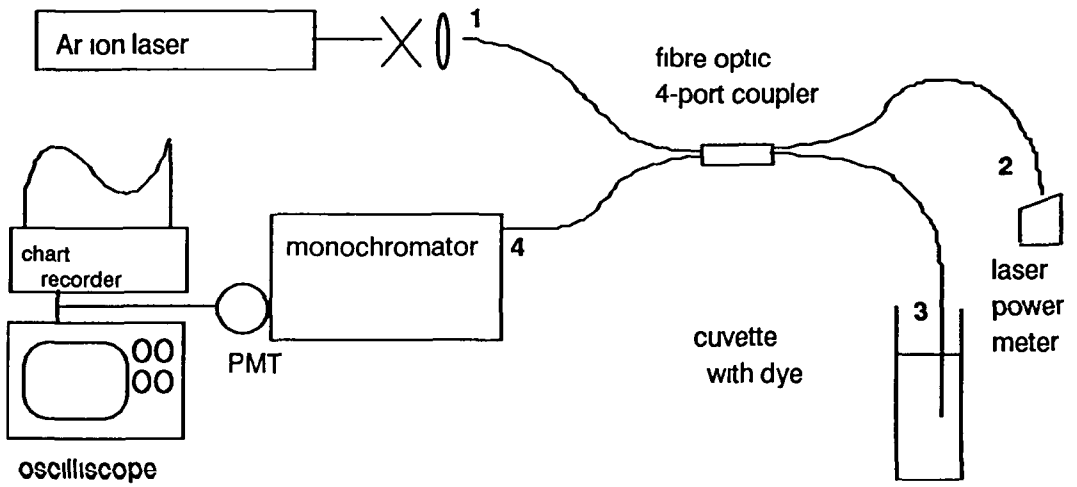

Figure II 6 Fibre optic cross coupler configuration

The four connections to the coupler were used as follows (§ Figure II.6):

- fibre #1: to carry the excitation light from the Ar ion laser.
- fibre #2: as a reference to monitor the power of the excitation light in the probe.
- fibre #3: to excite the fluorescent dye and to collect the fluorescent signal from the probe.
- fibre #4: to pass the fluorescence on to the detector.

The probe arm was immersed in a solution of Ru $(bpy)_3^{2+}$ and the fluorescence characteristic of Ru $(bpy)_3^{2+}$ was observed. The effect of different oxygen concentrations was investigated by bubbling either O_2 (100%), air (~21%) or N_2/Ar (0%) through the dye solution. Quenching was observed qualitatively as a decrease in intensity for increase in dissolved oxygen concentration on an oscilloscope connected to the PMT output.

It was attempted to try to observe fluorescence from Ru $(bpy)_3^{2+}$ immobilised on the end of a coupler fibre. It was found that HF etched a conical cavity in the end of the fibre (§ Chapter VI: Etching of optical fibres). The fibre was then washed in de-ionised water and left to dry. The end of the fibre was dip coated with 5% Nafion ion exchange resin powder dissolved in alcohol/water solution . The fibre was left to dry for 5 minutes and the application process was repeated for a total of six coatings. The fibre was left to dry for 30 minutes and then soaked in Ru $(bpy)_3^{2+}$ for 30 minutes. The apparatus was then tested as in Figure II.6. The fluorescence from the tip of the fibre was observed on an oscilloscope. The intensity of fluorescence was seen to drop in the presence of oxygen, but recovery in nitrogen was not complete. This lack of recovery was probably due to a combination of photo-induced decay and loss of polymer of the endface of the fibre. These will be discussed later in greater detail.

II:B(4) Filter box

It was decided to replace the monochromator by a filter based detector for several reasons. Firstly, the use of a broadband filter would pass a greater portion of the fluorescence from the fibre to the photomultiplier as compared to the narrow pass band of the monochromator. Secondly, the 488nm Ar ion excitation light was found to be scattered and diffracted within the monochromator, possibly due to the small dimensions of the optical fibres used with the coupler.

The filter box (§ Figure II.7) was built using a lens and filter holder. The lens (focal length = 5cm) was set so that the light from the fibre was focussed on the photo cathode of the PMT. A filter holder was placed between the lens and PMT, while a second filter holder for 26mm diameter filters was placed between the fibre and the lens. A number of different filters were used with this box. Two glass filters passing above 580nm (Illford 808 "Mercury Yellow" and Ealing

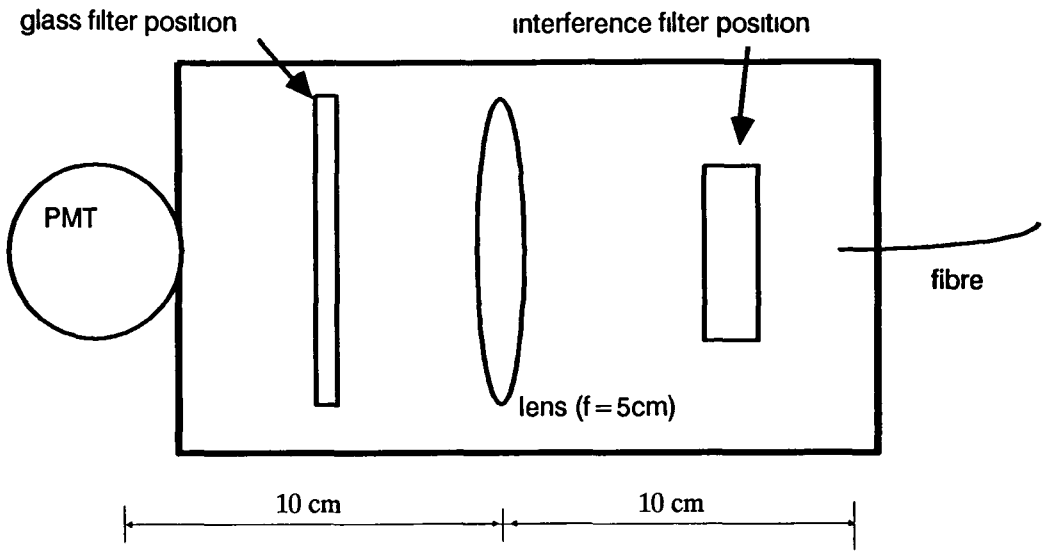

Figure II 7 Filter box layout
The position of the glass filter was chosen to optimise the beam filtering, as well as the filtering of the scattered light The interference filter was placed on the other side of the unit to accomodate a filter switching device

26-4366) were used for work with the Ruthenium compounds It was found that the filter had a fluorescence emission peaking at 580nm when excited by 488nm Ar ion laser light These filters were later replaced by a long pass interference filter (Ealing 35-5586) passing above 560nm A second interference filter was used for work with Os $(bpy)_3^{2+}$ (Ealing 35-5669) passing above 640nm

C) Oxygen quenching of fluorescent dyes

Several fluorescent dyes were characterised with respect to their oxygen quenching properties Measurements were made on a Perkin - Elmer L-5 luminescence spectrometer The dyes were tested in aqueous solution m a cuvette placed in the spectrometer sample chamber Gas was passed through the cuvette containing the fluorescent dyes in solution using microtubing The tubing was held in place using a cut cork with holes for the tubing and for a gas outlet The response to varying oxygen partial pressure was checked at the fluorescence maximum by setting the monochromator to the desired excitation and emission wavelengths and monitoring the fluorescent intensity on the chart recorder Three levels of dissolved oxygen partial pressure were available, Oxygen (1 0 bar), atmospheric air (0 21 bar) and Nitrogen, or Argon gas (0 00 bar) The results from different dyes tested are given in Table II 1

Table II 1 Summary of dyes tested

Name of dye	Excitation (nm)	Emission (nm)	Quenching observed	Quantum efficiency
Rhodamine 6G	520	535-580	No	0.35
Ru $(bpy)_3^{2+}$	450	610	Yes (30% in air)	0.10
Pyrene Butyrate	350	375, 395	Yes (25% in air)	0.09
Fluorol green gold	263	483	Yes (40% in air)	
Os $(bpy)_3^{2+}$	450	715	No	0.01
Ru $(phen)_3^{2+}$	450	610	Yes (35% in air)	0.08

D) Polymer and dye immobilisation

Two methods of immobilising the fluorescent dye Ru $(bpy)_3^{2+}$ on an optical fibre for use with the fibre optic oxygen sensor were investigated. The first method involved the incorporation of the dye into a polyacrylamide matrix which would be held on the end of the fibre. The second was the use of an ion exchange resin (Nafion), which was finally used due to its improved dye retention and concentrating properties, also being less bulky then the former. This former method was not practical for this oxygen sensor, but is included for completeness. A procedure is also included for sealing the oxygen probe with an oxygen permeable polystyrene coating so that the contents within the polymer remain constant.

II:D(1) Acryl amide polymerisation

Acryl amide crystals (0·5g) were dissolved in 10ml methanol and ~5mg Ru $(bpy)_3^{2+}$ crystals were added. This solution was illuminated using a focussed beam from a Deuterium lamp. This light source emits strongly in the UV part of the spectrum. Polymerisation was found to proceed along the walls of the plastic container where the solution was illuminated after approximately 15 minutes.

A cleaved optical fibre was held in the region where polymerisation occurred as shown in Figure II.8 and a spot of polyacrylamide was formed around the cleaved end of the fibre. The polymer had formed around the fibre after approximately 30 minutes and the fibre was withdrawn from the solution with the curing process completed in the direct light beam. This fibre was then tested by lateral illumination by the Argon ion laser (488nm) and a signal was observed. However, once the probe was immersed in water, the polymer was lost from the end of the fibre. The reason for this loss of polymer was that the polyacrylamide became swollen with water and therefore forced itself free of the fibre. An attempt to retain the polymer was made by preparing the fibre with surface silane groups that would be free to bind with the polymer.

The fibre was prepared by silanisation of the cleaved glass surface as follows. The fibre end was placed into a 10% solution of 3-aminopropyltriethylethoxy silane (APTS) (Aldrich 11,339-5) in a water bath at boiling point. The fibre remained in the silane solution for 45 minutes and was then immersed in acryloyl chloride (Aldrich A2,410-9) for 10 minutes, to activate the silylated surface. The fibre was rapidly transfered to the acryl aminde solution and the polymerisation process attempted. Formation of a stable polymer by this method on the end of an optical fibre

was not successful The acryl amide polymer remained only on the fibre end until it was immersed in water for probably the same reasons as stated above

Response of such a probe to different gaseous oxygen concentrations was noted, although the signal became very unstable as the polymer dried out

According to Iwai *et al* (1985), Ru $(bpy)_3^{2+}$ can be used to induce photopolymerisation of acryl amide It is based on the reduction of the photo-excited state of the fluorescent molecule to initiate the production of free radicals, which then polymerise A solution of Ru $(bpy)_3^{2+}$ in dimethyl formamide with acryl amide and triethylene amide was prepared The Ru $(bpy)_3^{2+}$ was excited using an Ar ion laser Polymerisation was observed when the solution was placed in the main 2 8W beam This polymerisation was not observed, however, when the excitation light was passed through a large diameter optical fibre at much reduced power levels for longer times This suggests that the observed polymerisation is due to heating of the monomer solution by the laser light, rather than a photo - chemical process

II D(2) Nafion ion exchange resin

Nafion is a registered trade mark of du Pont de Numours chemical company and the samples used were purchased from Aldrich Chemicals (27,470-4) The polymer comes as a 5% solution in a mixture of lower aliphatic alcohols and water Polymer formation occurs as the solvents evaporate

Initial tests with the Nafion polymer were carried out on narrow strips of rolled glass (microscope slides) The glass slide was dipped into the Nafion soluton and allowed to dry The slide was then immersed in an aqueous solution of Ru $(bpy)_3^{2+}$ for 5 minutes The polymer on the slide had

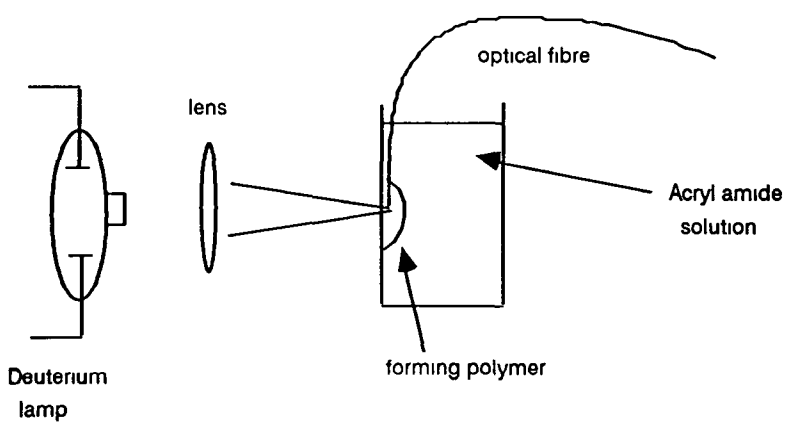

Figure II 8 UV curing of acryl amide

noticeably absorbed the dye, but had also come away from the surface of the glass slide. At the cleaved end of the slide, the polymer was retained and quite difficult to remove. This was attributed to the roughness of the surface rather than the polymer bonding to the freshly cleaved surface since the Nafion did not bind to a freshly cleaved fibre.

An etched Deeside 50μm multimode graded index glass fibre was dipped into a solution of Nafion, and allowed to dry. A total of six layers of Nafion were added in this way, allowing 5 minutes drying time between coats. The fibre was then soaked in Ru $(bpy)_3^{2+}$ solution for 30 minutes. The fibre was viewed under a microscope and the polymer had visibly been retained within the etched cavity of the optical fibre. Further tests were carried out to improve the adhesion of the polymer to the surface of the fibre, which involved the washing of the fibre in either HNO_3 or NaOH after etching in HF and then coating with the Nafion. The NaOH treated fibre was found to have a more strongly bound layer of Nafion along the fibre than the other combination of treatments.

The fibre at one port of the Canstar 4-port coupler was prepared by etching in HF for 5 minutes. The etched end was then washed sucessively in HNO_3, deionised water, and methanol for 10 minutes each. The fibre was then dip coated with Nafion and left to dry. Finally the probe was soaked in Ru $(bpy)_3^{2+}$ solution for 30 minutes. On viewing the end of the fibre under the microscope, the Ru $(bpy)_3^{2+}$ was clearly seen to be retained within the cavity. The polymer seemed stable in water over prolonged periods of time, but reimmersing in water after allowing the probe to dry out caused the Nafion to became detached from the cavity surface.

It was now necessary to ensure the bonding of the Nafion polymer to the surface of the optical fibre for stability reasons. The silanising of the fibre surface to allow bonding with the Nafion was explored based on a report by Szentirmay *et al* (1986). The choice of 3-aminopropyltriethoxy silane was made because of the intrinsic positive charge associated with the amino group, which allows easy ionic bonding to the SO_3^- chains in the Nafion (§ Figure I.11). To stabilise the structure of the Nafion itself, it was decided to investigate the effect of baking the dried Nafion in a furnace set to 200°C over a period of 2 hours. Various pre-silanisation, pre-coating, pre-curing processes were investigated, and the results are tabulated in Table II.2 and supplementary tests in Tables II.3 and II.4. A batch of Nafion solution based on dimethyl formamide (DMF) as solvent was prepared by adding 2 ml of DMF to 2 ml of original Nafion solution and gently boiling off the lower boiling point solvents (ie. alcohols and water) at 70°C (based on a report by Szentirmay *et al*, 1986). The resultant solution was topped up to make 2 ml and after a few such cycles was then considered water/alcohol free. This solution should then yield a more stable polymer that is

closer in character to the original sheet polymer The improved stability is due to curing the Nafion at higher temperatures, which improves long range order within the polymer structure

The treatment that yielded the most securely bound polymer with the required dye retention capabilities was as follows The fibre was cleaved, and etched in HF for 5 minutes and the fibre end was then washed in deionised water for 5 minutes The fibre end was inserted into a reflux apparatus containing deionised water and set to boiling for 24 hours This process thoroughly washed the surface of the fibre and ensured hydrolysis of the glass surface The water was then removed, and replaced with a 10% aqueous APTS solution This was allowed to reflux for a further 2 hours that resulted in a silanised surface The fibre was then removed and placed in a preset furnace at 200°C for 2 hours to activate the surface The fibre was then threaded through the drip coating apparatus (Figure II 9) so that the fibre end was well within the hot region of the furnace The syringe was filled with approximately 1 ml of Nafion solution in DMF that was allowed to drip slowly down the fibre As the drops left on the end of the fibre evaporated, a continuous layer of Nafion was built up Using a 5% Nafion/DMF solution, a very thick membrane of Nafion was left on the end of the fibre, while using a 1% solution, the polymer was of a more managable size The fibre was left for 2 hours in the furnace while being coated and to cure the Nafion The time of 2 hours in the furnace was found to be the minimum required to achieve a stable polymer.

When the fibre was removed from the furnace, it was ready for soaking in the sensing dye and the Nafion remained bound to the fibre during and after soaking

A method for fibre preparation was developed based on the above procedure which allowed fibres to be prepared in a much shorter time A cleaved fibre was etched for 5 minutes in 48% HF and

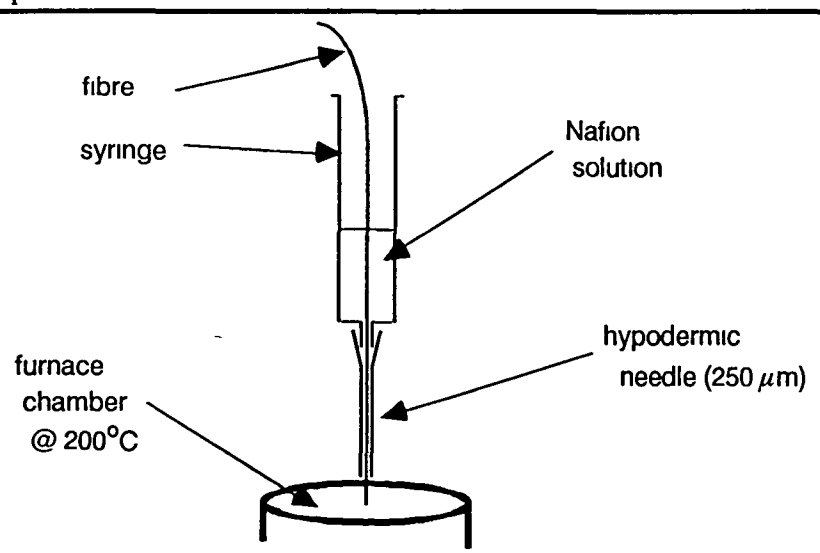

Figure II 9 Fibre coating apparatus

Table II.2: Fibre silanisation tests (1)

Etch in HF 5 minutes	Etch in HF 30 seconds	Etch in HF 10 seconds	Silanised in 3-APTS 2 hours	Furnace @ 2000C 2 hours	No furnace	Coated with 5% EtOH/H2O Nafion solution	Coated with 5% DMF Nafion solution	Furnace @ 2000C 2 hours	No furnace	Soak in Ru (bpy)32+ 5 minutes	
* *			*	*		*		*		*	good binding
*			*	*			*	*		*	polymer visible, no dye
	*		*	*			*	*		*	poor binding
	*		*	*		*		*		*	poor binding
	*		*	*		*			*	*	fragmented binding
		*	*	*		*		*		*	nothing
		*	*	*		*			*	*	no binding
* *			*		*		*	*		*	poor binding
* *			*		*	*		*		*	fragmented binding
*			*	*		*			*	*	poor binding on end
	*		*		*	*		*		*	nothing

Table II.3: Fibre silanisation tests (2)

Etch in HF 5 minutes	wash in DI water 5 minutes	soak in conc. NaOH 5 minutes	soak in mild NaOH 5 minutes	soak in dilute NaOH 5 minutes	wash in DI water 5 minutes	rinse in ethanol	rinse on acetone	rinse in methanol	no rinse	dry in air 15 minutes	silanise in APTS solution (as before)	
*	*	*			*	*				*	*	poor
*	*		*		*	*				*	*	poor
*	*			*	*	*				*	*	nothing
*	*	*			*		*			*	*	loose polymer
*	*	*			*			*		*	*	polymer in cavity
*	*	*			*				*	*	*	nothing
*	*			*	*	*				*	*	nothing
*	*			*	*			*		*	*	good
*	*			*	*				*	*	*	good
*	*			*	*	*				*	*	nothing

Table II.4: Fibre silanisation tests (3)

Cleave	Etch in HF 5 minutes	Wash in conc. NaOH 5 minutes	Wash in DI water 5 minutes	Wash in methanol 5 minutes	silanise in APTS / toluene soln 2 hours @ 75oC	Dip coat Nafion / alcohol solution	Funace @ 2000C 2 hours	Soak in Ru (bpy)32+	
*	*	*	*	*	*	*	*	*	good
*	*		*	*	*	*	*	*	excelent
*		*	*	*	*	*	*	*	poor
*			*	*	*	*	*	*	nothing

washed in ethanol The fibre was then allowed to dry in air and dipped into concentrated APTS solution (as supplied by Aldrich) The fibre was dried using a heat-gun operating at ~200°C The fibre was then coated with Nafion which was allowed to dry in air for 30 minutes before soaking with Ru $(bpy)_3^{2+}$ or Ru $(phen)_3^{2+}$ The Nafion polymer was found to be securely bound to the fibre surface This process can be completed within 45 minutes as opposed to 2 days for the full procedure and as a result was used for most of the work concerning Ru $(phen)_3^{2+}$.

II D(3) Polystyrene coating of the probe

The probe, as prepared by the method described above, can then be coated with polystyrene to provide an oxygen permeable membrane over the sensing tip This ensures that the concentration of dye within the probe stays constant, as no leaching will occur, and also that the concentration of water within the probe remains constant The response time of the probe is affected as the oxygen must now diffuse through a membrane before it can be measured

)

The probe tip was dipped into a dilute polystyrene / toluene solution to apply to O_2 permeable membrane As only a very thin membrane was required over the sensor, the concentration of the polystyrene in the toluene was kept to a minimum The quantity used was approximately 0.5 g polystyrene dissolved in 5 ml toluene The fibre is then dipped into the polystyrene solution and the toluene is allowed to evaporate It is important that the fibre be turned vertical, i e upside down, after dipping with the tip pointing upwards, otherwise, a drop of the polystyrene solution is held on the end of the fibre, leading to an unnecessarily thick membrane over the probe tip and therefore a longer response time

There is very little extra stability gained by such a coating, which implies that there is little or no leaching of dye from the Nafion resin The advantage of such a membrane is that the contents of the probe tip remain isolated from the external environment since the polystyrene will only pass gases

Chapter III: $Ru(bpy)_3^{2+}$ probe characterisation

A) Introduction

This chapter describes the experimental work carried out on the characterisation of the $Ru(bpy)_3^{2+}$ based oxygen sensor This work was used to qualitatively assess the properties of the oxygen probe using this dye Observations were made on the following Emission characteristics, signal decay, response to dissolved oxygen, temperature dependence and the rate of dye uptake These properties were not fully quantified as the dye $Ru(bpy)_3^{2+}$ was found to be less suited for use in an oxygen sensor when compared to the $Ru(phen)_3^{2+}$

However, this chapter is included in this thesis because of the importance of the dye $Ru(bpy)_3^{2+}$ in research and development of fibre optic oxygen sensors Such sensors (eg Lippitsch *et al*, 1988) use this dye to determine dissolved oxygen concentrations using similar techniques as those described here The results in this section may help in the understanding of the processes which influence the photochemical properties of the $Ru(bpy)_3^{2+}$ dye, especially when this dye is immobilised in the Nafion ion exchange membrane

B) Ru $(bpy)_3^{2+}$ probe· Experimental work

Probe fabrication process

- Cleave fibre
- Etch in 48% HF for 5 minutes
- Wash in ethanol for 5 minutes
- Coat with 5% Nafion solution
- Dry m air for 5 minutes
- Coat again with 5% Nafion and dry in air for 30 minutes
- Soak in Ru $(bpy)_3^{2+}$ for 10 minutes
- Store m de-ionised water

The wash after the HF etch may have been preceeded by washing m de-ionised water before the ethanol The Nafion used was purchased from Aldrich Chemicals (27,470-4), as was the Ru $(bpy)_3^{2+}$ (22,475-8)

III B(1) Emission characteristics

The emission spectrum recorded from the Ru $(bpy)_3^{2+}$ based oxygen sensor is the same as that for Ru $(bpy)_3^{2+}$ in aqueous solution (Figure III 1) The peak of maximum fluorescence in Nafion was found to be at 605nm in water The emission spectrum was analysed using an Applied Photophysics f/3 4 monochromator and a Hamamatsu R928 photomultiplier tube (§ Appendix A) A glass filter passing above 580nm (Illford 808 "Mercury Yellow", or Ealing 26-4366) was placed at the exit slit of the monochromator to remove scattering from the argon ion 488nm excitation beam The spectrum was recorded on a BBC micro using an A/D converter Typical scan ranges are from 500nm to 800nm The response of the detector system was found to be linear in the region of interest between 550-750nm

III B(2) Signal decay

The signal received from the PM tube while observing at 610nm using the monochromator was momtored on a chart recorder In later experiments, the monochromator was replaced with a filter and lens system. This allows much lower light levels to be achieved and therefore reduces the effects of intensity related signal decay

With high excitation powers, of the order of 200μW down the fibre, the fluorescence signal was

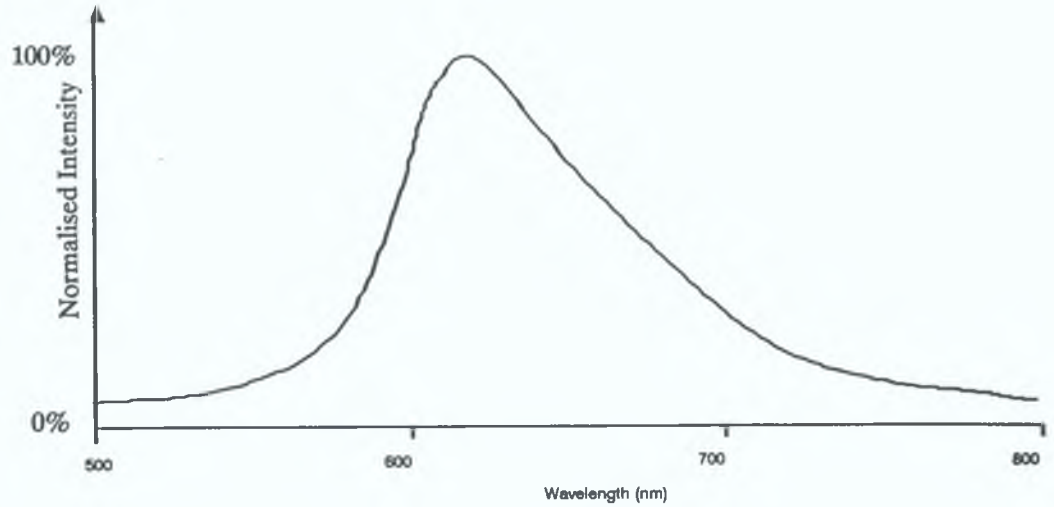

Figure III.1: Ru $(bpy)_3^{2+}$ probe:
Emission spectrum (λ_{ex} = 488nm).

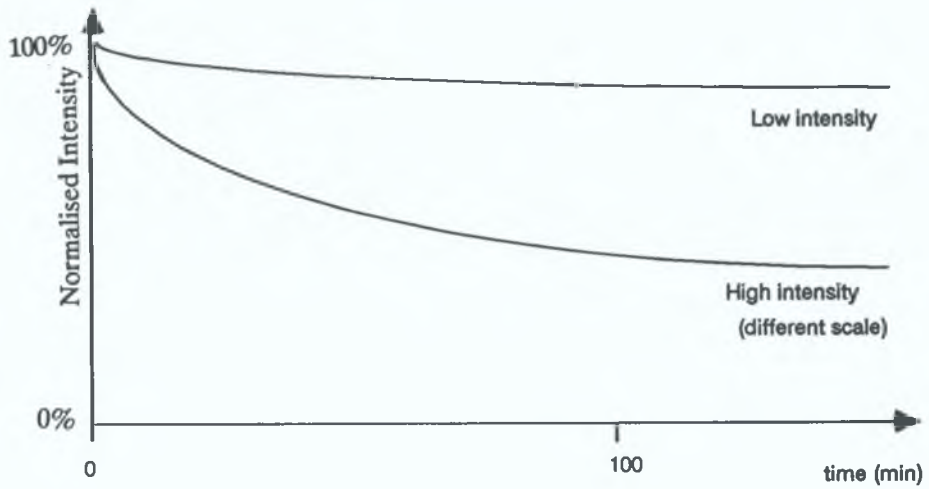

Figure III.2: Ru $(bpy)_3^{2+}$ probe:
Intensity dependent signal decay.

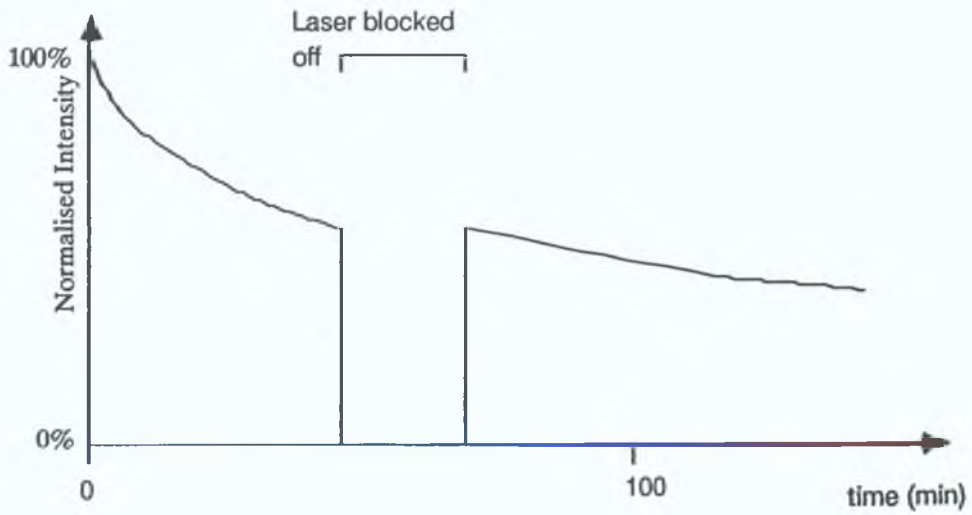

Figure III.3: Ru $(bpy)_3^{2+}$ probe:
Illumination dependence of photo-induced decay.

seen to decay rapidly (§ Figure III 2) The constant for this decay was calculated as the percentage decay per μW excitation power per minute exposure (§ Table III 1) An excitation power of 0 05μW is low enough that intensity effects are no longer significant and so gives an operating power level at which measurements of dissolved oxygen concentrations can be made

The decay of the signal under high intensity was shown to be illumination dependent This was verified by blocking the excitation light for a short period during the decay process The intensity of the fluorescence signal did not fall while the laser was blocked off (§ Figure III 3)

A second factor concerning the stability of the probe is the effect of temperature on the intensity of fluorescence This is discussed in a later section (§ Chapter III B(5) Temperature dependence / stability)

III B(3) Oxygen quenching of Ru $(bpy)_3^{2+}$ probe

Oxygen quenching measurements were carried out with the fibre probe immersed in a cuvette containing de-ionised water A small diameter plastic tubing was placed into the cuvette This tubing was connected to a gas mixing rig as shown in Figure III 4

The gas flow was controlled to a total of 0 75 litres per minute flow The dissolved oxygen partial pressures were set to 0 0, 0 2, 0 4, 0 6, 0 8, 1 0 bar, the balance of gas made up with nitrogen The gas from the mixing rig was allowed to flow freely for 10 minutes to fully purge the mixing cell The micro-tubing was then connected and inserted into the cuvette The gas was allowed to flow for a minimum of 5 minutes to set the new level of dissolved oxygen in the cuvette The detector configuration consisted of the interference filter and PMT Results were taken using a BBC micro computer and / or a chart recorder and such a scan is shown in Figure III 5

Table III 1 Ru $(bpy)_3^{2+}$ probe
Intensity decay data (extracted from a set of non-specific test scans over a period of time)

Power (μW)	Exposure (min)	%age change	Decay constant (%/μW/min)
0 3	45	8 1	0 6
0 95	15	30 2	2 19
1 7	20	74 7	2 2
4 6	10	57 7	1 25
5 0	10	34 7	0.69

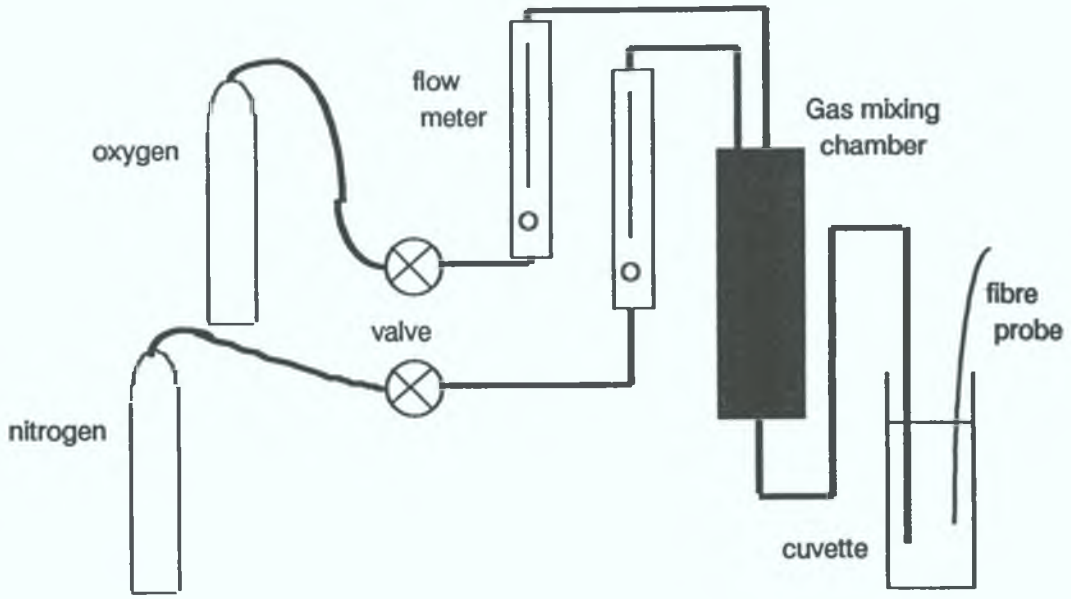

Figure III.4: Gas mixing rig.

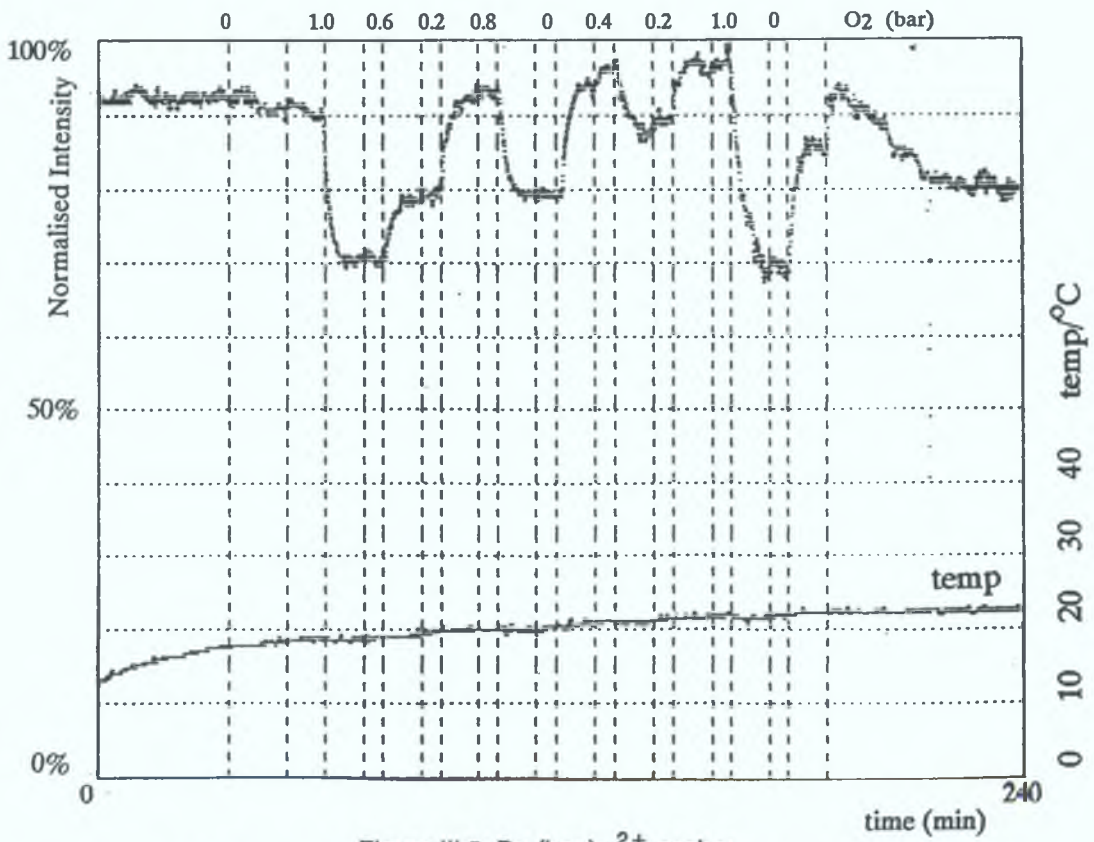

Figure III.5: Ru $(bpy)_3^{2+}$ probe:
Intensity monitored at various dissolved oxygen concentrations.

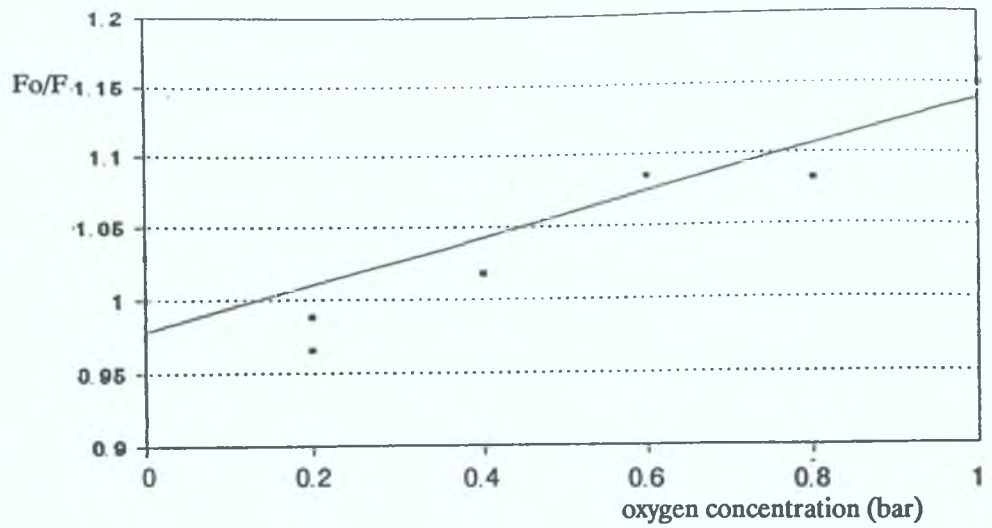

Figure III.6: Ru $(bpy)_3^{2+}$ probe:
Stern - Volmer plot using data from Figure III.5

III:B(4) Stern - Volmer plots for Ru $(bpy)_3^{2+}$ probe

The data obtained from the different levels of dissolved oxygen was plotted as a Stern - Volmer plot (§ Chapter 1: E: Quenching of fluorescence). This plot is an indication of how well the Stern - Volmer relation applies to this probe. This plot can be used to read dissolved oxygen concentrations given the maximum intensity (in the absence of oxygen) and the intensity at the oxygen concentration in question. The plot shown in Figure III.6 gives the intensity ratio as a function of the dissolved oxygen concentration. This concentration is given as a percentage of the dissolved gas as determined from the ratio of oxygen to nitrogen before passing to the water. To convert dissolved partial pressure to concentration in ppm, the conversion table given in Figure III.7 is used. The data for this conversion was obtained using a Hanna Instruments HI8543 Oxymeter portable dissolved oxygen meter.

II:B(5) Temperature dependence

The Ru $(bpy)_3^{2+}$ based sensor was found to be sensitive to changes in temperature. This can be attributed to the increase in the number of excited state relaxation pathways resulting in non-radiative decay. There is also an increase in the velocity of the solvent molecules that contribute significantly to the total quenching of the excited state. The solubility and diffusion of oxygen in water are temperature dependent. The decrease in the viscosity of water with temperature increases the proportion of solvent based quenching, thus also reducing the effective excited state lifetime of the fluorescent dye. The temperature dependence of the Ru $(bpy)_3^{2+}$ probe was not quantified since the other fluorescent dye Ru $(phen)_3^{2+}$ was found to be more suited for use in a fluorescence quenching based oxygen sensor due to its longer excited state lifetime (§ Chapter IV: Ru $(phen)_3^{2+}$ probe characterisation)

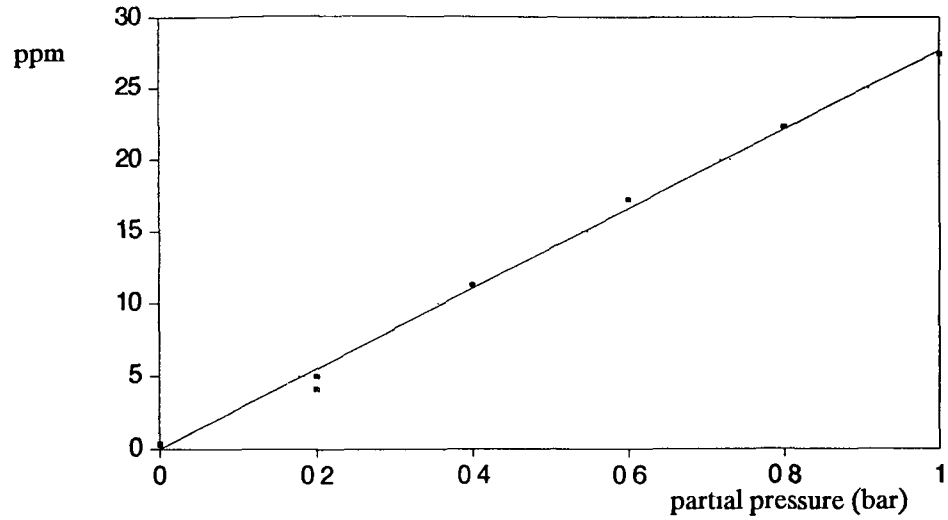

Figure III 7 Dissolved O_2 partial pressure to ppm conversion graph (@ 22°C) This data was used primarily to calibrate the commercial HI 8543 oxygen probe

III B(6) Dye uptake

In order to predict the intensity of fluorescence of a probe with respect to the time spent soaking in dye, it was necessary to monitor the intensity as a function of the time that the probe tip spent soaking in the stock dye solution The reasoning behind this is that if the concentrations of fluorescent dye within the Nafion polymer can be controlled, then it should be possible to place two dyes in the polymer, using specific dye uptake curves for each dye, so that similar intensities would be obtained This would then form the basis of the dual dye referencing of the sensor (§ Chapter V B Referencing the oxygen sensor) A second important reason for controlling the quantity of fluorescent dye within the Nafion matrix is to minimise the effects of concentration quenching The effects of concentration quenching due to the high density of dye obtained within the Nafion polymer are a significant factor in the fluorescence efficiency of the sensor probe Once the rate of dye uptake is known, then the time spent soaking in the stock dye solution can be optimised for maximum signal at minimum absorbed dye

The rate of Ru $(bpy)_3^{2+}$ uptake by the Nafion polymer was monitored using two methods In the first, the fibre is inserted into the stock solution of Ru $(bpy)_3^{2+}$ for short periods of time and then removed to a cuvette containing de-ionised water for intensity measurements The laser illumination remained off during the soaking periods In the second method, the intensity of fluorescence is continuously monitored as a function of the time that a freshly made probe spends in the stock solution The first method showed a peak in the soak time curve at 25 - 30 minutes (Figure III.8). This corresponds to a point where the constructive effect of high dye concentration was thought to be countered by the effect of self quenching

The first set of data was taken at an earlier part of the work for this project The experimental system consisted of the set-up described using a monochromator (§ Chapter II B(3)) The data was taken as follows The fluorescence spectrum was recorded and the intensity of fluorescence gauged from the height of the emission peak at 610nm The probe tip was left to soak in the stock solution of Ru $(bpy)_3^{2+}$ for periods of 10 minutes in the dark (no excitation) between spectral scans The results from this work is shown in Figure III 10 This data was found to be reproducible at the time between different stock solution concentrations and also for the dye Os $(bpy)_3^{2+}$. Each yielded approximately the same position of the optimum soak time at 25 - 30 minutes.

When an attempt was made to reproduce this data at a later stage (one year later), a different characteristic soak curve was obtained The method for monitoring the second set of data was the same in principle, but used the filter based configuration instead At first, a continuous measurement of the fluorescence intensity as the dye was taken in was made and is shown in Figure III 9 This curve is different to that obtained earlier and in an attempt to repeat earlier results, the same conditions were applied to the soaking probe The same Nafion polymer was used, the same fluorescent dye Ru $(bpy)_3^{2+}$ (as well as Ru $(phen)_3^{2+}$, Os $(bpy)_3^{2+}$); and the period of darkness during soaking yielded a different type of curve, which was fully reproducible at this stage The reason for this change is not understood, although the process of dye uptake is sensitive to subtle changes in the solutions used For example, if there was a presence of small cations in the stock solution of dye, they too would be taken up by the Nafion and so would initially reduce the rate of Ru $(bpy)_3^{2+}$ uptake in the Nafion due to their greater mobility If the Ru $(bpy)_3^{2+}$ has a greater affinity for the Nafion resin than these cations, then as time passes, the cations will be forced out of the polymer and the concentration of Ru $(bpy)_3^{2+}$ within the resin increases It is not thought that such a process was responsible as the same dye solution was used

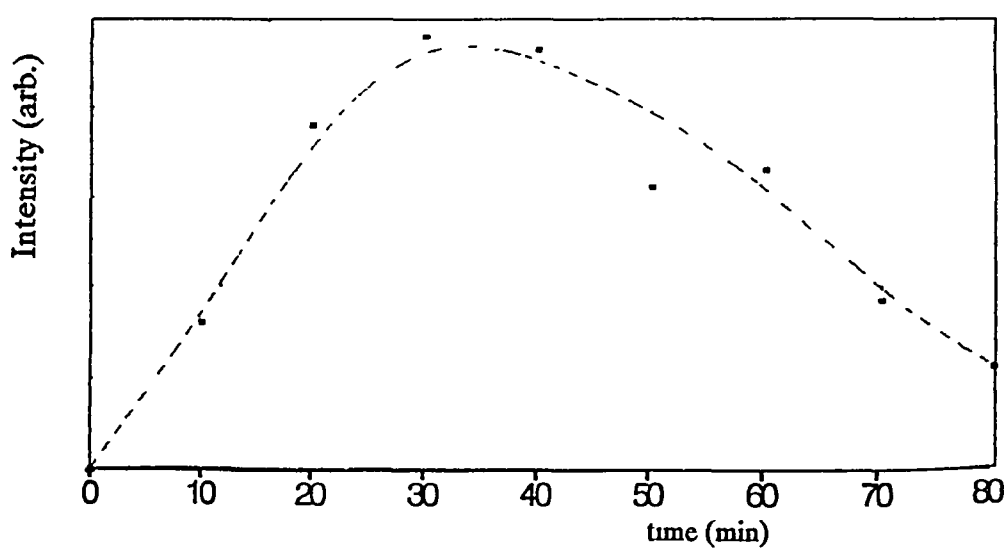

Figure III 8 Ru $(bpy)_3^{2+}$ probe
Dye uptake by probe tip early work

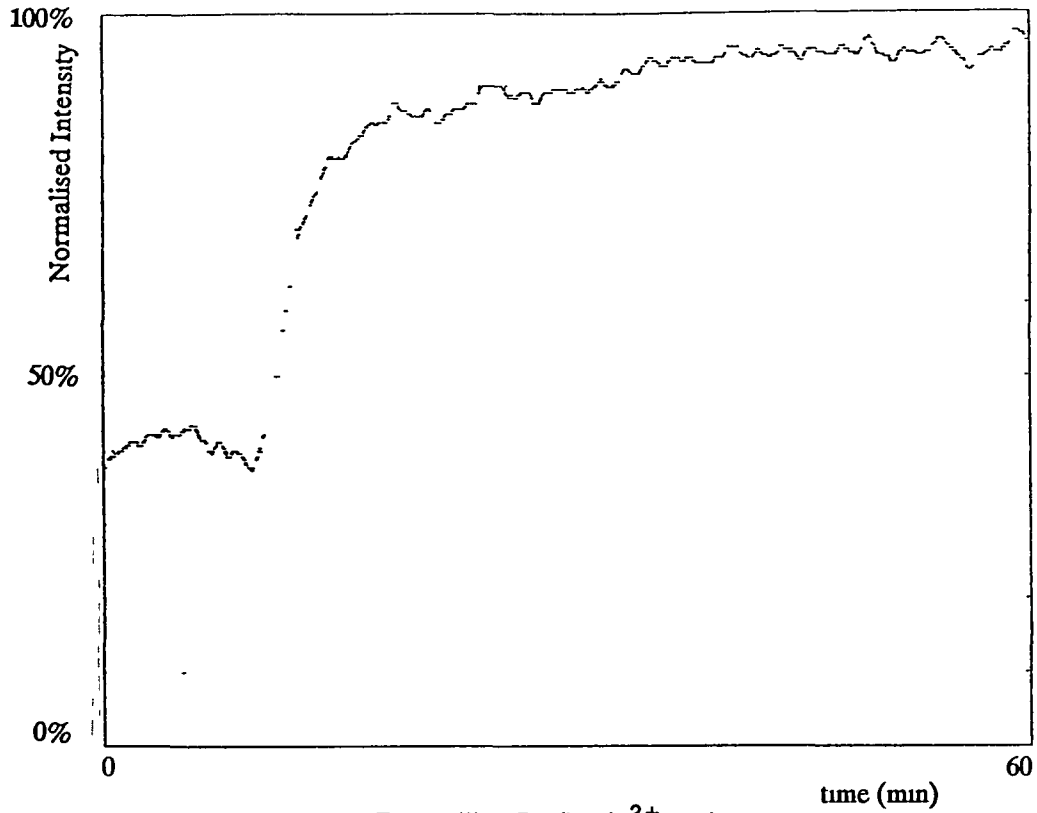

Figure III 9 Ru $(bpy)_3^{2+}$ probe
Continuous monitoring of fluorescence intensity during dye uptake at 5μW excitation power

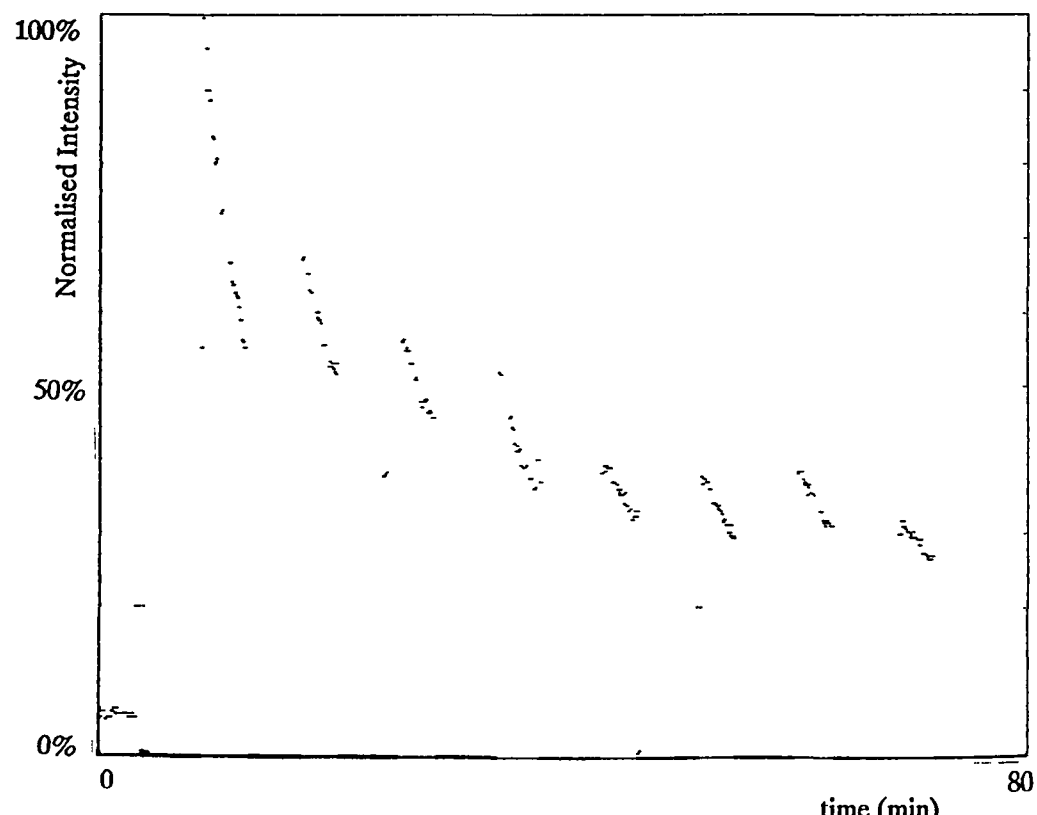

Figure III 10 Ru $(bpy)_3^{2+}$ probe
Dye uptake with no excitation light during soaking
Excitation power 50μW

in the later experiments There are two main differences between the two sets of experiments Firstly, the power of Ar ion laser excitation light was of the order of 40μW in the first set and up to 15μW in the second While the excitation intensity strongly influences the decay portion of the soak curve, its significance in the early period of dye uptake is not clear The higher excitation powers may be responsible for the formation of Ru $(bpy)_3^{3+}$ which is not retained by the Nafion polymer This can influence the uptake of Ru $(bpy)_3^{2+}$ as the concentration of free sites at the Nafion / dye solution interface is thus lowered The dye in the Nafion polymer may also be converted to the 3+ state which is then lost to the solution This transition from 2+ to 3+ requires the presence of an oxidising agent, for which there was no evidence in either the dye solution or in the Nafion polymer (the oxidising agent would have had to come from external contamination)

The second major difference between the two sets of dye uptake data may be due to the solution of Nafion used During experimental work with Nafion, a small quantity of Nafion solution obtained from Aldrich was stored in a glass container, from which the fibres were coated As the solvent in this container was found to evaporate over long periods of time, the Nafion used during the second set of data was from the same stock solution, but a different sample If the sample used in the first experiments was contaminated, then this contaminant was not transferred to the second set of experiments This contaminant would have to modify the character of the Nafion in such a way as to reduce its dye uptake facility, for example if a high boiling point alcohol was added to the Nafion solution, then the "dried" polymer would be more easily dissolved in the dye solution as it was not fully cured This may account for the slower uptake of dye from the bulk solution Again it is not confirmed that this was the case, but a polymer dependent change may account for the reproducibility of the results taken during that period

The downward slope of the dye uptake curve may be explained by such effects as self-quenching and also photo-mduced decay of the resident dye The latter is quite plausible as in early times, high intensities of excitation light were used, but even under high illumination during the repeat experiments, this dramatic effect was not reproduced Unfortunately, the first set of results was not reproduced at the later date, but even as such cannot be discarded or ignored The process that may cause the presently observed curves is discussed in more detail in Chapter IV I

C) Conclusion

Although the fluorescent dye, Ru $(bpy)_3^{2+}$ is quite popular for use in an optical based oxygen sensor, the results shown in this chapter suggest that this dye does not have the required stability for use in such a device This conclusion is drawn mainly from the data obtained in the section about the decay of the observed fluorescence signal with time during probe illumination (Chapter III B(2)), as well as from the irreproducibility of some of the data taken in the other sections As the fibre optic probe can only be used while it is under illumination, this problem has no simple solution For this reason, other fluorescent dyes were sought which had properties better suited for use in this fibre optic oxygen sensor, especially stronger π-bonding between the metal and ligand The most promising of these dyes was the compound Ru $(phen)_3^{2+}$ and the properties of a sensor based on this fluorescent dye are described in the next chapter

Chapter IV: Ru (phen)$_3^{2+}$ probe characterisation

A) Introduction

This chapter describes the experimental work carried out to characterise the properties of the oxygen sensor based on the fluorescent dye Ru (phen)$_3^{2+}$ Several different aspects of the sensor were investigated and an attempt was made to quantify their behaviour The properties investigated were the signal stability, oxygen dependence and the temperature dependence, as well as response time and sensitivity An attempt to fit a set of equations to the experimental data taken during this work resulted in a compound equation that describes the operation of the sensor and is characterised by a set of parameters unique to each sensor These parameters are given as the rate of illumination dependent signal decay (%/μW/mm), the Stern - Volmer quenching constant given (mol^{-1}) and the temperature dependence constant (^{o}C^{-1}) Once these parameters are estabhshed, the operational readings from the sensor can be standardised

Both the response time and the sensitivity of the sensor were determined by the procedures described The mechanical stability of the oxygen sensor was also mvestigated

The final section describes work carried out in testing the operation of the sensor in a gaseous environment The idea of possibly operating a fibre optic oxygen sensor in both aqueous and gaseous environments is new and unique to this sensor The procedure for producing the probe is the same as that used in the other parts of the chapter, differing only in the fact that the probe was let dry out for this work

B) Ru (phen)$_3^{2+}$: Experimental Work

The fluorescent dye Ru (phen)$_3^{2+}$ was chosen for several reasons. Firstly, its excited state lifetime is 850ns in water at 300 K and so is more suited than Ru (bpy)$_3^{2+}$ (τ = 580ns) to the role of oxygen sensing by the method described here. Secondly, and more importantly, the excited state of Ru (phen)$_3^{2+}$ is less reactive than that of Ru (bpy)$_3^{2+}$. This means that it is less prone to decomposition under illumination than the bpy compound because of stronger π-bonding between the ligands and the central metal ion. The luminescence quantum yield (0.08) is large enough to allow the development of an optical based instrument when compared to that for Ru (bpy)$_3^{2+}$ (0.10).

Probe fabrication process:

A modified procedure was adopted for the fabrication of the probes used in this set of characterisation experiments and tests. The procedure differs from that given earlier for Ru (bpy)$_3^{2+}$ in two ways: firstly, the fibre was silanised before being coated with Nafion to ensure bonding of the polymer to the fibre surface (§ Chapter I:F; Chapter II:D(2)); secondly, the Nafion used was given by Dr. J.M. Kelly, T.C.D., instead of the Aldrich product used earlier and did not contain solubility stabilisers.

- Cleave fibre
- Etch in 48% HF for 5 minutes
- Wash in ethanol for 5 minutes
- Dip coat with conc. APTS solution
- Heat fibre with heat gun (~200°C)
- Coat with 6% Nafion
- Dry in air for 30 minutes
- Soak in Ru (phen)$_3^{2+}$ for 10 minutes
- Store in de-ionised water

IV:B(1) Emission characteristics

There is no significant difference between the emission spectrum of Ru (phen)$_3^{2+}$ in aqueous solution (§ Figure I.7) and that observed in the probe (§ Figure IV.1). There may be a slight blue shift of the fluorescence maximum of approximately 5-10nm due to the hydrophobic nature of the internal structure of the Nafion membrane, but this is not serious as most measurements are taken using a broad band filter system. The apparatus for recording the emission spectrum is shown in Figure IV.5.

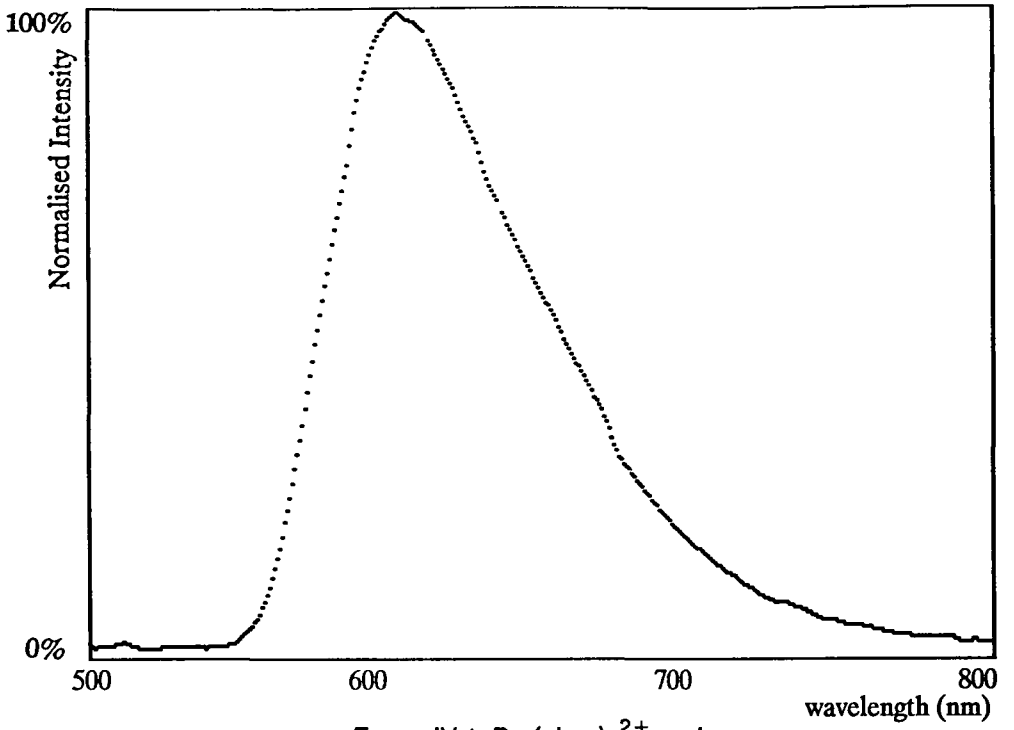

Figure IV 1 Ru (phen)$_3^{2+}$ probe
Emission spectrum at λ_{max} = 488nm

Table IV 1 Ru (phen)$_3^{2+}$ probe
Intensity decay data assuming linear approximation

Power P_{ex} (μW)	Exposure (min)	%age change	Decay constant D_C (%/μW/min)
0 05	20	3 7	3 7
0 25	20	4 7	0 94
0 52	20	8	0 76
1 03	20	10	0 48
2 05	20	10 4	0 26

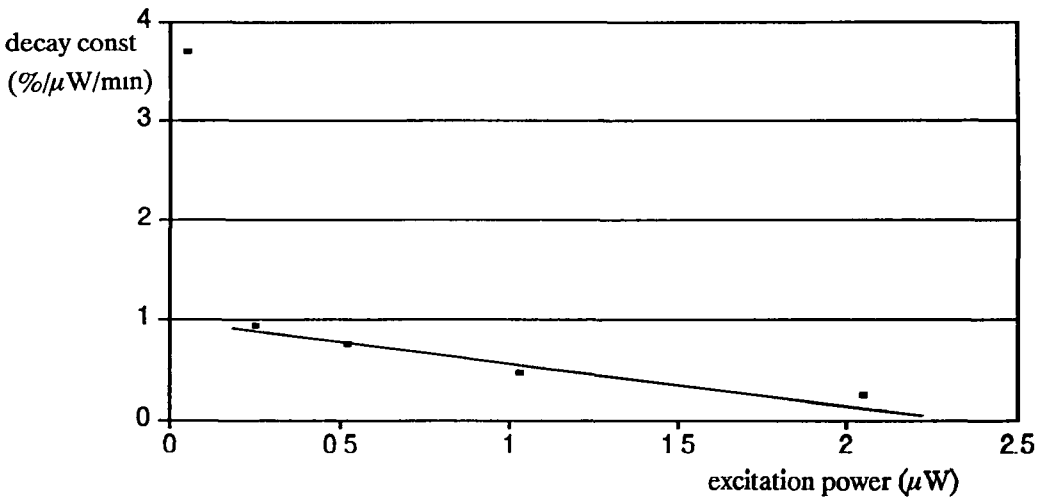

Figure IV 2 Ru (phen)$_3^{2+}$ probe
Plot of decay time constant against excitation power
Stray point is due to the relatively high noise level in the low excitation power data set which makes short term decay difficult to quantify

IV.B(2) Signal stability

The signal recieved from the detector was monitored over a large excitation power range (30μW - 0 02μW) on a BBC micro computer using the filter based detector system described in Chapter II B(3) This work was done with a view to identifying the extent of intensity related decay of the probe when illuminated When high excitation powers were used, the fluorescence signal was seen to decay rapidly, while when very low levels were used, the signal was found to be stable The decay time constant was found by calculating the percentage decay per minute for a given excitation power level assuming a linear decay approximation and is given the units %/μW/min. The data found from these experiments is displayed m Table IV 1 and the decay constant was plotted against the excitation intensity shown in Figure IV 2

The signal change from initial value I_o to intensity I_t , at time M minutes is defined as

$$I_t = I_o \left((100 - D_C P_{ex} M) / 100 \right)$$

where P_{ex} is the excitation power in μW, D_C is the decay constant m %/mW/min. M is the time in minutes of the exposure of the probe to excitation power P_{ex} The value for D_C comes from Table IV 1

The decay of the signal was also shown to be illumination dependent by temporarily blocking the

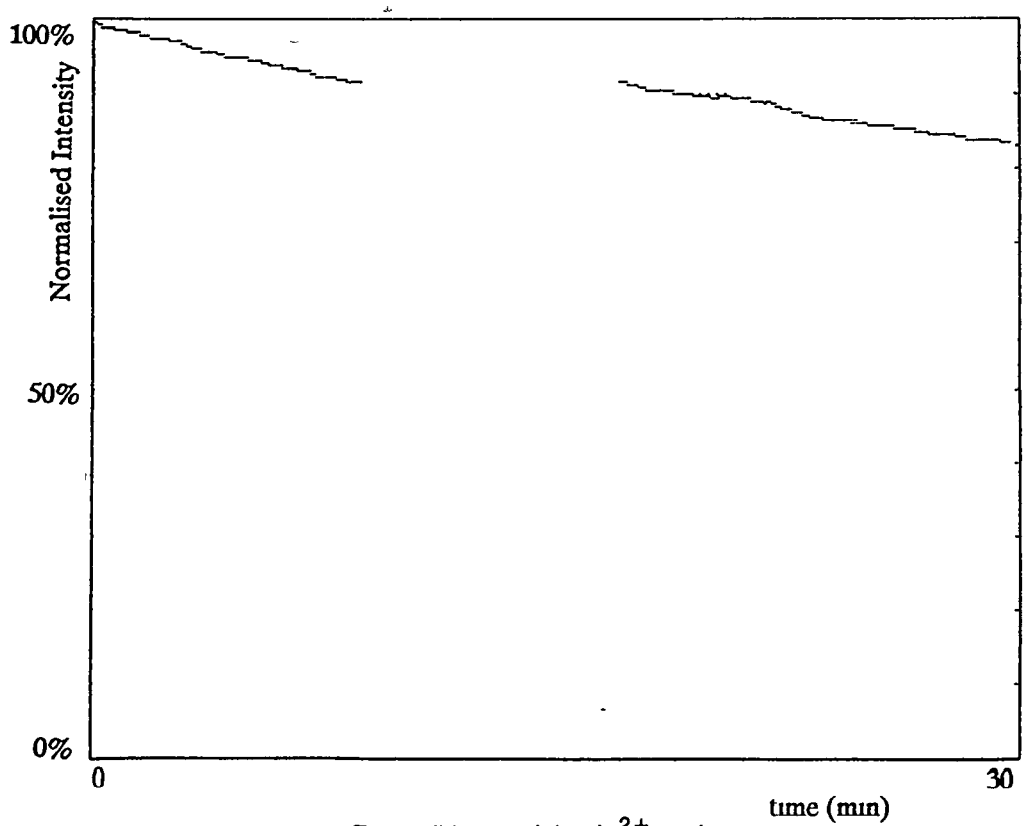

Figure IV 3 Ru $(phen)_3^{2+}$ probe
Illumination dependence of signal decay

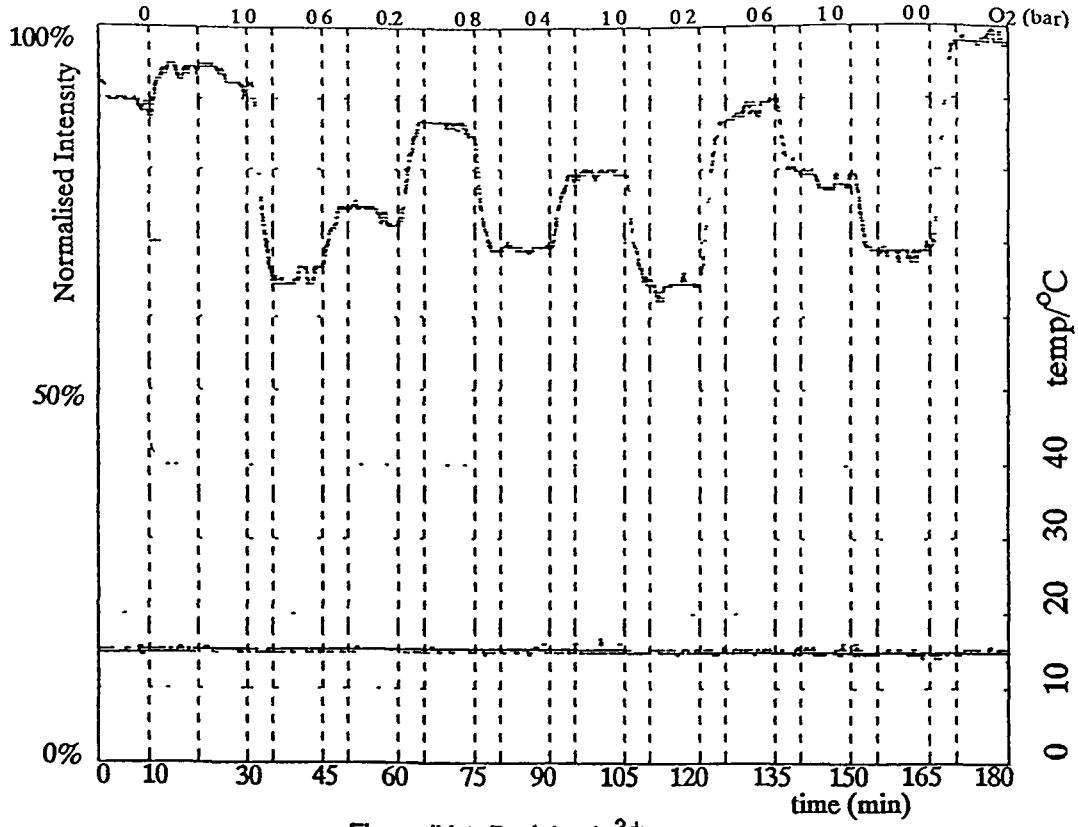

Figure IV 4 Ru $(phen)_3^{2+}$ probe
Monitor scan of probe signal at various dissolved oxygen concentrations

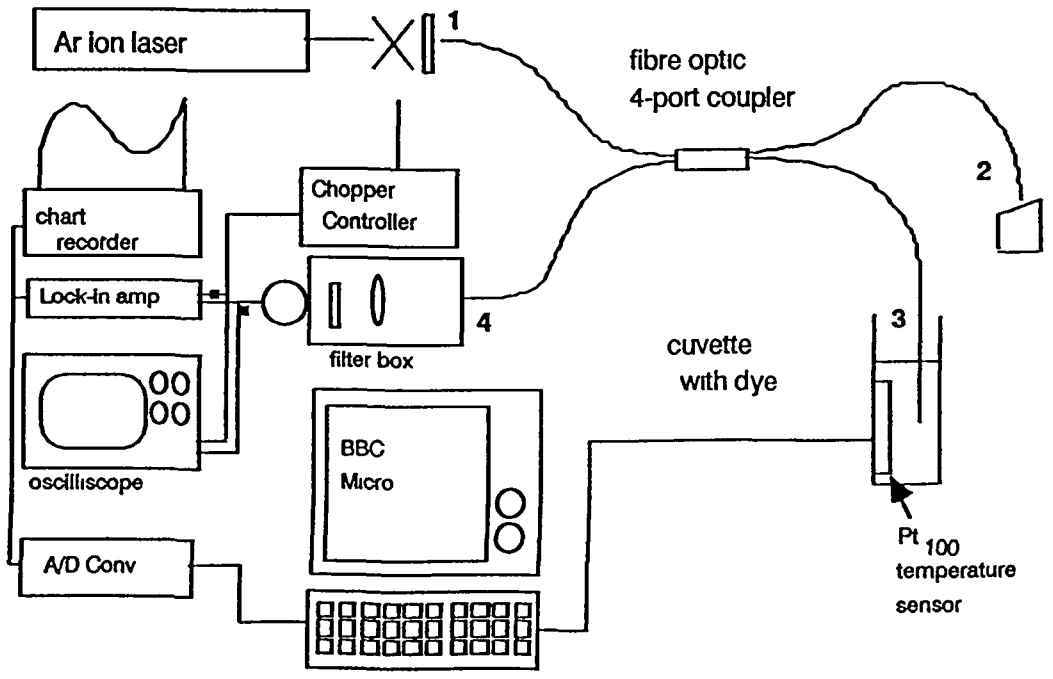

Figure IV 5 Experimental system with filter based detector

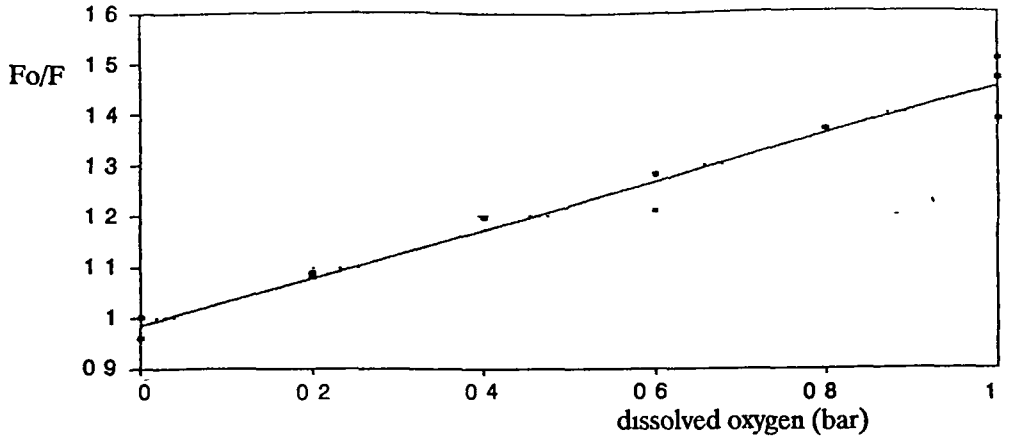

Figure IV 6 Ru $(phen)_3^{2+}$ probe
Stern - Volmer plot for uncorrected data from Figure IV 4

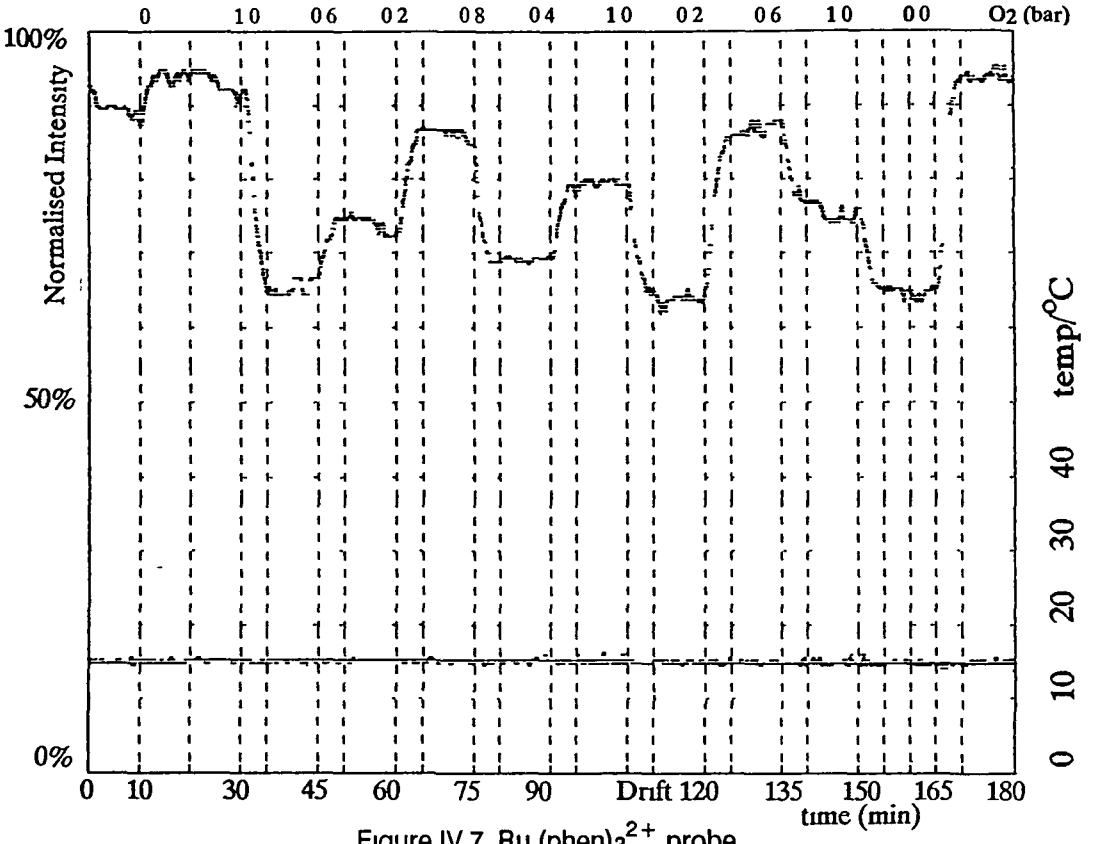

Figure IV 7 Ru $(phen)_3^{2+}$ probe
Monitor scan of probe signal at various dissolved oxygen concentrations with data corrected for drift as described in the text

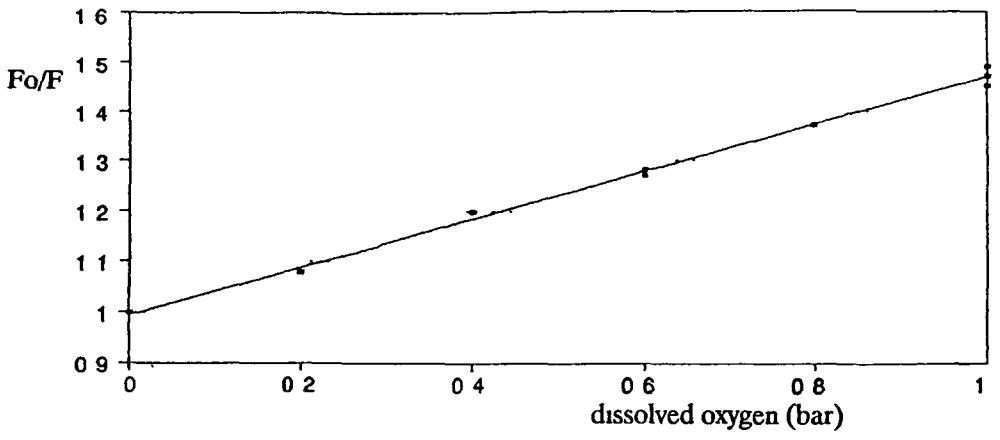

Figure IV 8 Ru $(phen)_3^{2+}$ probe
Stern - Volmer for drift corrected data from Figure IV 7

excitation light and observing the intensity of fluorescence when the excitation source was restored This effect is shown in Figure IV 3 The observed decay of the signal was seen to continue once the excitation light was restored, proving the illumination dependence

IV B(3) Oxygen quenching of Ru $(phen)_3^{2+}$ probe

The oxygen quenching properties of the Ru $(phen)_3^{2+}$ probe were investigated using the experimental set-up with the filter based detector system (Figure IV 5) The intensities of fluorescence of the Ru $(phen)_3^{2+}$ probe at different oxygen concentrations at room temperature (usually at approx 22°C) were taken for the following dissolved oxygen partial pressures 0 0, 0 2, 0 4, 0 6, 0 8, 1 0 bar, the balance of gas being made up with nitrogen An intensity monitoring scan with such cycling of dissolved oxygen concentration is shown in Figure IV.4 It was found that a solution purged with Nitrogen was Oxygen free after a purging time of 10 minutes as monitored using the Hanna Instruments Oxymeter It was noticed that a background signal was measured in the absence of any dye in the probe This level was found to be approximate 38% of maximum for Ru $(phen)_3^{2+}$ scans and thus was removed from the data where necessary

IV B(4) Stern-Volmer plots for Ru $(phen)_3^{2+}$ probe

The monitor scan shown in Figure IV 4 was used to extract data for the Stern - Volmer plot which characterises the oxygen response of the fluorescent dye used in the probe The data points were measured at intervals along this scan where the gas in solution had come to an equilibrium This data was then plotted as shown in Figure IV 6 There is, however, a noticable drift in the latter half of the scan Although the reason for this change is not understood, if a linear drift is assumed, then removing this drift from the original data greatly improves the Stern - Volmer plot of the data The drift corrected scan is shown in Figure IV 7 and the corresponding Stern - Volmer plot in Figure IV 8 The drift compensation function assumes a linear drift between two points on the graph that are known to be at the same intensity The program calculates a straight line between these two points and subtracts this line from all points in the selected region For a complete listing of the program employing this and other data presentation features, see Appendix D The reasons for probe drift in the plot shown in Figure IV 4 are not fully identified and are thought to be a combination of temperature effects, possible alignment change, dye mixing within the polymer, dye decomposition and other effects Although these effects have been investigated in some detail, there is still some process present that has not been identified and which may affect the short term stability of the probe as used at present

It was noted that the signal reduction due to oxygen quenching increased with increasing temperature This implied that the quantity F_0/F increases with temperature, which verifies that

the process responsible for the quenching is indeed collisional in nature (§ Chapter I E, Figure I 10)

The signal from the probe decreases as the oxygen concentration in solution increases according to the relation

$$I = I_o \quad \frac{1}{1 + K_D [Q]}$$

where Q is the partial pressure of oxygen, in bar, in equilibrium with the solution, K_D is the Stern - Volmer quenching constant

A value of K_D = 0 5/bar was derived from the slope of the line in Figure IV 8 It should be noted that this value only applies to sensors based on Ru $(phen)_3^{2+}$, but values for other dyes can be found similarly

IV B(5) Temperature dependence

The Ru $(phen)_3^{2+}$ probe was found to be very sensitive to temperature fluctuations This is attributed to the long lifetime of the dyes excited state, which at higher temperatures finds alternative non-radiative relaxation pathways of the excited state that are equivalent to quenching This temperature dependence is observed as a decrease in intensity for an increase in temperature The temperature at the probe was monitored continuously using a Pt_{100} platinum film temperature sensor connected to the A/D converter on the BBC micro computer The temperature was also measured directly using a Maplin digital thermometer for certain experiments and also for calibration of the computer temperature log

The intensities of fluorescence for the Ru $(phen)_3^{2+}$ probe were recorded as a function of temperature Several different systems were used for the characterisation of the temperature dependance Firstly, the temperature and intensities were noted as the temperature of the system stabilised over several hours, mainly due to the heat generated in the laboratory by the Ar ion laser which was air cooled Such a monitor scan is shown in Figure IV 9 It shows that the intensity of the probe has stabilised once the temperature of the solution in which the probe was immersed has reached equilibrium The intensity was plotted against temperature for this data as is shown in Figure IV 10 and is exponential in nature Further temperature measurements were made by exposing the probe to step changes in temperature Temperatures below room temperature were achieved by placing a water bottle into an ice bath, while higher temperatures by using a water bath at ~80°C The temperature of the probe was thus cycled between three basic temperature

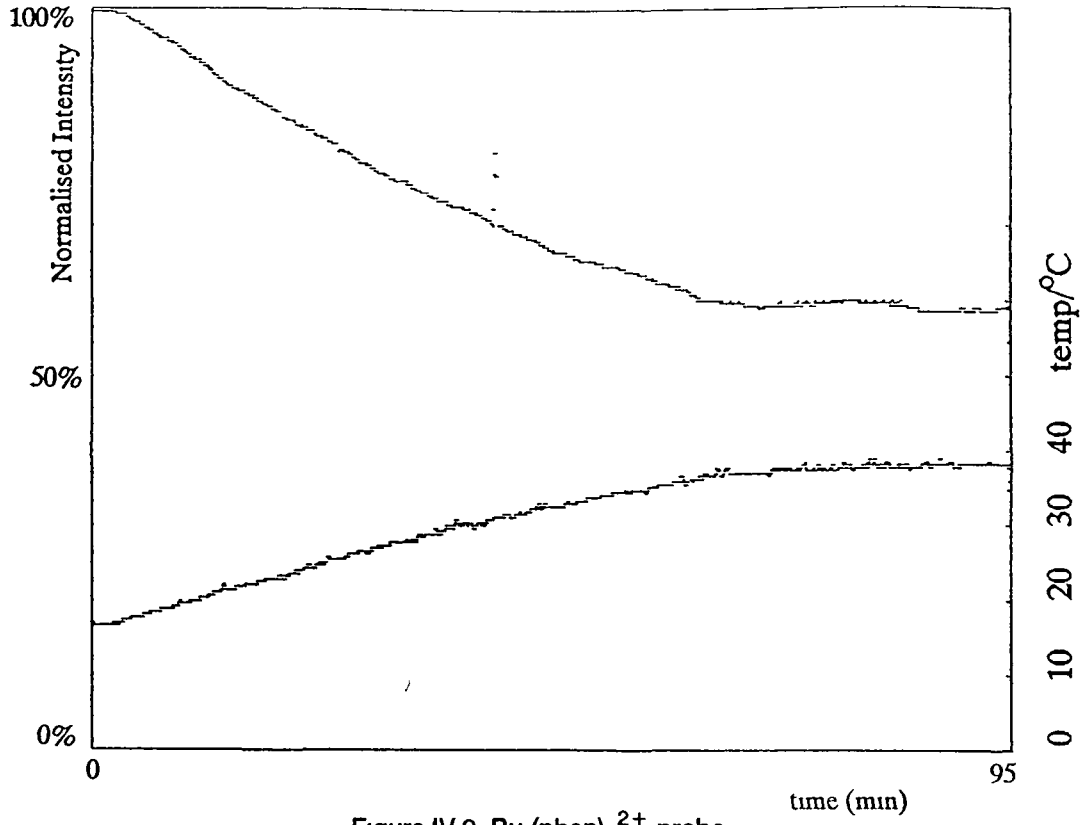

Figure IV 9 Ru $(phen)_3^{2+}$ probe
Intensity monitor scan with continuous probe temperature monitoring

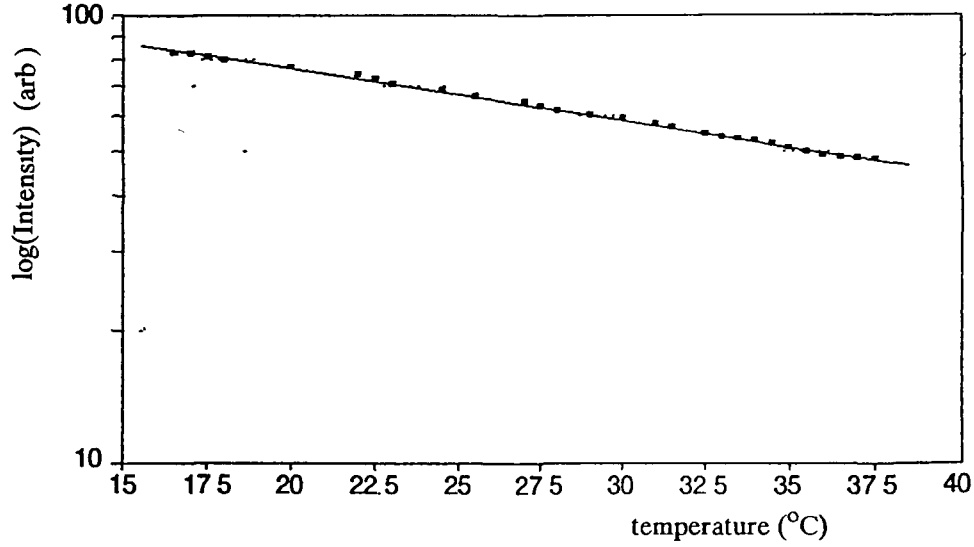

Figure IV 10 Ru $(phen)_3^{2+}$ probe
Logarithmic plot of Intensity against temperature in air saturated de-ionised water using data from Figure IV 9
The data was first corrected for 0 2 bar dissolved oxygen and then for illumination dependent decay with $D_C = 0\ 025\%/\mu W/min$

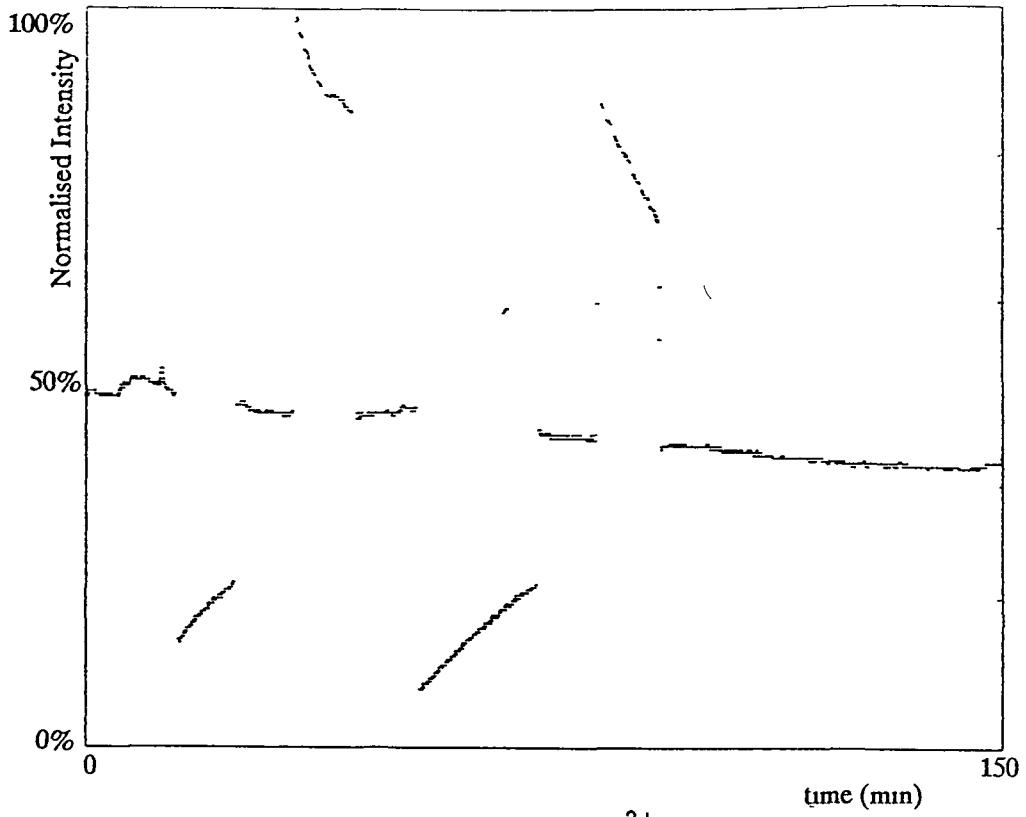

Figure IV 11 Ru $(phen)_3^{2+}$ probe
Intensity monitor scan showing step changes in temperature
of nitrogen purged de-ionised water

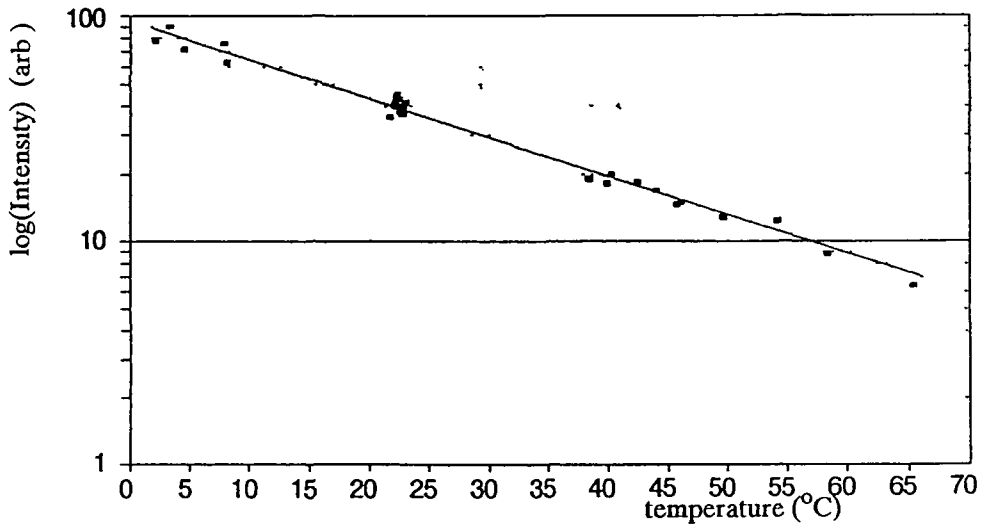

Figure IV 12 Ru $(phen)_3^{2+}$ probe
Logarithmic plot of intensity against temperature with data from
Figure IV 11 The data was corrected for illumination dependent
decay with D_C = 0 025%/μW/min

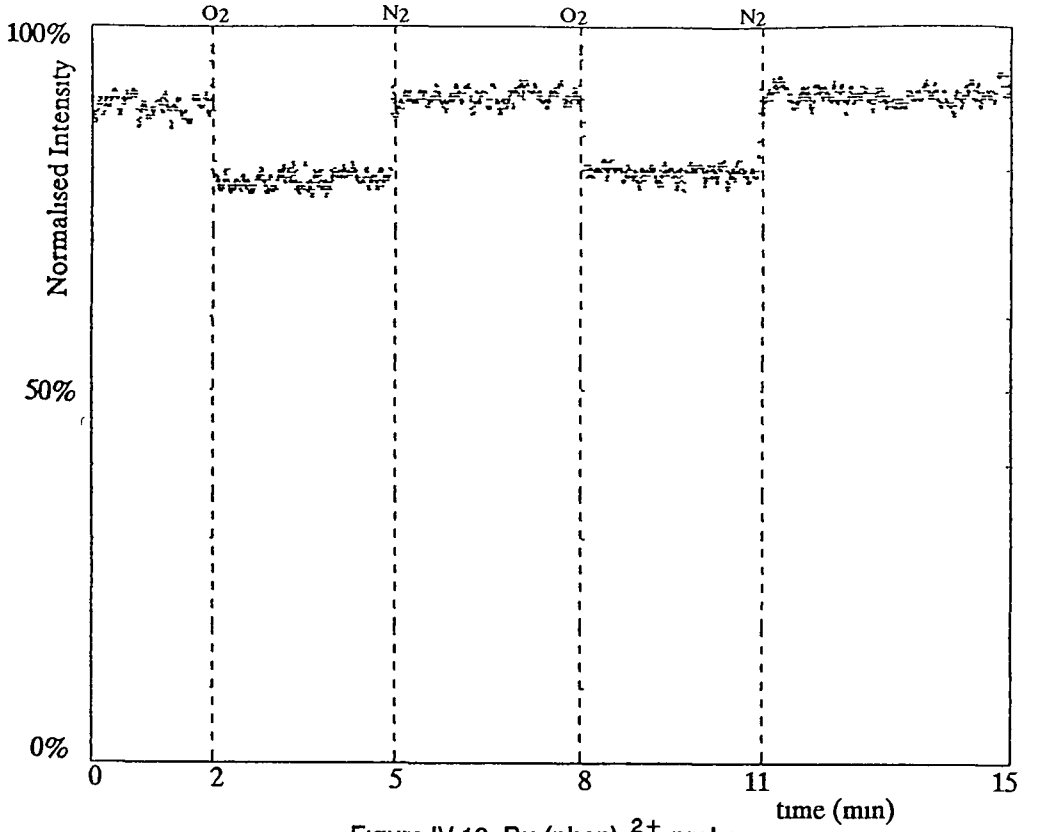

Figure IV 13 Ru $(phen)_3^{2+}$ probe
Intensity monitor scan for probe response time with step dissolveod oxygen concentration changes with 3 sec lock-in amp post-filter smoothing

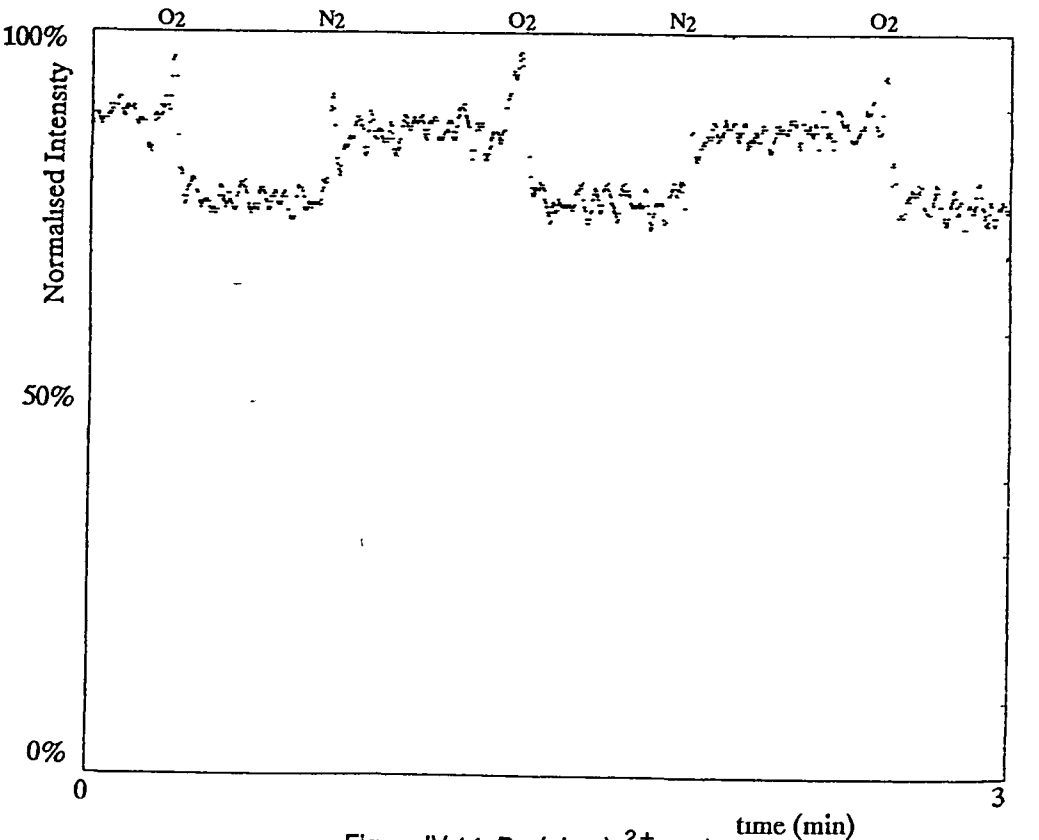

Figure IV 14 Ru $(phen)_3^{2+}$ probe
Intensity monitor scan for probe response time with step oxygen concentration changes with 3ms lock-in amp post-filter smoothing

levels. The monitor scan for this work is shown in Figure IV.11. The signal usually returns to the level shown for room temperature that corresponds to the temperature of the probe bath returning to that of the surroundings. This data was used to calibrate the probe used with respect to temperature and a temperature factor was calculated from the graph shown in Figure IV.12. This factor was found by fitting the data to the equation $I = I_o (10^{-Ct})$, where C is the component that defines the probe's response to temperature.

IV:B(6) Response times for Ru $(phen)_3^{2+}$ probe

The response time of the Ru $(phen)_3^{2+}$ probe is the time required to reach 67% $(1 - 1/e)$ of final change when the oxygen content in solution is changed. In the present case, the change was from an oxygen purged solution to an oxygen saturated solution. The experimental value for the response time was found by first placing the probe in nitrogen purged de-ionised water and then changing this for oxygen saturated water. The change over time of the dissolved oxygen concentration should have been small compared to the response time and so the response time was calculated from a series of such changes. The intensity monitor scans obtained during this work are shown in Figures IV.13 and IV.14. The response time was found to be of the order of 55 seconds for a lock-in amp post-filter time constant of 3 seconds and 5 seconds for 3ms integration. These values lead to the conclusion that the response time of the probe is not limited in practice by the rate of diffusion of oxygen within the probe, but rather by the response of the electronics used to measure the signal. The signal averaging period can be reduced at the cost of signal to noise ratio, but it is felt that a working post filter time constant of 3ms is adequate for most work as the data can be later smoothed by the display software (§ Appendix D). The fast oxygen diffusion within the probe is a result of the fluorocarbon nature of the Nafion matrix, which has a high diffusion constant for oxygen.

IV:B(7) Dye uptake

The fluorescence signal from a freshly made probe was monitored as it was allowed to take up the dye Ru $(phen)_3^{2+}$ using the filter based detector system over a period of 30 minutes. Two different methods were used, firstly the intensity was sampled at given intervals during the dye uptake. This method involved blocking the laser light while the probe was in the dye solution and unblocking it while the measurements were taken. The dark soak period was 5 minutes and the illuminated scan period was 3 minutes. The intensity monitor scan for this work is shown in Figure IV.15. The second method was to continually monitor the fluorescence as a function of the soak time. The experimental setup was the same as that used for the low intensity work using the filter box and an excitation intensity of $\sim 0.05 \mu W$. The scan for continuous monitoring is shown in Figure IV.16. The results described here are consistent with those shown in the later

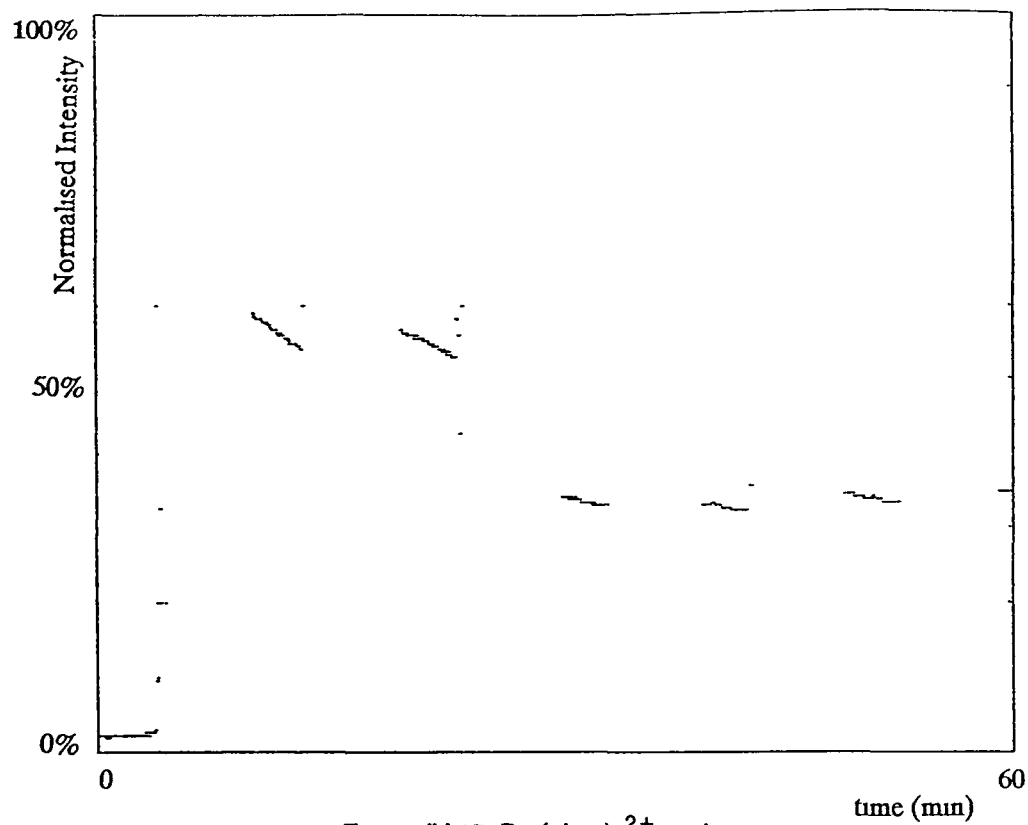

Figure IV 15 Ru $(phen)_3^{2+}$ probe
Intensity monitor scan for dye uptake Excitation power
@ 2μW in fibre No excitation light during soaking

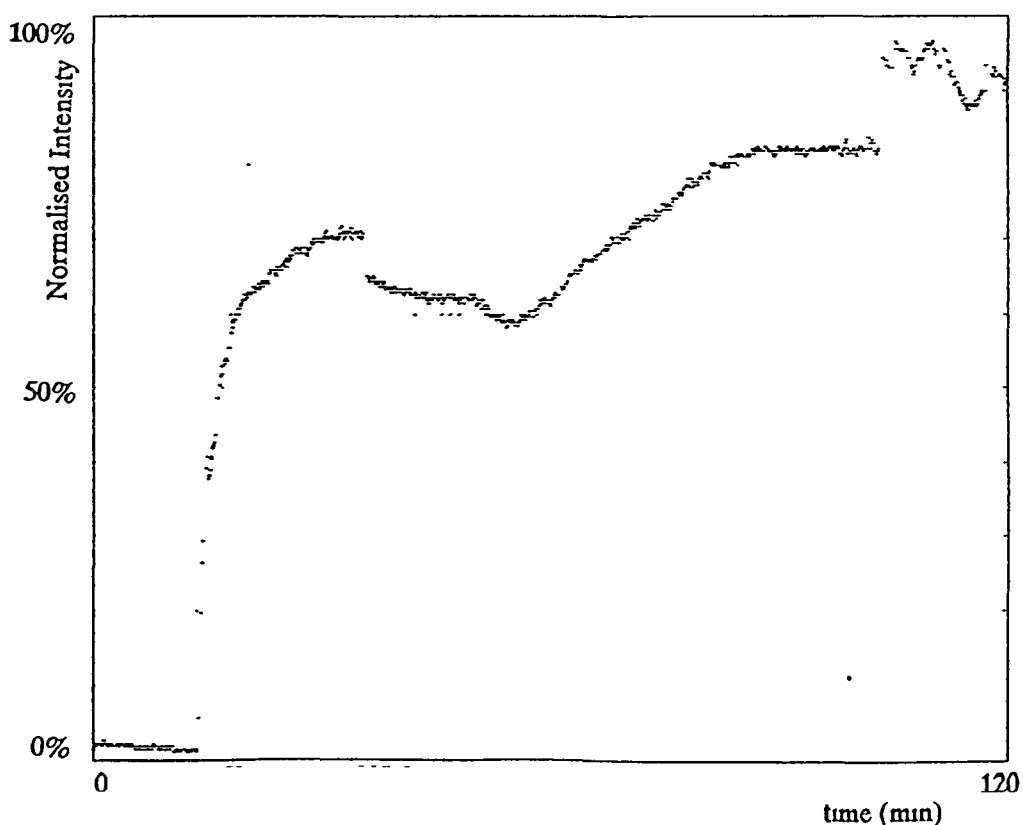

Figure IV 16 Ru $(phen)_3^{2+}$ probe
Intensity monitor scan for dye uptake Continuous illumination
0 02μW excitation power in fibre

work for the dye Ru $(bpy)_3^{2+}$, although differing from the early work for that dye (§ Chapter III B (6)) This similarity is to be expected as both dyes have very similar chemical properties

The soak curve observed for Ru $(phen)_3^{2+}$ into Nafion ion exchange resin can be interpeted as follows Since the Nafion ion exchange resin actively attracts cations, the dye is taken up very rapidly initially, which is observed as the sharp increase in intensity as the probe is immersed into the dye solution This uptake process is then limited both by the diffusion of dye within the polymer and diffusion in the bulk solution to the polymer / solution interface, which accounts for the plateau in the intensity observed after 10 minutes While this may explain the results observed here, it does not allow for those observed for the Ru $(bpy)_3^{2+}$ probe

IV B(8) Sensor characterisation

This sections attempts to tie together the individual dependencies of the Ru $(phen)_3^{2+}$ probe on temperature, dissolved oxygen concentration and exposure to the excitation radiation The equations derived in the earlier sections are now combined to yield a formula which may be applied to any Ru $(phen)_3^{2+}$ based oxygen sensor to fully characterise that probe This equation is explained as follows

The intensity dependent decay when assumed to be linear (good approximation for low excitation powers) can be given by $D_C P_{ex} M$ % after M minutes exposure time at P_{ex} μW excitation power with a decay constant of D_C, which comes from the data in Table IV 1 The oxygen dependnece is expressed from the Stern - Volmer equation given by $I = I_o / (1 + K_D[Q])$ where the quenching constant K_D was found to be 0 5 for a Ru $(phen)_3^{2+}$ based probe The temperature dependence was found to be described by the exponential relation $I = I_o\ 10^{-Ct}$, where C was found to be 0 011 /°C and t is temperature in °C These three relations can be combined to give the following equation

Table IV 2 Ru (phen)32+ probe
Data for sensor characterisation

Intensity (arb)	time (mm)	temp(°C)	$[O_2]$ (bar)	calc $[O_2]$ (bar)
90	10	15	0 0	0 000
62	37	15	1 0	1 090
71	55	15	0 6	0 612
82.5	70	15	0 2	0 179
66	85	15	0 8	0 832
76	100	15	0 4	0.380
61	115	15	1.0	1 090
83	130	15	0.2	0 131
71	145	15	0 6	0.553
62	160	15	1.0	1 000
89	175	15	0 0	-0 050

$$I = I_z \left(\frac{(100 - (D_C P_{ex} M))}{100} \right) \left(\frac{1}{1 + K_D[Q]} \right) \left(\frac{1}{10^{Ct}} \right) + O_c$$

O_c = signal offset constant, possibly caused by light leakage into detector system

I_z = calculated initial intensity without offset

[Q] = partial pressure (bar) of oxygen in equilibrium with the solution

M = exposure time (mm)

t = temperature (°C)

D_C = illumination decay constant (%/μW/min) eg 0 5 %/μW/min for 0 05 μW.

Pex = excitation power (μW)

K_D = Stern - Volmer quenching constant (0 5)

C = temperature decay constant (/°C) eg 0 011/°C for Ru $(phen)_3^{2+}$ at 0 05 μW

This equation was verified with data taken with the oxygen probe When the values for intensity, temperature, total exposure time (from the beginning of the scan), and oxygen concentrations taken from Figure IV 7 (§ Table IV 2) are inserted in to the above equation, two parameters are obtained, the initial intensity I_z and the offset O_c A best fit program such as that in Appendix B gives I_z = 97 7±2 9 and O_c = 6 7±2 0 for the data in Table IV 2 It should be noted that a different sensor will give different values The value obtained for I_z is statistically significant and shows that the equation describes the behavior of the sensor The equation can then be rearranged to allow the oxygen concentration to be determined when the intensity, temperature and exposure time are known, assuming that at least two calibration points are taken at known dissolved oxygen levels in order to determine I_z and O_c A program listing for the determination of oxygen concentrations from known parameters is given in Appendix F

The equation was also applied to the plot shown in Figure IV 17 which has a large temperature range It can be seen that the data in Figure IV 18 is quite constant, although a certain amount of drift above the noise level can be seen towards the end of the scan

The free variables can be quantified during a start-up procedure where a number of data points are taken under calibration conditions, so that the important values of I_z and O_c can be determined It is also possible to calibrate the sensor for the constants D_C, C, K_D using a similar method

A start-up sequence to characterise a fresh probe may take the following format

- Place the probe into de-oxygenated water at set temperature without excitation light

- Turn laser light on - calculate illumination decay constant after 10 minutes illumination
- Change temperature - calculate temperature dependence after equilibrium
- Blow oxygen through solution - calculate Stern - Volmer constant after equilibrium
- Take 10 data points over 30 minutes at known temperature, illumination time and dissolved oxygen concentration and hence calculate I_z and O_c from this data
- The probe should now be characterised and ready for use

Care should be taken that the probe is operated at excitation powers for which the linear approximation to the illumination decay still holds This limit is at an excitation power of approximately 0 50μW, and so the sensor as used in this work is generally operated below this The Stern - Volmer quenching constant is expected to be temperature sensitive, as temperature affects the lifetime of fluorescent molecules, but the variation of D_C from 16 5°C to 23°C was found to be 0 5 to 0 54/bar It may also be necessary to quantify this constant at the temperature at which the probe is being operated

IV B(9) Sensor sensitivity

The sensitivity for this sensor was calculated from a sample scan (§ Figure IV 7) where the noise level was estimated at 1 7% over a full scale signal change from 900 to 615 (N_2 to O_2 saturated water) This gives a sensitivity of 0 053 bar for the Ru $(phen)_3^{2+}$ based oxygen probe This value for the sensitivity assumes that there is no signal drift other than that quantified in the previous section (Chapter IV B(8))

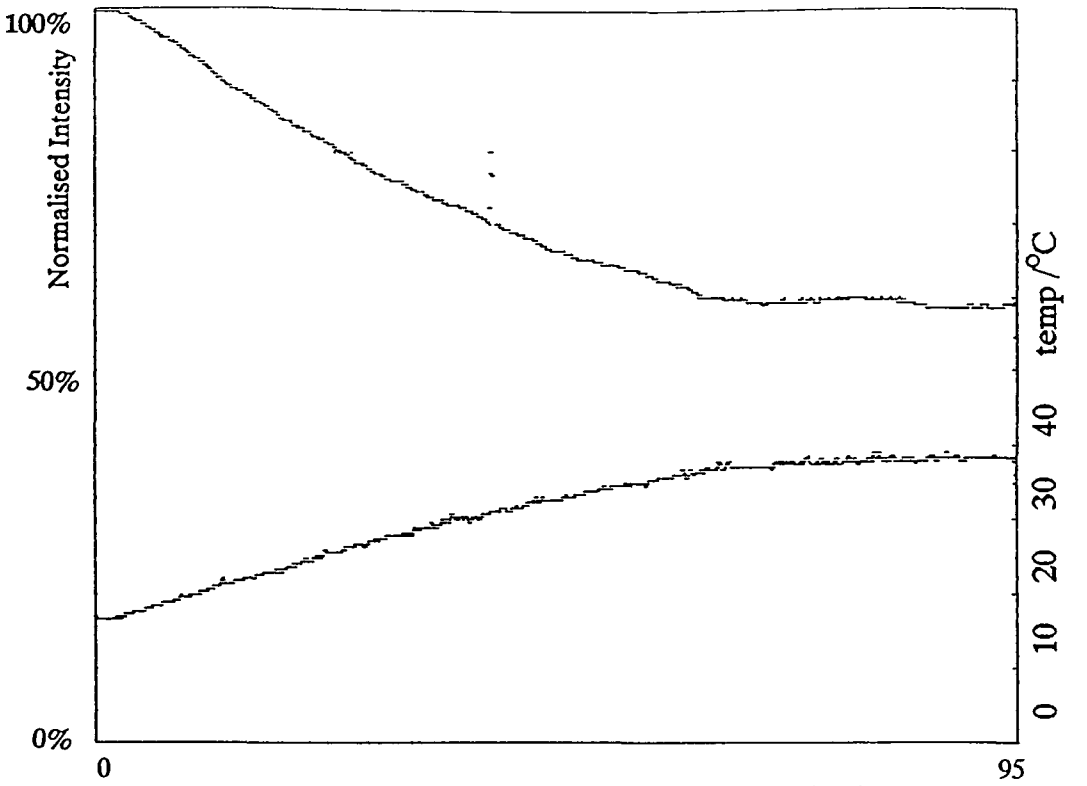

Figure IV 17 Ru $(phen)_3^{2+}$ probe
Sample scan before correction formula is applied

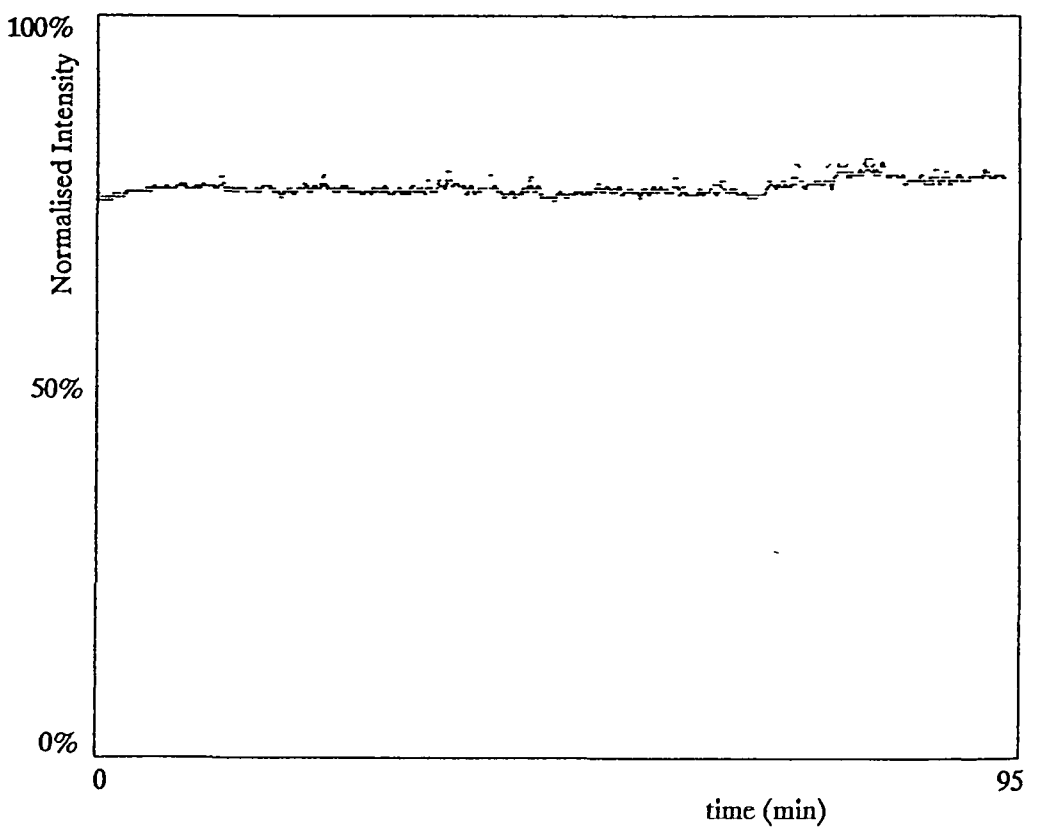

Figure IV 18 Ru $(phen)_3^{2+}$ probe
Sample scan for probe after correction formula is applied to data

IV B(10) Mechanical stability

It is important when designing a sensor to ensure that the probe can operate fully within certain limits of mechanical vibration This system was tested for such susceptibility to mechanical shocks and vibrations The work that follows was performed by monitoring the intensity of fluorescence from the probe over a period of time There are three parts of the sensor which may be influenced by such vibrations Firstly, the launching optics need to be secure The set-up used is immune to minor alignment changes as there is no focussing system involved The beam of the Ar ion laser is approximately 1mm in diameter, while the fibre used has core diameter of 50μm This means that as long as the fibre is placed centrally in the beam, it is allowed to move 0 25mm before the intensity of excitation light is significantly affected This was borne out by the observations that there was no change in signal when the bench on which the sensor was set up was knocked

Secondly, the detector was also found to be stable under the same conditions mentioned above Finally, the mechanical stability of the probe tip was investigated The tip was placed in a cuvette containing de-ionised water A stirrer paddle was made and used to see if the probe responded to mechanical stirring of the water No effects were observed as long as the polymer was firmly bound to the fibre surface (§ Chapter II C (3)) This was important to note as it was not desirable that the sensor respond to the mechanical action of blowing gas through the cuvette

Thus it can be concluded that the probe is not influenced by external mechanical effects within reasonable limits

C) Use of Ru (phen)$_3^{2+}$ probe as a gaseous oxygen sensor

The fibre optic oxygen sensor was tested for oxygen response in a gaseous environment, as opposed to the aqueous environment used to date The probe was made by the usual procedure and left to dry m air overnight The tip of the probe was placed into a glass tube with gas tubing attached to one end The output from the gas mixing rig (§ Chapter III B(3), Figure III 4) was connected to this flow cell The intensity from the oxygen sensor was monitored as the gaseous oxygen concentrations were changed The gas flow was controlled at 0 75lt/min

It can be seen from the monitor scan shown in Figure IV 19 that the Ru (phen)$_3^{2+}$ probe behaves as well m air as it does when kept in an aqueous environment The oxygen sensitivity of the probe m air was calculated to be 0 042 bar from the data in IV 19 This compares favourably with the result shown in IV B(9) of 0 053 for the probe in an aqueous environment The reason for this difference is thought to be due to a difference m the fabrication procedure between the two individual probes resulting in different concentrations of dye in the polymer which then changes the excited state lifetime The Stern - Volmer plot shown in Figure IV 20 shows a good degree of fit of the experimental data taken from the previous monitor scan (Figure IV 19) This data is not corrected for temperature or illumination

This short section thus describes an aspect of this fibre optic oxygen probe which has not been documented before, that is that the same fibre optic probe can be used for measuring oxygen m both an aqueous and gaseous environment, although there may be some adjusting time between changing environments

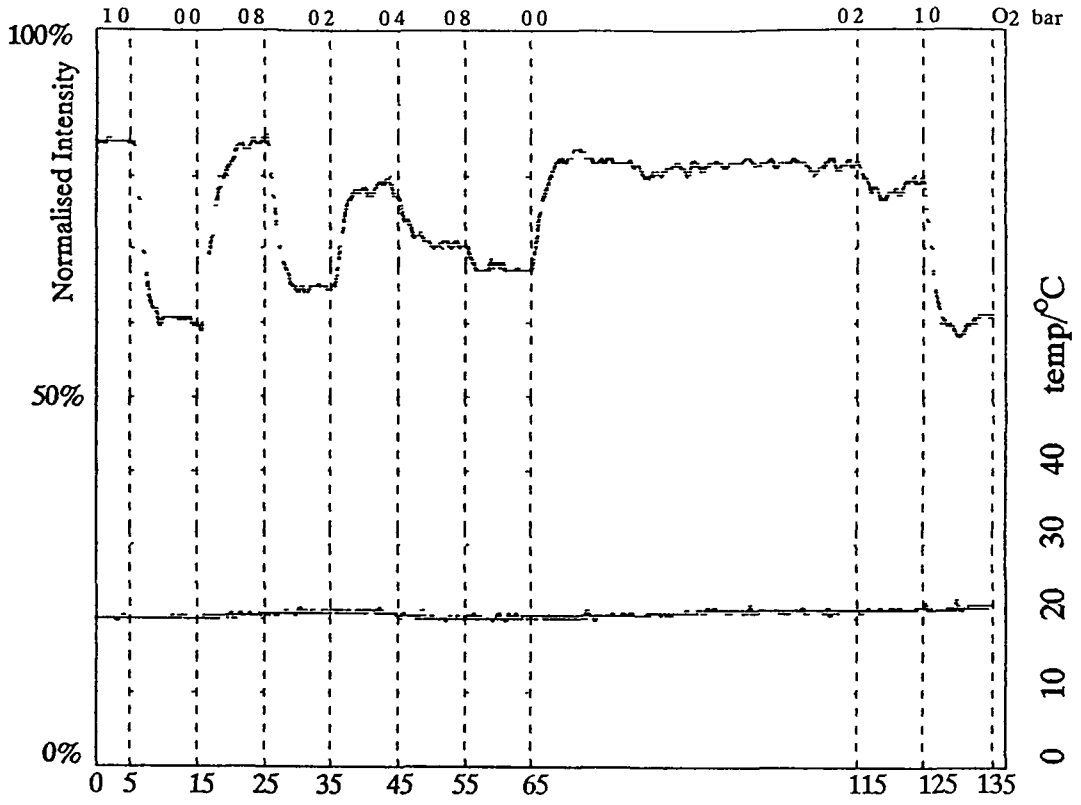

Figure IV 19 Ru $(phen)_3^{2+}$ probe
Use of probe as a gaseous oxygen sensor with oxygen concentration cycling

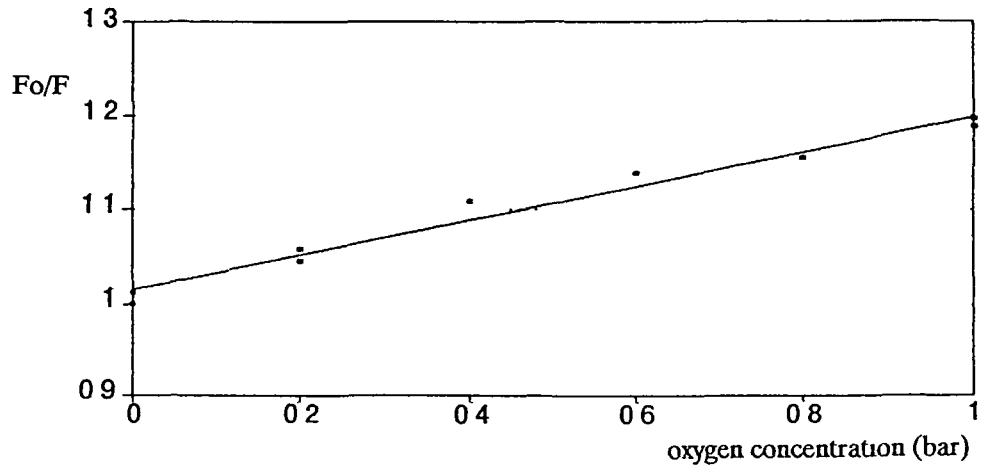

Figure IV 20 Ru $(phen)_3^{2+}$ probe
Stern - Volmer plot for data from Figure IV 19

Chapter V: Further developments

A) Introduction

This chapter describes relevant work that was carried out in addition to that described for the basic sensor The first section is concerned with the development of a referencing system for the Ru $(bpy)_3^{2+}$ based sensor While the information described here was not found to improve the performance of the sensor, it is included to aid general understanding of the problems encountered during the development of the oxygen sensor

The second section describes work carried out in relation to a possible development of a hand-held instrument for the determination of ambient oxygen concentrations based on a silicon carbide LED as light source In such a case, the fluorescent dye may be immobilised in a polymer coating on the surface of the LED dome, or on a glass slide in front of the LED and that the fluorescence intensity is monitored using a photodiode This work is also partially applicable to the use of a SiC LED as light source in place of the Ar ion laser in the fibre optic probe The idea of the hand held probe was not fully developed as it was thought to be too much of a side line to the core problems encountered in this project

In the final section, there is a brief description of an application for the fibre optic oxygen sensor described in this thesis This application would involve the measurement of the radial dissolved oxygen profile in Calcium alginate bioreactor pellets that are used by the Biotechnology industry The experimental work for this project was not carried out due to lack of time and also due to dissatisfaction with the degree of stability that was required of the probe for such measurements

B) Referencing the Ru $(bpy)_3^{2+}$ based oxygen sensor

In order to improve the accuracy of the Ru $(bpy)_3^{2+}$ based fibre optic oxygen sensor, some method of reference is required to allow the readings to be corrected for external factors such as temperature, excitation light source power, detector instability and mechanical vibrations In order to reference the probe from such factors, it was decided to investigate the use of a second fluorescent dye along with the sensing dye Ru $(bpy)_3^{2+}$

The complex Os $(bpy)_3^{2+}$ is chemically quite similar to that of Ru $(bpy)_3^{2+}$, with two important differences The first is the fluorescence maximum, which lies at 715nm as opposed to 608nm for Ru $(bpy)_3^{2+}$ This allows relatively easy separation of the two fluorescence peaks The second difference is that the Os $(bpy)_3^{2+}$ excited state has a much shorter lifetime (19ns , Creutz *et al*, 1980) than that for Ru $(bpy)_3^{2+}$ (580ns in water at 300K) This renders the Os $(bpy)_3^{2+}$ insensitive to oxygen quenching It is possible to encorporate the Os $(bpy)_3^{2+}$ into Nafion ion exchange resin (Anson *et al*, 1984) by the same process as for Ru $(bpy)_3^{2+}$ This potentially allows the probe tip to contain both dyes in the same polymer with the effect that the Os $(bpy)_3^{2+}$ acts as a reference Therefore, by ratioing the fluorescence intensities of both dyes, the dissolved oxygen concentration can be determined

The fibre from one arm of the Canstar 4-port coupler was cleaved and etched in HF for 5 minutes and coated with Nafion after washing in de-ionised water The probe was left to soak in Os $(bpy)_3^{2+}$ solution for 45 minutes The emission spectrum taken by the system of the probe yielded the same as that for the fluorescence spectrum for Os $(bpy)_3^{2+}$ using a spectrometer The probe was then immersed in a solution containing Ru $(bpy)_3^{2+}$ for 15 minutes A probe spectrum was found to contain the emission peak associated with Ru $(bpy)_3^{2+}$, but the intensity of the Os $(bpy)_3^{2+}$ peak had decreased significantly Further soaking of the probe in either Ru $(bpy)_3^{2+}$ or Os $(bpy)_3^{2+}$ had no significant effect

A mixture of the two fluorescent dyes, Ru $(bpy)_3^{2+}$ and Os $(bpy)_3^{2+}$ was made up which gave the maximum of the respective fluorescence intensities to be similar This is important as the Os $(bpy)_3^{2+}$ has a much lower quantum efficiency (1%) than Ru $(bpy)_3^{2+}$ (10%) and thus requires approximately 10 times the concentration of the Ru $(bpy)_3^{2+}$ This mixture was monitored using a Perkin-Elmer L-5 luminescence spectrometer Spectra of this mixture were taken as small amounts of nitrogen were passed throught the mixture, each spectrum being superimposed on the previous one The process was reversed when air was bubbled through the solution The resultant plot is shown in Figure V 1

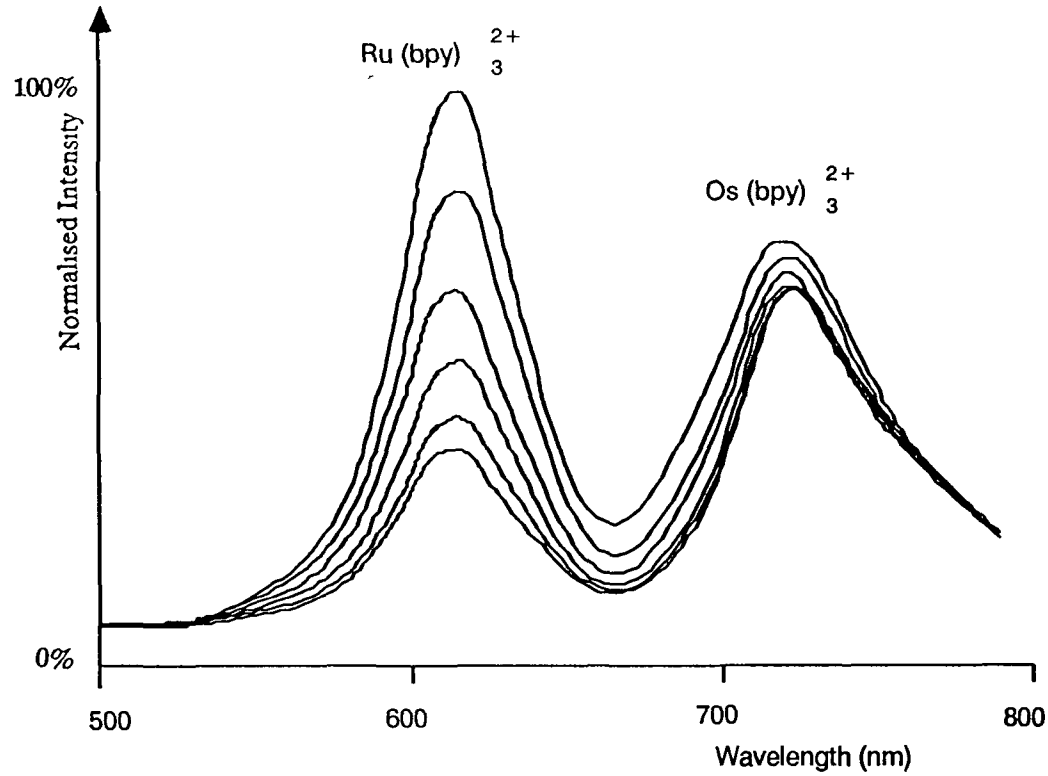

Figure V 1 Ru $(bpy)_3^{2+}$ / Os $(bpy)_3^{2+}$
Fluorescence sprectra of combined dyes at various dissolved oxygen concentrations taken with luminescence spectrometer

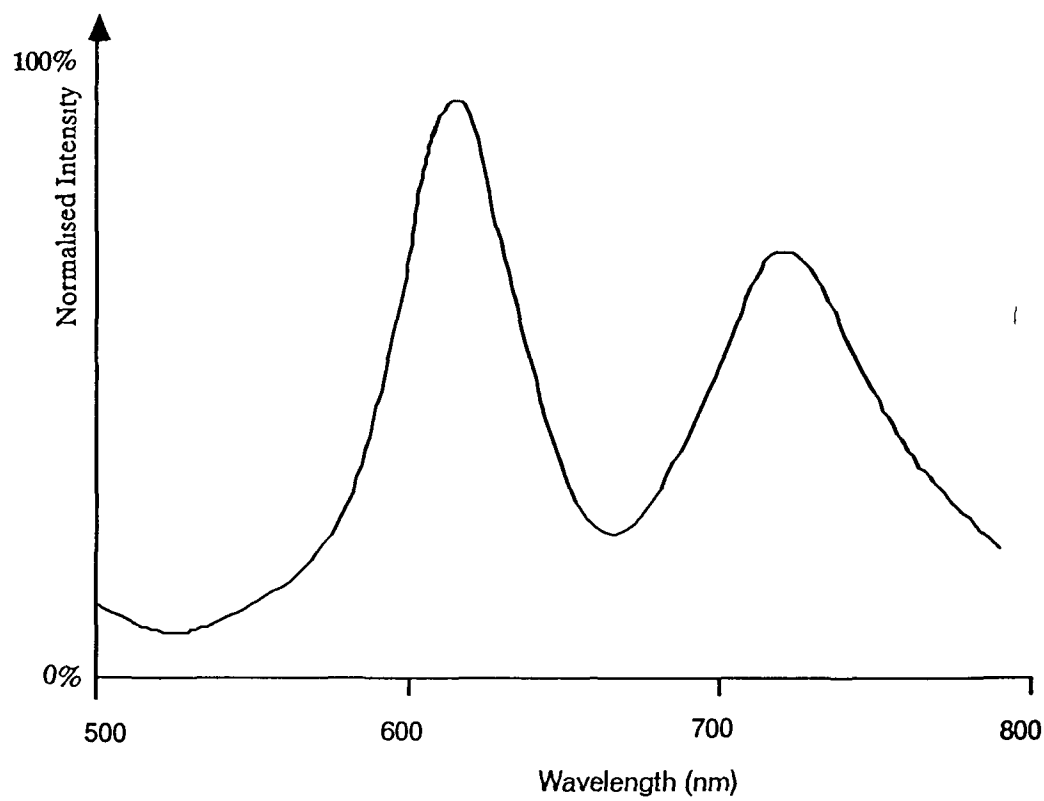

Figure V 2 Ru $(bpy)_3^{2+}$ / Os $(bpy)_3^{2+}$
Fluorescence spectrum of both dyes in Nafion on fibre tip

The important point to note in these spectra is that the intensity of the 715nm peak changes with oxygen levels This is not due to oxygen quenching of the Os $(bpy)_3^{2+}$ fluorescence, but due to the tail of the spectrum of Ru $(bpy)_3^{2+}$ overlapping with the Os $(bpy)_3^{2+}$ maximum

Having observed the oxygen response of a mixture of Ru $(bpy)_3^{2+}$ and Os $(bpy)_3^{2+}$, it was decided to make a probe containing both dyes A coated fibre was left soaking in the solution described above overnight Initially, only the Ru $(bpy)_3^{2+}$ fluorescence could be seen, but after soaking in de-ionised water, the Os $(bpy)_3^{2+}$ emission peak began to appear When oxygen was bubbled through the water containing the fibre probe, a reduction in the intensity of the Ru $(bpy)_3^{2+}$ fluorescence was observed, with a slight increase in the fluorescence of the Os $(bpy)_3^{2+}$ No increase in the relative intensity of Ru $(bpy)_3^{2+}$ was observed with nitrogen purge

A dye uptake curve of Os $(bpy)_3^{2+}$ was generated in the same manner as that described in Chapter II D (6) for Ru $(bpy)_3^{2+}$ The plot obtained was identical to that shown in Figure III 8 for the dye Ru $(bpy)_3^{2+}$ (§ Chapter III B (6)) Both plots showed a maximum intensity at approximately 25 minutes soaking By soaking for a time that corresponds to regions on these curves with a positive slope, that is of the order of 10 minutes, the concentration within the Nafion should be low enough to minimise concentration effects, such as self quenching

A solution was made up which contained equivalent quantities of Ru $(bpy)_3^{2+}$ and Os $(bpy)_3^{2+}$ A fibre freshly prepared and coated with Nafion was prepared in the usual manner This probe was immersed in the dye mixture for 10 minutes and stored in de-ionised water A fluorescence spectrum was taken of the probe formed (Figure V 2) This probe was tested for stability by taking spectra at different intervals It was noted that the heights of the two fluorescence maxima changed with time and also relative to one another As a result, it was not possible to take referenced readings from the probe in this manner

The reason for this instability, which was observed on many occasions, is not understood Although it has been seen earlier that the Ru $(bpy)_3^{2+}$ decomposes in the presence of Ar ion laser excitation, this is not thought to be responsible for the fluctuations observed as a relative increase of the intensity of Ru $(bpy)_3^{2+}$ was also observed It is thought that there is some interaction between the two fluorescent dyes that is not constant It is possible that one dye has a higher diffusion rate within the Nafion and as a result there are initially localised regions of high concentrations of this dye This would have two consequences Firstly, if this dye diffuses more rapidly into the Nafion, it would tend to occupy those regions closer to the Nafion / fibre interface

This would have the effect that the relative strength of the observed fluorescence from this dye would be much stronger (higher excitation intensity, spectral absorption of the other dye's fluorescence, less self-absorption, more light launched back into the fibre due to the geometry) As time progresses, a gradual mixing of the two species would occur, so that the fluorescence intensity from the second dye would become stronger than at first There is another factor that should be taken into account when considering the present system The concentration of Os $(bpy)_3^{2+}$ is ~10 times greater than that for Ru $(bpy)_3^{2+}$ because of the difference in fluorescence quantum yields This will also generate problems in reaching a stable equilibrium between the two dyes in question It may be possible to overcome this problem of mixing of the two dyes by applying each separately A proposed method to achieve this is to prepare a fibre in the normal manner and then to apply a Nafion coating The fibre is then soaked with Os $(bpy)_3^{2+}$ for ~10 minutes (enough to give an appreciable signal) A thin layer of polystyrene should then be applied to seal the first Nafion layer A second coating of Nafion is then apphed and is soaked with Ru $(bpy)_3^{2+}$ or Ru $(phen)_3^{2+}$ for a time of the order of 7 minutes This probe is finally coated with polystyrene to seal the complete unit This probe has the advantage that there is no mixing between the two dyes and then once each layer has reached equilibrium, the signals from the two dyes should behave in a predictable fashion The detector system proposed to be used is a slight variation of the filter unit, with the addition of a filter changing mechanism for alternately viewing the fluorescence of either dye With the aid of a computer controller, the referenced signal could then be calculated

C) Working with Silicon Carbide blue LED

The silicon carbide blue light emitting diodes (Siemens LB5410) have a peak emission at 480nm with a spectral bandwidth of 90nm. This light source is suited for work with the fluorescent dyes used in the development of this sensor which have strong absorption at that region. The LED typically delivers between 2 and 5 mcd luminous intensity and was measured to be at 0.65μW over the full emission angular range.. The SiC LED has a rise time of 700ns and a fall time of 800ns allowing it to be modulated up to 500kHz.

The earlier parts of the work described here are concerned with designing a handheld portable instrument for the measurement of ambient oxygen concentrations. The second use of the LED is as a light source for the fibre optic oxygen sensor. This is advantageous since it eliminates the need for an Ar ion laser, thus reducing the cost of the sensor and also allowing for its portability.

V:C(1) Ru $(bpy)_3^{2+}$ bulk fluorescence

A cuvette containing a dilute solution of Ru $(bpy)_3^{2+}$ in water was placed in a sample chamber and illuminated by the blue LED. The fluorescence signal was viewed at right angles to the excitation direction and the spectrum was recorded on a chart recorder.

This spectrum is the same as that taken for Ru $(bpy)_3^{2+}$ on the luminescence spectrometer (Chapter I.D(1)).

V:C(2) Ru $(bpy)_3^{2+}$ in Nafion on glass slides

Some Nafion was bonded on glass slides and soaked with Ru $(bpy)_3^{2+}$. Four different configurations were tested where the orientation of the Nafion and slide were changed. Spectra were recorded for each configuration. These spectra showed the LED emission as well as the fluorescence of the Ru $(bpy)_3^{2+}$. This was expected as the tail of the LED emission spectrum is still visible at 600nm which causes the two spectra to overlap. The emission spectrum of the Ru $(bpy)_3^{2+}$ is clearly identified when the Nafion / Ru $(bpy)_3^{2+}$ film is illuminated from the rear. The four configurations of slide / polymer orientations are shown in Figure V.3. The schematics in the top-right hand corners of each cell show the orientation of the polymer with respect to the blue LED and monochromator. The polymer is shown as the thicker line with the glass slide represented by the longer thin line. The spectra suggest that there is significant difference in the fluorescent intensities when the polymer film is illuminated from the side that was exposed to the dye solution and when illuminated from behind. The lower signal obtained when the polymer is front illuminated possibly illustrates the effects of concentration quenching on the fluorescence

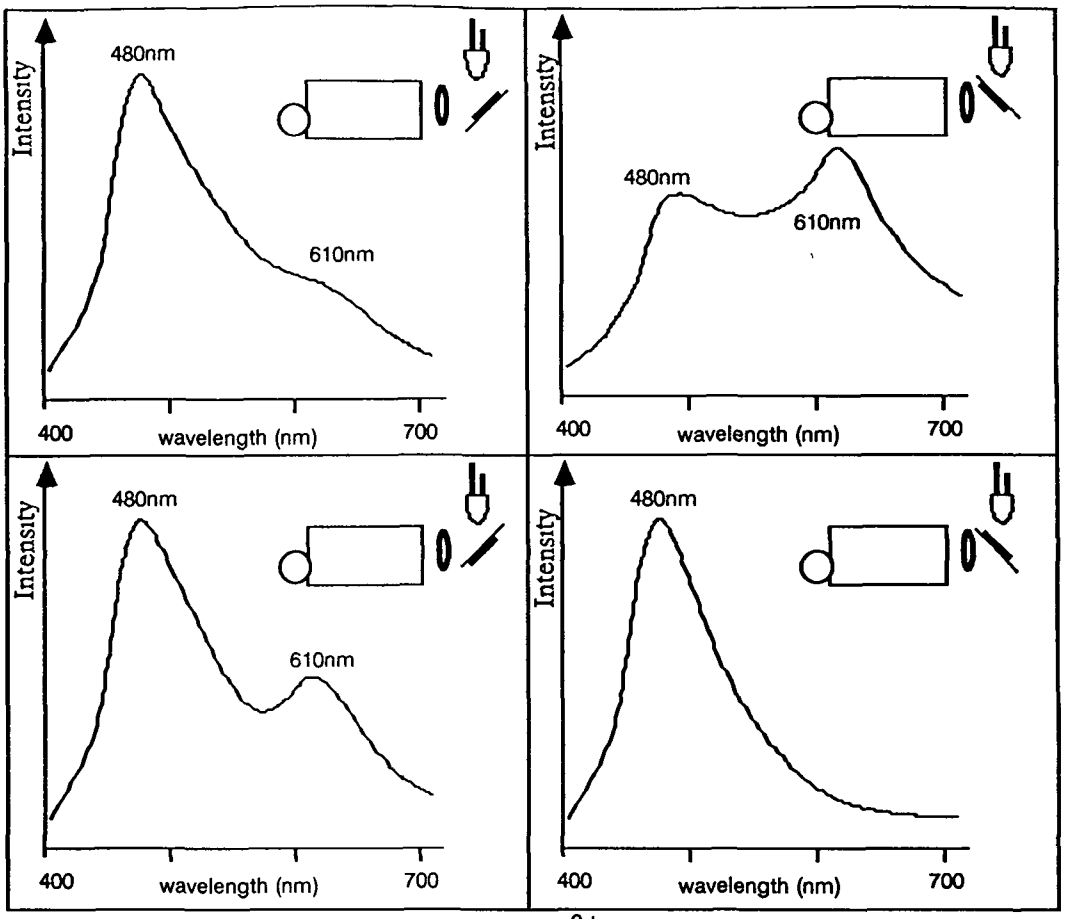

Figure V 3 Ru $(bpy)_3^{2+}$ / SiC LED
Fluorescence emission spectra recorded for different experimental configurations of LED and Nafion containing dye

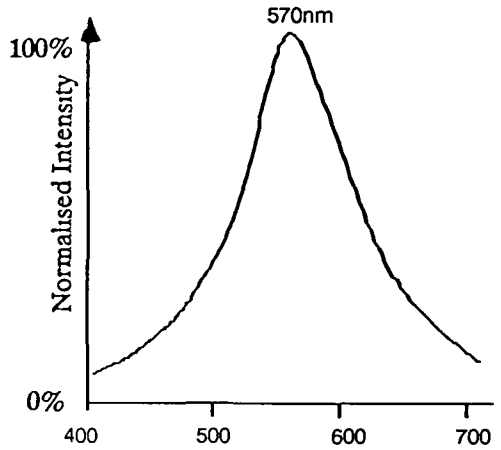

Figure V 4 Ru $(bpy)_3^{2+}$ in Nafion on LED dome surface

signal, as this region of the polymer is expected to have a much higher concentration of dye than the inner regions because of the slower diffusion of dye within the Nafion matrix

V C(3) Ru $(bpy)_3^{2+}$ in Nafion on LED dome surface

Some Ru $(bpy)_3^{2+}$ was incorporated into a Nafion film which had been applied to the surface of the LED Spectra were taken of this setup with a monochromator system This yielded some unusual results Neither the spectrum from the LED or Ru $(bpy)_3^{2+}$ were clearly visible, but rather a combination of the two that resulted in a peak at 570nm as shown in Figure V 4 This was explained as an overlap of the LED spectrum and the fluorescence emission spectrum of Ru $(bpy)_3^{2+}$, and therefore peaks at 570nm

V C(4) Use of LED with fibre optic sensor

Since the power levels of excitation light have steadily fallen, the feasibility of using an LED as light source for the fibre optic oxygen sensor is tested here The operating power levels of the sensor using the Ar ion laser beam are approximately 0 02μW which yields an observed signal of 10-20mV from the PMT when using the filter box configuration (§ Appendix A) These light levels are comparable to those which can be launched from an LED This has several advantages over a chopped laser source The first is that the power consumption of the sensor is greatly reduced (laser consumes approx 5kW) The second is that the need for a chopper is removed and that the LED can be driven at modulation rates of up to 500kHz The latter means that lifetime measurements should be possible for the fluorescent dyes used at present (Wolfbeis *et al*, 1988) The possibility of using lifetime measurements removes the need for a reference as the lifetime is independent of intensity, launching, detection etc (§ Appendix C)

D) Application of fibre optic oxygen probe

The fibre optic oxygen sensor described in this work was initially developed for use in measuring the radial oxygen concentration profile across Calcium Alginate beads Such pellets are used by the biochemical industry for the growth of micro-organisms in bioreactors for the production of drugs and other chemicals These pellets form the basic matrix for sustaining the organisms, which are nourished by the solution in which the pellets are placed It is important when making these pellets to optimise their size, as one of the major limiting factors is the diffusion of oxygen through the pellets If the pellets are too large, then the oxygen will not diffuse through to the centre of the pellet, as it is consumed by the growing cells If the pellets are too small, then the space in the bioreactor is not efficiently used Much work has been performed in modelling the process of the oxygen diffusion through living pellets (Walker *et al*, 1986)

The spatial resolution of the fibre optic oxygen probe (50nm calculated from the diffusion constant for oxygen in water and from the lifetime of the dye, § Chapter I F) is much less than the diameter of the fibre core which is given at 50μm, so this 50μm is taken as the minimum resolution The diameter of the Ca alginate pellets is approximately 4mm (although some of 10mm diameter have been made), and thus stepping across the pellet with 0 1mm spacing, an oxygen concentration profile can be built up The proposed experimental apparatus is described in Figure V 5 The probe would have to be operated at 37°C in the bioreactor environment, which means that effects of temperature on quenching become prominent The signal from the probe was found to

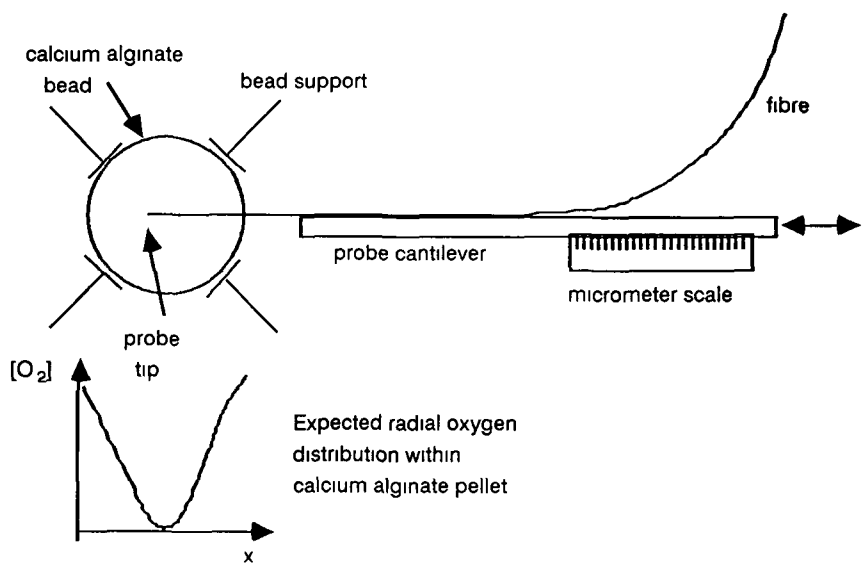

Figure V 5 Use of fibre optic oxygen sensor in measuring the radial oxygen concentration profile in Calcium alginate bioreactor pellets

decrease by 60% when the operating temperature of the probe went from 16°C to 38°C This poses the problem of increasing the signal noise This is a major problem as the probe is already operating with a relatively high noise level, thus increasing it will reduce the oxygen concentration resolution of the sensor At this time it is not known what procedures can applied to improve the sensitivity of the instrument at such temperatures

Chapter VI: Etching of optical fibres.

A) Introduction

Much work has been documented on etching SiO_2 using HF acid (Judge, 1971) and buffered HF (BufHF), where the buffered solution is typically composed of 9 parts 40% NH_4F to 1 part 48% HF This technology when applied to optical fibres has been used for creating microlenses on the ends of monomode communications fibre (Kayoun *et al*, 1981, Kawachi *et al*, 1982, Eisenstem and Vitello, 1982) and for splicing optical fibres with minimal losses (Svaasand *et al*, 1978, Hopland and Berg, 1979) In order to make microlenses on optical fibres, the cladding is etched away leaving portion of the core exposed as a raised mesa on the fibre end face The fibre end is then softened in a flame and a smooth lens is formed due to surface tension The mesa left over when the cladding is etched, has a height dependent on the relative rates of etching of the doped and undoped silica glass and the etch time The shape of the mesa depends on the radial distribution of the dopants Thus etching can be controlled by knowing the etch rates and how they are determined by the dopant profiles, as an increase in dopant is not always accompanied by an increase in etch rate (Hopland and Berg, 1979) The etched shape can be designed using multiple dopants with different etch rates

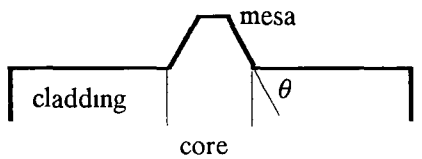

Kawachi *et al* (1982) described the sequence of events for etching a mesa onto the fibre end using step index fibres in BufHF They described a process in which the angle of the side of the mesa with respect to the base of the cladding remains constant and is given by the equation

$$\cos\theta = v_1 / v_2$$

where v_1 is the etch rate of the core, and

v_2 is the etch rate of the cladding

The same relation holds for a step index fibre etched in HF, except that a cavity is formed in place of a mesa

During the work for this thesis, a pattern of fibre etching in HF has been identified that does not follow the pattern described by Hopland and Berg (1979) even allowing for graded index fibre instead of step index. P_2O_5 doped graded index fibres etched in 48%HF were found to form a conical cavity. The development of this cavity was found to be unusual. When viewed under an optical microscope, the cavity was found to grow with constant apex angle. Further investigation using a scanning electron microscope showed that complex processes are responsible for the development of the etched cavity. The mechanism responsible for the cavity formation was investigated and the results from that study are shown here.

The fibre used for these investigations was 125/50μm multimode P_2O_5 doped graded index glass fibre supplied by Optical Fibres, Deeside, Clydd. Optical fibres, Deeside, have confirmed that the refractive index profile is bell shaped, but have not given the precise profile. Short samples of this fibre were cleaved and etched in 48% Hydrofluoric acid (HF) for varying lengths of time.

B) Observations of etched cavity.

There are several distinct features visible under electron microscope examination of samples of etched fibres. When the fibre is etched in HF for a short period, a set of concentric corrugations are visible that are thought to correspond to the various dopant concentrations required for the

During the work for this thesis, a pattern of fibre etching in HF has been identified that does not follow the pattern described by Hopland and Berg (1979) even allowing for graded index fibre instead of step index P_2O_5 doped graded index fibres etched in 48%HF were found to form a conical cavity The development of this cavity was found to be unusual When viewed under an optical microscope, the cavity was found to grow with constant apex angle Further investigation using a scanning electron microscope showed that complex processes are responsible for the development of the etched cavity The mechanism responsible for the cavity formation was investigated and the results from that study are shown here

The fibre used for these investigations was 125/50μm multimode P_2O_5 doped graded index glass fibre supplied by Optical Fibres, Deeside, Clydd Optical fibres, Deeside, have confirmed that the refractive index profile is bell shaped, but have not given the precise profile Short samples of this fibre were cleaved and etched in 48% Hydrofluoric acid (HF) for varying lengths of time

B) Observations of etched cavity

There are several distinct features visible under electron microscope examination of samples of etched fibres When the fibre is etched in HF for a short period, a set of concentric corrugations are visible that are thought to correspond to the various dopant concentrations required for the refractive index grading These corrugations are visible in Figure VI 1 showing a fibre etched for 15 seconds This feature is thought to be associated with the fabrication of the dopant profile (Figure VI 3, region B) The dopant P_2O_5 is added in discrete steps during the Outside Vapour Deposition (OVD) process used in the formation of the boule from which the fibre is drawn yielding step changes in composition dependent etch rate The second feature is the formation of the conical cavity that seems to etch at constant rate irrespective of dopant concentration

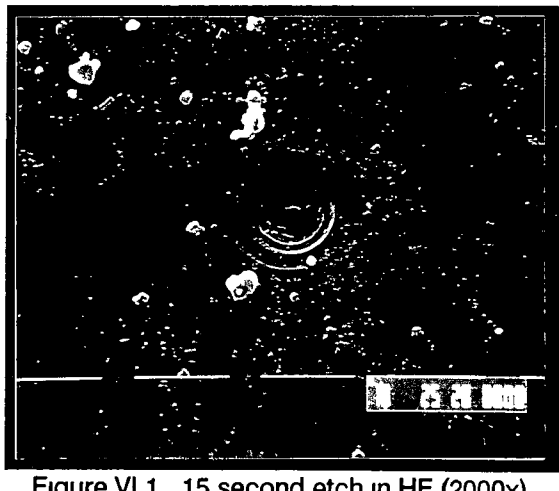

Figure VI 1 15 second etch in HF (2000x) (graded index P_2O_5 doped glass fibre)

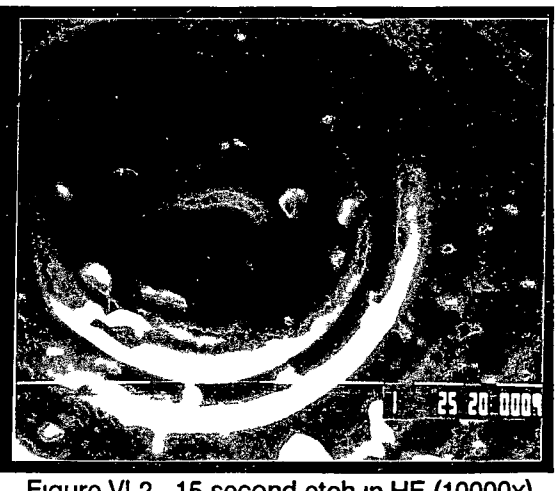

Figure VI 2 15 second etch in HF (10000x) (graded index P_2O_5 doped glass fibre)

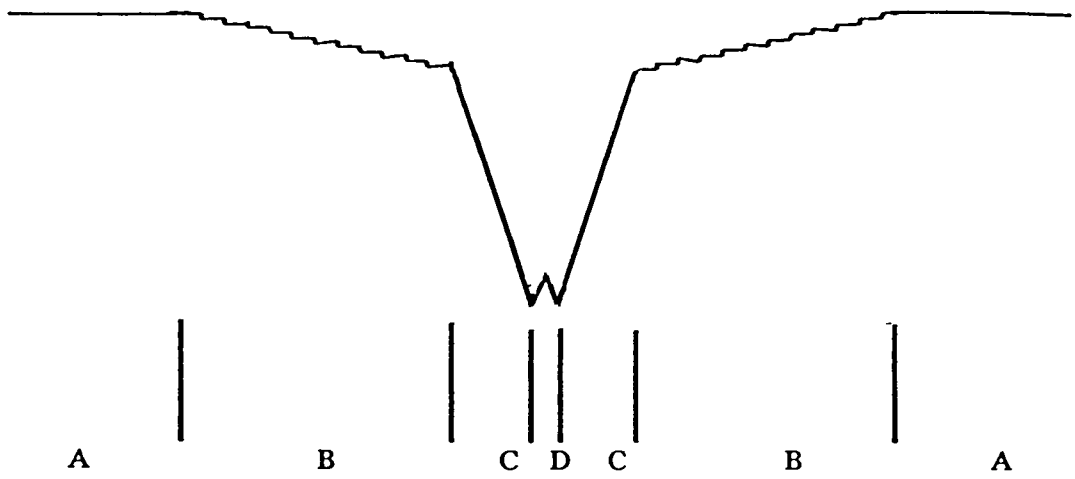

Figure VI 3 Structure of etched cavity
(Multimode fibre in48% HF)

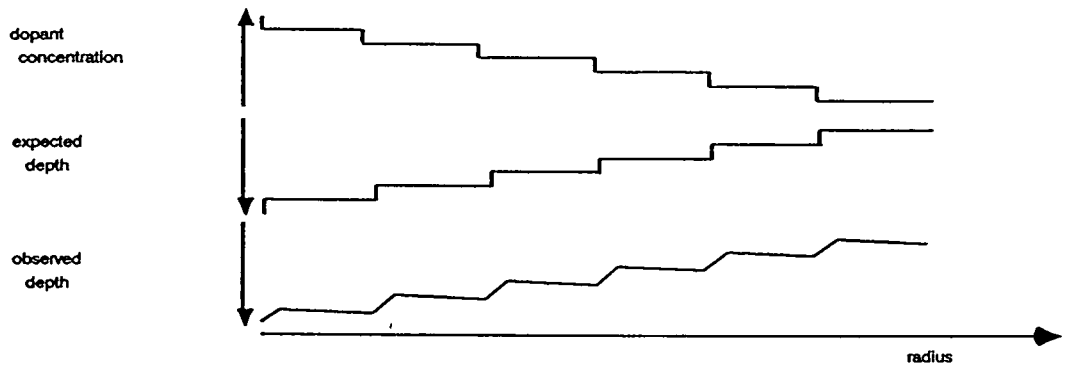

Figure VI 4 Observed dopant dependant structure
observed when etched in HF acid

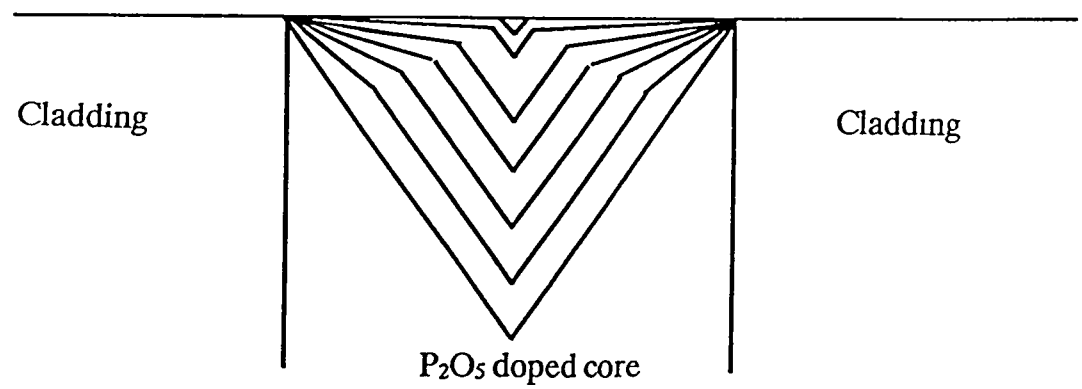

Figure VI 5 Progression of cavity etched in multimode
fibre in 48% HF etchant

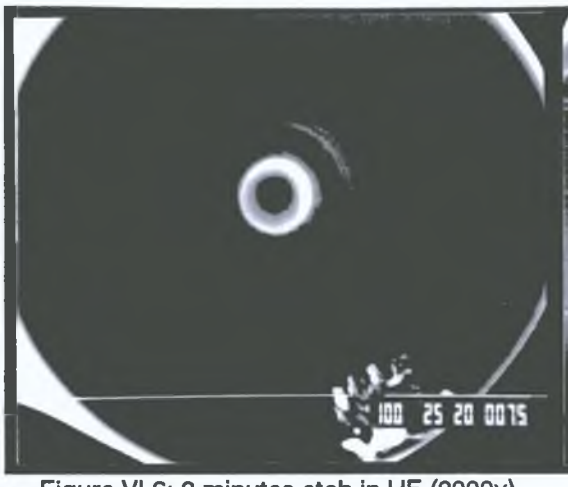

Figure VI.6: 2 minutes etch in HF (2000x)
(graded index P_2O_5 doped glass fibre)

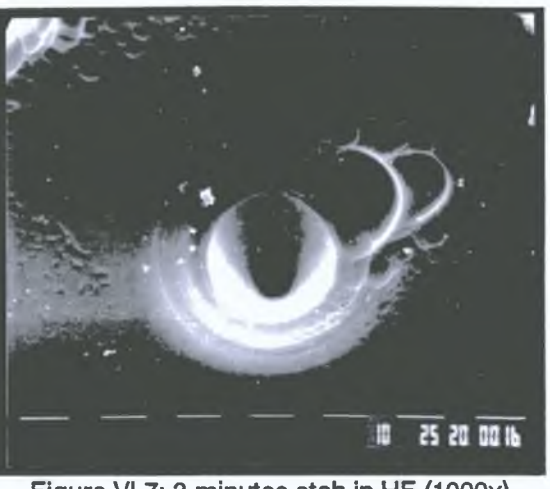

Figure VI.7: 3 minutes etch in HF (1000x)
(graded index P_2O_5 doped glass fibre)

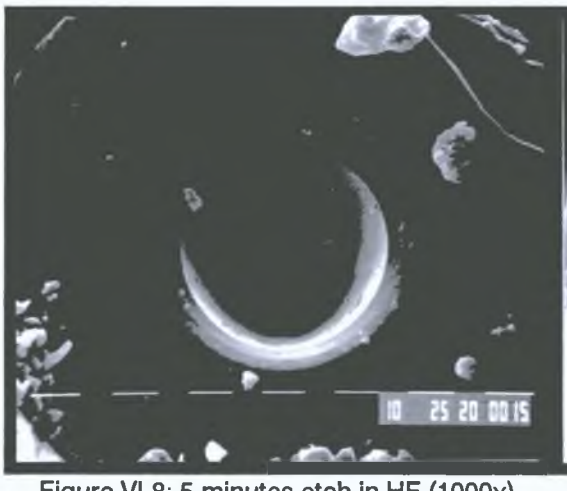

Figure VI.8: 5 minutes etch in HF (1000x)
(graded index P_2O_5 doped glass fibre)

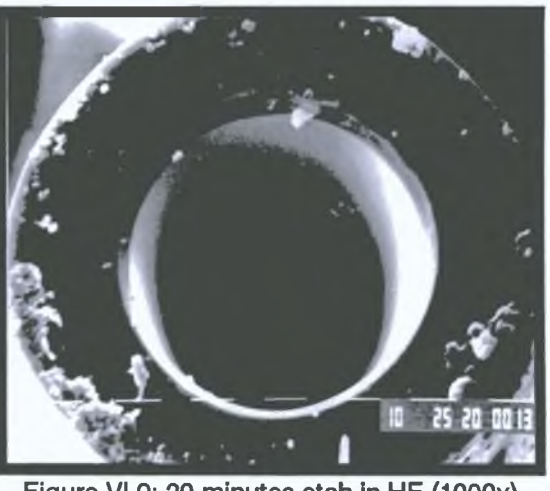

Figure VI.9: 20 minutes etch in HF (1000x)
(graded index P_2O_5 doped glass fibre)

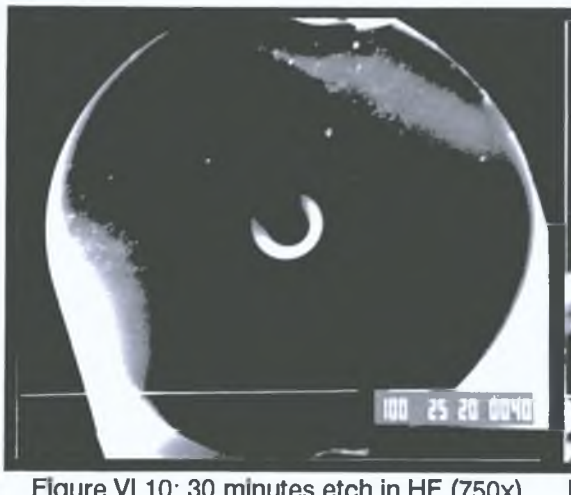

Figure VI.10: 30 minutes etch in HF (750x)
(step index GeO_2 doped glass fibre)

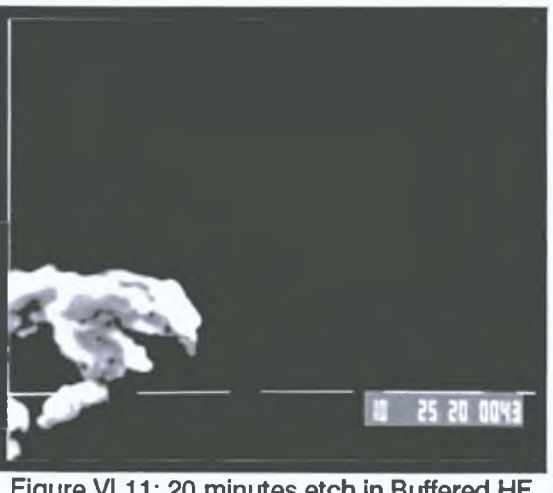

Figure VI.11: 20 minutes etch in Buffered HF
(step index GeO_2 doped glass fibre, 750x)

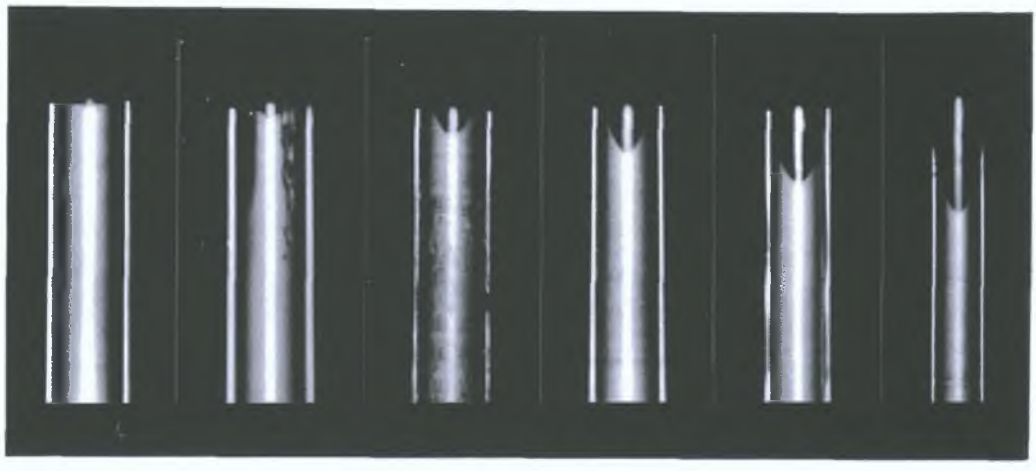

Figure VI.12: Sample P_2O_5 doped fibres
etched in 48% HF showing cavity development using conventional microscopy.
Etch times (left to right): 1 min; 2 min; 5 min; 10 min; 15 min; 20 min.

(Figure VI.3, region C). This cavity begins as a small indentation and grows steadily into the fibre end, deepening and widening, but maintaining a constant apex angle until it meets with the outside of the fibre. The cavity size is not limited to the doped core region, as the first described process is, and the etch rate normal to the surface seems constant with time. It can be seen from the electron micrographs in Figures VI.7, VI.8, VI.9 that the surface of the cavity has a different texture to that of the remaining fibre surface. This may be a deposited layer resultant from the etching process. X-ray analysis with the SEM yielded no additional information on the nature of this layer, but this is partially due to the overlap of the observed x-ray spectral lines for the gold coating (used in the preparation of the samples) and phosphorous / silicon. There is also a third process visible in the central region where a bump appears in the bottom of the cavity (Figure VI.3, region D). This is thought to be associated with the refractive index dip associated with OVD fibres. The region marked A in Figure VI.3 is that corresponding to the cladding, which is etched at the rate for undoped SiO_2.

C) Explanation / theories:

The first process mentioned above (observed as in Figure VI.3, region B), although assumed to be associated with the doping of the boule, does not precisely yield these step changes. On close examination, the steps observed in Figure VI.2 are not flat, but seem to be sawtooth in profile as shown in Figure VI.4. A further observation on these rings is that they are no longer visible after approx. 10 minutes etching. This may be due to the same process that governs etching at a step change as was discussed for monomode fibres.

The cavity region marked as C in Figure VI.3 is that which is not explained by the dopant distribution within the fibre. This part of the cavity is present from the start, and can be seen even after 5 seconds etching in HF. This cavity then seems to develop with constant cone apex angle of approximately 20° as estimated using the electron microscope. This cavity seems to grow irrespective of the dopant concentration and reveals no detailed structure. It should be noted that the walls of this central cavity have a different texture to the rest of the fibre. This is seen as a changed in the colour of the cavity wall on the electron micrographs. After 40 minutes, the walls steepen as the cavity deepens, but the apex angle remains the same forming a pointed barrel shaped cavity. After 60 minutes, the central etched cavity meets with the outside of the fibre, which has also etched inwards at the rate for undoped silicon. This fast growing cavity is not limited to the doped core of the fibre as expected from a dopant dependent process. The progression of the etched cavity is schematically shown in Figure VI.5. This drawing is based on observations from electron micrographs such as those shown in Figure VI.6, VI.7, VI.8 and VI.9 as well as fibres examined under conventional microscopy.

The central region (Figure VI.3, region D) which is seen as a small bump in the base of the cavity may be explained by the presence of a refractive index dip associated with CVD fibres. The refractive index dip is a region in the centre of the boule that is low in dopant due to dopant loss on completion of the deposition process.

Two models have been developed to explain the process of cavity formation, but at this time it is not possible to determine which of these models is correct.

VI:C(1) Model 1: Dopant related catalyst:

The first model put forward for the etching mechanism responsible for the constant angle conical cavity is as follows. When doped glass is etched, the dopant residue may act either as a catalyst for further etching of the SiO_2 or as a coating over the SiO_2 which limits access of HF to the surface. In either case, the etch rate becomes constant and independent of the dopant concentration. There is some evidence to support this in that several fibres were etched in HF containing 3 grammes of P_2O_5 in 10ml 48% HF and resulted in much larger than normal cavities. The etch rate for this dopant containing etchant was estimated to be approximately 2.5 times that for straight HF. There was no further increase in etch rate observed as the dopant concetration within the HF was increased. It is known that the P_2O_5 dopant is highly soluble in water and so will dissolve in the etchant before it is removed chemically. This can then yield localised regions of high P_2O_5 concentrations near the surface of the fibre being etched as well as having the effect of increasing the surface area of that region due to making the surface porous. It may be possible

that the dopant combines with the HF to form an intermediate compound which is responsible for the fast etch Such a compound would explain the presence of the coating visible on the walls of the cavity when viewed under an SEM The diffusion dependence of the etching process was investigated by placing the bottle containing the HF solution in an ultrasonic bath while the fibre was etched It was hoped that the cavitation would prevent buildup of a coating, but no change in the observed cavity was seen However, this may have been due to the polythene container for HF absorbing the ultrasound waves

The development of the secondary conical cavity can be explained by the high dopant concentration (~25%) in the center of the fibre (ignoring the presence of a refractive index dip for the present) which is dissolved out of the fibre and caused the enhanced etching process to proceed As the etching continues, more dopant or dopant / HF compound is liberated and allowed to diffuse through the newly formed cavity The super etch may then be limited by the rate at which the etched material can be removed from the surface The super etch process is thus independent of the concentration of P_2O_5 dopant within the fibre, but rather dependent on the concentration of dopant in solution at, or deposited on the fibre surface The constant shape of the cavity is explained by the etching process proceeding normal to the surface of the developing cavity This also explains how the observed cavity can grow beyond the doped region of the fibre and also why the corrugations observed at the early stages are no longer visible at later stages of etching (the super etch is much faster than the dopant concetration dependant etching) The chemistry of this P_2O_5 catalysed etching is not well understood and no reference was found in the literature to any process for optical fibres comparable to the one described above

VI C(2) Model 2 Stress enhanced etching

A second model was developed based on the influence of the structure of the fibre on the etch

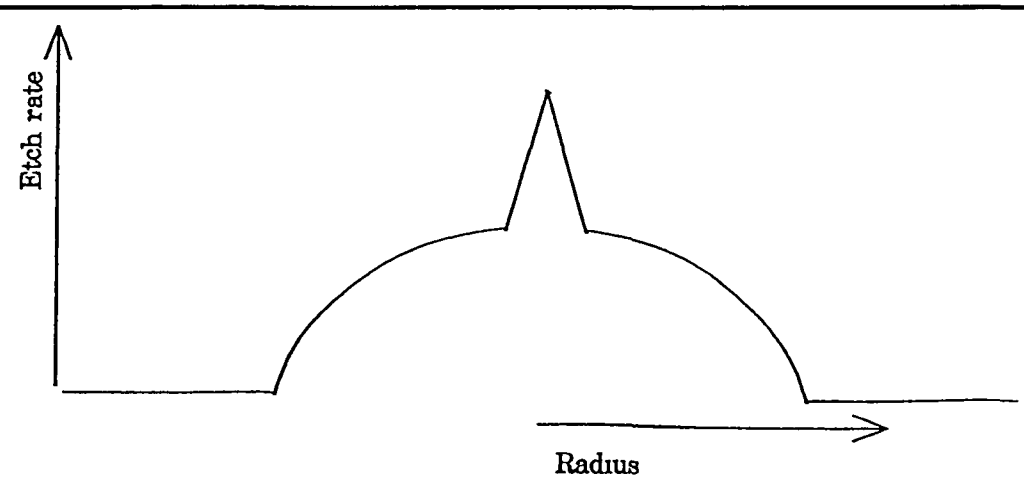

Figure VI 13 Etch rate profile for computer simulation of etching program (Appendix E)

rate If an etch potential curve is plotted (Figure VI 12) where the dopant distribution is superimposed on etch enhancing features and this curve is then given to an etching simulating program (§ Appendix E), the shape of the extra features can be investigated so that the observed cavity is developed It was found that if there existed an abnormally high etch rate in the centre of the fibre, then the two distinct cavity regions could be identified using the program listed in Appendix E The operation of the program is based on knowing the etch rate at a point and calculating the quantity of material removed This quantity is determined by the time interval, the etch rate and the surface area over which the etching can proceed The latter factor is calculated from knowing whether the point of interest is above or below the surrounding area If below, then etching can only proceed from above, and so this factor is zero, while if the point is proud of the surroundings, then etching can also take place from the sides This program was found to yield the observed result for step index fibres using the same calculations as those for the graded index fibres The nature of such a high etch rate is not understood, but a number of possible explanations exist The most plausible may be due to stresses induced during the cooling of the glass fibre shortly after being drawn If the thermal expansion coefficient for doped silica is greater than that for pure silica, then as the drawn fibre cools the cladding exerts a tensile force on the core due to the greater contraction of the core A second region of stress occurs where the doped core contracts around the refractive index dip (pure silicon), generating compressive stresses in the centre of the fibre The stress induced in the centre of the fibre is much greater than that at the cladding / core interface since the transition from pure to doped silicon is much steeper Further stress instability may be caused by the action of cleaving the fibre This would explain why

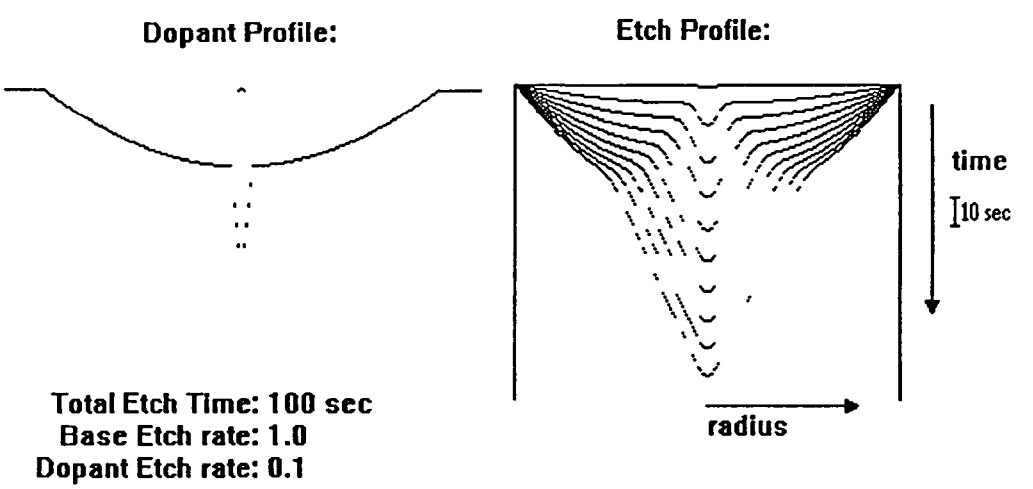

Figure VI 14 Results of computer simulation using data from Figure VI 13

the central region of the fibre is etched almost immediately as the fibre is inserted into the HF solution

The corrugations visible during the early stages of etching were seen not to be flat, but sawtooth shape as shown in Figure VI 4 The above theory may explain this, since there is a region of higher stress associated with every step change in dopant concentration

One feature which the simulation does not account for is that the corrugations are no longer visible after 5 minutes etching in HF This may be explained by limiting the stress factor to only be active during the early stages of etching that may be due to high stress regions at the surface of the freshly cleaved fibre due to the action of cleaving destroying the balance of forces in the fibre structure It may be that after the initial stages, other more conventional processes take over

D) Conclusion

Both models account for some of the features observed The most likely situation is where both theories are combined to explain the complete etching process The assumptions made for the second model would serve to explain what happens during the initial phase, while the first model would explain the development of the conical cavity

To determine the full process responsible for the etching of fibres in HF, more complete specifications for the composition of the fibre used in the work needs to be obtained Although this information was requested from the manufacturers, it was not released The chemistry of the etching of silica and P_2O_5 doped silica needs to be understood, especially the nature of products formed in the process It is also necessary to explore the etching of fibres manufactured using other dopants This was carried out partially by the etching of monomode fibres that are GeO_2 doped The action of annealing fibres before etching can also be explored to examine the stress component of the etching, especially during the early stages

The explanations offered for the etching process causing the constant angle conical cavity observed in graded index P_2O_5 doped silica describe how the mechanism may proceed, although it does not account for the detailed chemical and physical processes that occur

Chapter VII: Discussion

This work has described an oxygen sensor based on the quenching of fluorescence of Ruthenium compounds immobilised on 50μm core optical fibres The sensor has a fast response time and high spatial resolution Good short term stability has been shown, although long term stability was at times poor This sensor has a number of distinct advantages over other fibre optic oxygen sensors which are described below

The design of this sensor is based on the use of a single 50μm core multimode glass optical fibre Other fibre optic sensor systems use either a multi-fibre system or large diameter (typically 200μm) fibres in their designs In multi-fibre systems, usually one fibre carries the excitation light and the remaining fibres return the emitted light to the detector In our sensor design, we have used a fibre optic 4-port coupler to allow for the alignment between the light source and fibre, fibre and detector to be simplified This has not been used before The spatial resolution of the probe is calculated from the interaction distance between the oxygen molecules and the excited fluorescent dye molecules, which was calculated at 50nm (§ Chapter I E), and the volume in which the quenching interaction can take place The latter sets an upper limit of the resolution at the diameter of the fibre core (50μm) which is the value adopted here The resolution in the direction of the fibre axis is very much better than this value at 50nm, but the localised oxygen concentration can only be calculated accurately to within one fibre diameter This is the highest spatial resolution obtained to date using a fibre optic oxygen sensor and is due to the use of a single fibre

In this work, a novel method for dye immobilisation on optical fibres was developed for use with positively charged fluorescent dyes This method involves the use of an ion exchange resin, Nafion, which is bound to the fibre using silamsation techniques (§ Chapter I F, II D(2)) This polymer film was found to be securely bound to the fibre and immune to most mechanical abrasion This dye entrapment also has the advantage of limiting the size of the fibre probe to the diameter of the fibre as the thickness of the film is $< 5\mu$m as was found during examination of fibre tip under an electron microscope This feature along with the etched cavity makes for a compact sensing element which is smaller than others described in the literature The sensing element which retains the active dye usually takes the form of an envelope surrounding the fibre / fibres This greatly increases the diameter of the probe as well as reducing the mechanical stability of the tip The thinner polymer used in this sensor greatly influences the response time which was determined to be of the order of 5 seconds (§ Chapter IV B(6)) using short lock-in amplifier integration times The effective response time is a compromise between the excitation intensity dependent signal decay, and the size of the signal to noise ratio required for accurate readings An optimum

excitation power was found to be at 0 05μW with a lock-in post filter integration time of 3 seconds The levels of excitation light intensities are many orders of magnitude smaller than those commonly used in previous systems (normally using 50W filtered white light source and yielding several milliwatts of power at the sensing tip) The sensor described in this work uses 0 05μW of Ar ion laser excitation light at the sensing tip This has several advantages The longevity of the sensing dye is improved as photobleaching, photodecomposition and other photo-induced decay processes are greatly reduced at these light levels This is of importance when considering the sensing dyes used in the sensor The fluorescent species Ru $(bpy)_3^{2+}$ is quite active photochemically as it was initially designed for splitting water using visible light, and thus any reduction in excitation light will reduce the effects of this activity This reduction in excitation power also improves the performance of the other dye used, Ru $(phen)_3^{2+}$ The second advantage of the use of low excitation intensities is that the safety of the sensor in hazardous environments is improved as the output light level is well within the recomended safe limits (§ Chapter I B(4)) The lower excitation intensity also means that the possibility of the light from the sensor causing spurious effects in biological systems is also reduced

The sensitivity of the Ru $(phen)_3^{2+}$ based sensor was estimated at 0 053 bar dissolved oxygen partial pressure from a signal with noise level of 1 2% and a full scale signal change from 900 to 615 (N_2 to O_2 saturated water) This sensitivity was offset, however, by signal drifts observed which could not be explained or quantified The presence of this drift is evident from the intensity monitor scans shown in Chapter IV Ru $(phen)_3^{2+}$ probe characterisation

The Ru $(phen)_3^{2+}$ probe was found to operate well in a gaseous environment During the work investigating this aspect of the sensor operation, a probe was let dry fully in air (§ Chapter IV 11) The dry probe was then inserted into a gas blending chamber which was set to various concentrations of oxygen The probe was found to respond similar to that for dissolved oxygen, and the stability of the probe was not affected during gaseous operation The use of an oxygen permeable membrane such as polystyrene (§ Chapter II D(4)) allows the sensor to operate freely in both aqueous and gaseous environments without adversely affectmg the probes performance The sucess of the probe in gaseous environments is attributed to the high diffusion rate of oxygen in the fluorocarbon matrix in the Nafion polymer which then removes the dependence of the sensor probe on water It should be noted that the probe tip was dried in laboratory air with 40% - 70% relative humidity and not dried using a dessicator with the result that the polymer matrix may contain water which serves to keep the Ru $(phen)_3^{2+}$ in an aqueous environment

The choice of Ruthenium based fluorescent dyes was made on the basis of the oxygen sensitivity,

the quantum fluorescence efficiency and most important, the excitation and emission wavelengths which show a large Stoke's shift The dye Ru $(bpy)_3^{2+}$ has been well documented in the literature, especially for sensitising Nafion coated electrodes The Ru $(bpy)_3^{2+}$ was not found to have the required stability for use with a sensor such as this, which resulted in the use of Ru $(phen)_3^{2+}$ This dye has essentially the same optical characteristics as the Ru $(bpy)_3^{2+}$, while showing stronger π bonding between the Ru metal ion and the "phen" ligand This greatly improves the performance of this dye resulting in reduced photo-induced decay A third dye was tested, Ru $(bdt)_3^{2+}$, and was found to be less suited to the present probe Although the "bdt" ligand has stronger π accecptance than "phen", it has fluorescence emission maximum at 660nm and a lower quantum efficiency (0 001) (Fennema *et al*, 1991) which makes using it in an optical instrument more difficult No improved stability was observed for a probe using the Ru $(bdt)_3^{2+}$ as sensing dye

The idea of referencing the probe with a second insensitive dye has not been used before For short term stability, there may not be any need to reference the probe, but for long term reliability, this is necessary The use of a short life time dye (Os $(bpy)_3^{2+}$, τ = 15ns) in conjunction with the sensing dye (Ru $(bpy)_3^{2+}$, τ = 580ns) should result in a probe which chemically behaving like one containing only one species and allowing all but the oxygen dependence of the sensor to be characterised The difference in the fluorescence maxima of the two dyes (608nm and 715nm) is well suited to simultaneous monitoring of the sensor and reference dyes, as simple filter arrangements can be used The use of a second reference dye was investigated (§ Chapter V B), but instabilities were found in the form of an interaction between the two dyes which made it impractible to use the second dye The instabilities were observed as fluctuations in the relative intensities of the two dyes This suggests that there is constant mixing of the two dyes within the polymer matrix which does not reach a stable equilibrium The mixing of two dyes in solution is expected to reach thermodynamic equilibrium, but this may not be the case when two dyes in Nafion are considered This state of no equilibrium may be due to the high concentrations of dye in the Nafion polymer, where there can be no stable state with the process of dye retention active in the ion exchange resin This process may also be responsible for the unexplained medium term instabilities observed in the sensor using just one dye, either Ru $(bpy)_3^{2+}$ or Ru $(phen)_3^{2+}$, but no solid evidence was found to support this A method is outlined at the end Chapter V B which may overcome the problems observed, but this was not attempted due to lack of time

The fluorescence signal from the fibre optic probe was found to be very temperature sensitive, with the observed signal dropping to 60% when changing from 16°C to 38°C The dependence was found to be exponential in nature and can be removed from the data once the probe in use

was characterised with respect to temperature This dependence was found to take the form of $I = I_0 10^{-Ct}$, where the constant C was calculated experimentally to be approximately 0 011°C^{-1} and t is temperature given in Celcius

The oxygen probe based on the use of Ru (phen)$_3^{2+}$ as the sensing dye was characterised to determine the intensity at a given time using constants determined experimentally for probes operating with excitation intensities of 0 05μW (§ Chapter IV B(8)) This equation takes into account the effects of temperature, excitation light exposure and the presence of oxygen The Stern - Volmer quenching constant was found to be 0 5 (§ Chapter IV B(4)), while the illumination decay constant was found to be 0 025 %/μW/min These terms can be combined to give the following equation

$$I = I_z \left(\frac{(100 - D_C P_{ex} M) / 100}{(1 + K_q [Q]) 10^{Ct}} \right) + O_c$$

where

O_c = constant offset, possibly caused by light leakage into detector system
I_z = calculated initial intensity without offset
[Q] = partial pressure (bar) of oxygen in equilibrium with the solution
M = exposure time (mm) of probe to P_{ex} excitation power
t = temperature (°C)
D_C = illumination decay constant (%/μW/mm) eg 0 5%/μW/min @ 0 05μW
P_{ex} = excitation power (μW)
K_q = Stern - Volmer quenching constant (0 5/bar)
C = temperature decay constant (/°C) eg 0 011/°C for Ru (phen)$_3^{2+}$ @ 0 05μW

There still exist a number of discrepancies which remain unresolved, namely the stability of the two dye system mentioned above, the long term stability of the probe and the process responsible for the dye uptake into the Nafion ion exchange resin The long term stability of the probe was generally found to be quite good where old probes were tried after long periods of disuse For example, a probe which was stored in air for a period of 3 months was used and found to behave as well as a similarly prepared fresh probe There are certain instabilities associated with the probe which appear to be random in nature This drift has been observed for the Ru (phen)$_3^{2+}$ probe as a maximum 5% change in intensity over 30 - 60 minutes, although no drift was observed during several monitor scans

According to Gierke (1982), the internal structure of the Nafion membrane is constantly evolving

with old cavities collapsing and new cavities being formed If this were the case in the Nafion used in this sensor, then this would have the following implications The precise effect that this evolving structure has on the fluorescence properties of a dye retained in this cavities is not known, but it is estimated that this changing environment can be seen as a change in intensity The reason for this change may be that the dye may be exposed alternately to hydrophobic and hydrophilic environments which will affect the fluorescence emission Such a changing environment may not only account for the instabilities observed for the Ru $(phen)_3^{2+}$ probe, but also for the case where the two fluorescent dyes, Ru $(bpy)_3^{2+}$ and Os $(bpy)_3^{2+}$ were incorporated into the same polymer, where there does not seem to be a stable equilibrium state for the two dyes

Alternate explanations for the drifting observed in the intensity form the fibre probe may be associated with the launching of the excitation light, where the modal power distribution accross the laser beam is changing, with the result that the intensity of light launched changes

It was mentioned that there is a discrepancy in results taken for characterising the rate of uptake of Ruthenium dyes by the Nafion polymer The fluorescent intensity was found initially to be maximised after 30 minutes soaking in Ru $(bpy)_3^{2+}$ (§ Chapter III B(6)), while one year later, this maximum was found to occur within 30 seconds (§ Chapter IV B(7)) The reason for this difference is not known, although it is suspected that there was a difference between the two samples of Nafion used during the experimental work The stock solution of Nafion was found to behave as expected and this was verified by using a freshly purchased Nafion solution It is thus possible that the sample of Nafion used initially had changed in nature in such a way as to reduce the ion exchange capacity of the polymer The details of such a change are not known, but may take the form of a contaminant, partial crystalisation of the Nafion is solution, or a change in the solubility stabilisers used in the commercial product

Conclusion

The work described in this thesis results in a fibre optic based oxygen sensor which has a well characterised sensitivity and stability The spatial resolution of the sensor is quite high at 50μm minimum and a fast response time of 5 seconds Although temperature dependence is quite high, it has been well characterised and is a known quantity Work was done on referencing the probe by using a second dye incorporated with the sensing dye Supplementary work was performed on the study of the etching of glass optical fibres in HF acid and developing models to account for the sequence of events observed

References and bibliography:

This reference section is intended to give the reader a list of material which is related to the work described in this thesis While all the references made in the text are contained here, many of the papers listed give a more detailed account of some of the more specialised aspects of the sensor development, such as the bonding of Nafion to glass and the etching of optical fibres in HF Those papers marked with (*) are core to the work described here, while the others are intended for the more enthusiastic reader

Ainsley K.J , Seales K J , Cooper D M and Day C R
Fabrication and evaluation of MCVD single-mode fibres with and without central index depression
Elect Lett Vol 18 No 19 (Sept 1982) pp 908-811

Angel P F Daley S M and Kulp T.J
Optical chemical sensors for environmental monitoring
Proc Symp Chem Sens Vol 87-9 (1987) pp 484-489

*Anson F C , Tsou Y and Saveant J M
Outer-sphere oxidation of ascorbate with Os trisbippy incorporated in Nafion coatings on graphite electrodes
J Elect Chem Vol 178 (1984) pp 113-127

Armstrong N R
Silylation reactions applied to attachment of dye molecules to semiconductor electrodes
Midland Macromol Monogr Vol 7 (1978) pp 159-171

Bacci M , Baldini F , Brenci M , Conforti G , et al
Model for optical fibre pH sensor
SPIE Vol 713 (1986) pp 88

*Bacon J R and Demas J N
Determination of oxygen concentrations by luminescence quenching of a polymer-immobilised transition-metal complex
Anal Chem Vol 59 (1987) pp 2780-2785

*Balzani V , Moggi L , Manfrin M F , Bolletta F and Laurence G G
Quenching and sensitisation process of coordination compounds
Coord Chem Rev Vol 15 (1975) pp 321-433

Barbieri E , Roxey T , Khoury A and Abela G S
Evaluation of optical properties and laser effects on arterial tissue using a microlens tipped optical fibre
SPIE Vol 713 (1986) pp 166

*Bataillard P , Clechet P and Jaffrezic-Renault N
Silanisation of Si/SiO_2 structures for detection of silver ions
J Electrochem Soc (Aug 1986) pp 1759-1760

*Baumgartl H and Lubbers D W
Microcoaxial Needle sensor for polarographic measurement of local O_2 pressure in the cellular range of living tissue
Polarographic O_2 sensors Vol (1983) pp 37

Bear P H
Microlenses for coupling single-mode fibres to single-mode thin-film waveguides
Appl Opt Vol 19 No 17 (Sept 1980) pp 2906

*Benson D M, Knopp J A and Longmuir I S
Intracellular oxygen measurements of mouse liver cells using quantitative fluorescence video microscopy
Biochem Biophys Acta Vol 591 (1980) pp 187-197

*Bergman I
Rapid response atmospheric oxygen monitor based on fluoresence quenching
Nature Vol 218 (April 1968) pp 396

*Bergman I
Metalised membrane electrode Atmospheric oxygen monitoring and other applications
Nature Vol 218 (April 1968) pp 266

Bibby G W, Ross J N, Dakin J P and Pratt D J
Raman Thermometry using optical fibres
Anal Proc Vol 22 (Jul 1985) pp 213

Birch D J S and Imhof R E
Kinetic interpetation of fluorescence decays
Analytical Instrun Vol 14 No 3&4 (1985) pp 293-324

*Blatt E and Sawyer W H
Depth dependant fluorescence quenching in micelles and membranes
Biochem Biophys Acta Vol 822 (1985) pp 43-62

Bradley P G, Kress N, Hornberger B A and Dallinger R F et al
Time resolved resonance raman study of $Ru(bpy)_3^{2+}$ and related complexes Definite evidence for the localised MLCT
J Am Chem Soc Vol 103 (1981) pp 7441-7446

Brady R, Miller W V and Vaska L
Luminescence of d8 complexes of iridium and rhodium and its quenching by molecular oxygen and other gases
J C S Chem Comm Vol (1974) pp 393-394

Bright F V, Vickers G H and Hieftje G M
Use of time resolution to eliminate bilirubin interference in the determination of fluorescein
Anal Chem Vol 58 (1986) pp 1225-1227

*Bright F V, Poirier G E and Heiftje G M
A new ion sensor based on fibre optics
Talanta Vol 35 No 2 (Feb 1988) pp 113-118

*Buell S L and Demas J N
Heterogenous preparation of singlet oxygen using ion-exchange-resin-bound trisbipyridyl ruthenium photosensitiser
J Phys Chem Vol 87 (1983) pp 4675-4681

*Buttry D.A and Anson F C
Electrochemical control of the luminescent lifetime of Ru $(bpy)_3^{2+}$ incorporated in NAFion films on graphite electrodes
J Am Chem Soc Vol 104 (1982) pp 4824-4829

Buttry D.A and Anson F C
Effects of electron exchange and single file diffusion on charge propogation in Nafion films containing redox couples
J Am Chem Soc Vol 105 No 4 (Feb 1983) pp 685-689

Caspar J V , Kober E M , Sullivan B P and Meyer T.J
Application of the energy gap law to the decay of charge-transfer excited states
J Am Chem Soc Vol 104 (1982) pp 630-632

Christian L M and Seitz W R
An optical ionic-strenght sensor based on polyelectrolyte association and fluorescence energy transfer
Talanta Vol 35 No 2 (Feb 1988) pp 119-122

*Cirlot G B , Kelly J M , Lyons M E G and McCormack D E
Electrochemical properties of Ruthenium oxidex and some photo-induced electron transfer reactions in Nafion ionomers
J ElectroChem (1989)

Cohen L G , Kaiser P , MacChesney J B and O'Connor P B
Transmission properties of a low-loss near-parabolic-index fibre
Appl Phys Lett Vol 26 No 8 (Apr 1975) pp 472-474

Coleman J , Eastham J F and Sepamak M J
Fibre optic based sensor for bioanalytical absorbance measurements
Anal Chem Vol 56 (1984) pp 2246-2249

*Creutz C , Chou M , Netzel T L , Okumura M and Sutin N
Lifetimes, spectra and quenching of the excited states of polypyridine complexes of Iron(II) Ruthemum(II) & Osmium(II)
J Am Chem Soc Vol 102 No 4 (Feb 1980) pp 1309-1319

*Dakin J P
Spectral filtering optical fibre sensors
Anal Proc Vol 22 (Jul 1985) pp 214

*Delapierre G
Micro-Machining A survey of the most commonly used processes
Sensors and Actuators Vol 17 (1989) pp 123-138

*Demas J N and Crosby G A
Quantum efficiencies of transition metal complexes Charge transfer luminescence
J Am Chem Soc Vol 93 No 12 (Jun 1971) pp 2841

*Doremus R H
Glass Science Chemical reactions
Glass Science (Wiley) (1973) pp 247

*Duportail G and Weinreb A
Photochemical changes of fluorescent probes in membranes and their effect on the observed fluorescence amsotropy values
Biochem Biophys Acta Vol 736 (1983) pp 171-177

*Durham B , Caspar J V , Nagle J K and Meyer T J
Photochemistry of $Ru(bpy)_3^{2+}$
J Am Chem Soc Vol 104 (1982) pp 4803-4810

Durham B , Wilson S R , Hodgson D.J and Meyer T J
Cis-trans photoisomerisation in $Ru(bpy)_2(OH_2)_2^{2+}$ Crystal structure of trans-$[Ru(bpy)_2(OH_2)(OH)](ClO_4)_2$
J Am Chem Soc Vol 102 No 2 (Jan 1980) pp 600 607

Edmonds T E and Ross I D
Low-cost fibre optic chemical sensors
Anal Proc Vol 22 (Jul 1985) pp 206

*Eickhoff W and Weidel E
Measurmg method for the refractive index profile of optical glass fibres
Opt Quant Elect Vol 7 (1975) pp 109-113

*Eisensein G and Vitello D
Chemically etched conical microlenses for coupling single-mode lasers mto single-mode fibres
Appl Opt Vol 21 No 19 (Oct 1982) pp 3470

*El-Hoshy A H
Measurement of P-etch rates for boron-doped glass films
J Electrochem Soc Solid State Science Vol 117 No 12 (Dec 1970) pp 1583-1584

*Elliott C M and Redepenning J G
Aqueous and non-aqueous electrochemistry in thick-film Nafion/mercury modified electrodes
J Electroanal Chem Vol 181 (1984) pp 137-152

*Elmer T H
Glass surfaces
Midland Macromol Monogr Vol 7 (1978) pp 1-30

*Ennis P M , Kelly J M and O'Connell C M
Preparation and photochemical properties of water-soluble polymers with pendant tris(2,2'-bipyridyl)ruthemum(II) groups
J Chem Soc Dalton Trans Vol (1986) pp 2485

Erickson H H , Cholvin N R , Swift C S and Pearson P T
Reflection oxymetry its use during cardiopulmonary bypass and artificial heart studies
Int Conf Med Bio Eng Vol 7th (1967) pp 18-10

Evans C C , Macrae J C and Wilson S
Determination of ruthenium and chromium by X-ray fluorescence spectroscopy and the use of inert ruthemum(II)phenantroline
J Agric. Sci. Comb Vol 89 (1977) pp 17-22

Fales E M and Penneys R
Further experiments *in vitro* with a platinum oxygen microelectrode
Int Conf Med Bio Eng Vol 7th (1967) pp 18-8

Federer J I
The effect of reactive gasses on oxygen sensor responses
J Electrochem Soc ElectroChem Science and Tech Vol 131 No 4 (Mar 1984) pp 755 - 760

Fennema B D.J R , deGraaff R A G, Hage R and Vos J G
Ruthenium(II) compounds containing a novel strong π accecpting ligand, 2,2'-dimethyl-5,5'-bis 1,3,4-thiadiazole
J Chem Soc , Dalton Trans (in press)

Fetterolf M L and Offen H W
Luminescence of Ruthenium(II) and Osmium(II) polypyridyls in acetonitrile at high pressures
J Phys Chem Vol 89 (1985) pp 3320-2233

*Fuh M S , Burgess L W , Hirschfeld T and Christian G D
Single fibre optic fluorescence pH probe
Analyst Vol 112 (Aug 1987) pp 1159

*Gabardi D R and Shealy D L
Coupling of domed light-emitting diodes with a multimode step-index optical fibre
Appl Opt Vol 25 No 19 (Oct 1986) pp 3435

*Gebel G , Aldebert P and Pineri M
Structure and related properties of solution-cast perfluorosulfonated ionomer films
Macromolecules Vol 20 (1987) pp 1425-1428

*Gehrich J , Lubbers D , Opitz N and Hansmann D
Optical fluorescence and its aids in application to an intravascular blood gas momtoring system
IEEE Biomed Eng Vol BME-33 No 2 (Feb 1986) pp 117

Ghosh P K and Spiro T G
Photoelectrochemistry of tris(bipyridyl)ruthemum(II) covalently attached to n-type SnO_2
J Am Chem Soc Vol 102 (1980) pp 5543-5549

*Gleria M , Minto F , Beggiato G and Bortolus P
Photochemistry of tris(2,2'-bipyridine)ruthenium(II) in chlorinated solvents
J C S Chem Comm Vol (1978) pp 285

*Gierke T D , Munn G E and Wilson F C
J Pol Sc Pp Vol 19 No 11 (1981) 1687 - 1704

*Gierke T D , Munn G E and Wilson F C
Acs Symp S Vol 180 (1982) 195 - 216

Goswami K , Klainer S M and Tokar J M
Fibre optic chemical sensor for the measurement of partial pressure of oxygen
SPIE 1988 Vol 990 (1988) pp 111-115

*Gottesfeld S , Raistrick I D and Srinivasan S
Oxygen reduction kinetics on a platinum RDE coated with a recast Nafion film
J Electrochem Soc Vol 134 No 6 (June 1987) pp 1455-1462

Grimnes S
Catheter electrode for absolute determination of oxygen tension
Int Conf Med. Bio Eng Vol 7th (1967) pp 18-9

*Grot W
Use of Nafion perfluorosulfonic acid products as seperators in electrolytic cells
Chem Ing Tech Vol 50 No 4 (1978) pp 299-301

*Grot W G
Nafion membrane and its applications
Electrochem Ind Vol (1980) pp 73-87

Guckel H , Smegowski J.J , Christenson T R and Mohney S
Fabrication of micromechanical devices from polysihcon films with smooth surfaces
Sensors and Actuators Vol 20 (1989) pp 117-122

*Hager G D and Crosby G A
Charge transfer excited states of ruthenium(II) complexes I) Quantum yield and decay measurements
J Am Chem Soc Vol 97 No 24 (Nov 1975) pp 7031-7042

Harmer A L
Guided-wave chemical sensors
Proc Symp Chem Sens Vol 87-9 (1987) pp 409-427

*Harrell S.A and Peoples J R
SiO_2 etch rate in HF solutions I Addition of H_2SiF_6 to buffered HF
Electrochem Soc Vol 112 (1965) pp 247-249

Harrison D J , Turner R F B and Bates H P
Characterisation of perfluoroulfonic acid polymer coated enzyme electrodes and a miniaturised integrated potentiostat for glucose analysis in whole blood
Anal Chem Vol 60 (1988) pp 2002-7

Henning T P , White H S and Bard A J
Polymer films on electrodes Biconductive polymers produced by incorporation of tetrathiafulvalenium in a Nafion matrix
J Am Chem Soc Vol 103 (1981) pp 3937-3938

Hillard L A
Application of single optical fibres to remote absorption measurements
Anal Proc Vol 22 (Jul 1985) pp 210

*Hills P C
Intrinsic safety of optical fibres in combustible environments
Elect Lett Vol 26 No 23 (Nov 1990) pp 1982-3

Hirschfeld T , Deaton T , Milanovich F and Klainer S
Feasibility of using fibre optics for monitoring groundwater contaminants
Optical Eng Vol 22 No 5 (Sept 1983) pp 527

Hirschfeld T , Miller F , Thomas S , Miller H and Gaver R
Laser-fibre-optic "Optrode" for real time *in vivo* blood carbon dioxide level monitoring
IEEE J Lightwave Tech Vol LT-5 No 7 (July 1987) pp 1027

Hoggard P E and Porter G B
Photoanation of the Tris(2,2'-bipyridine)ruthenium(II) cation by thiocyanate
J Am Chem Soc Vol 100 No 5 (Mar 1978) pp 1457-1463

*Hopland S
Removal of the refractive index dip by an etching method
Elect Lett Vol 14 No 24 (1978) pp 757-759

*Hopland S
Characteristics of the etching of undoped silica in MCVD-fabricated optical fibres with buffered HF
Mater Res Bull Vol 20 (1985) pp 1367

*Hopland S and Berg A
Fabrication of coupling fibres with spherical end faces by a selective etching/melting technique
Fifth Euro Conf on Optical Fibres (1979) pp 9 3-1

Hosaka T , Okamoto K., Miya T , Sasaki Y and Edahiro T
Low-loss single polarisation fibres with asymetric strain birefringence
Elect Lett Vol 17 No 15 (23 July 1981) pp 530

*Hsu W Y and Gierke T D
Plastic theory for ionic clustering in perfluorinated ionomers
Macromolecules Vol 15 (1982) pp 101-105

Imoto K , Sano and Maeda M
Plastic optical fibre star coupler
Appl Opt Vol 25 No 19 (Oct 1986) pp 3443

*Iwai K , Uesugi M and Takemura F
Tris(2,2'-Bipyridine)Ruthemum(II)- sensitised photopolymerisation of acrylamide
Polymer J Vol 17 No 9 (1985) pp 1005-1011

Jervis L and Pettit N M
Purification of ribonuclease T1 on porous glass affinity adsorbents
J Chromatography Vol 97 (1974) pp 33-38

Jones J D and Jackson D A
Monomode fibre optic temperature sensors
Anal Proc Vol 22 (Jul 1985) pp 207

*Jones R F and Cole-Hamilton D J
The substitutional photochemistry of tris(bipyridyl)- ruthenium(II) chloride
Inorg Chem A-L Vol 53 (1981) pp L3-L5

*Judge J S
A study of the dissolution of SiO_2 in acidic flouride solutions
J Electrochem Soc Vol (Nov 1971) pp 1772

Kalyanasundaram K
Direct observation of substitutional photochemistry in tris(bipyrazyl)ruthemum(II)
J Phys Chem Vol 90 (1986) pp 2285-2287

Kalyanasundarum K and Neumann-Spallart M
Influence of added salts on the cage escape yields in the photoredox quenching of $Ru(bpy)_3^{2+}$ excited states
Chem Phys Lett Vol 88 No 1 (Apr 1982) pp 7-12

Kawabata R Tahara Y , Imasaka T and Ishibashi N
Fibre-optic calcium(II) sensor with reversible response
Anal Chim Acta Vol 212 (1988) pp 267-271

Kawabata Y , Imasaka T and Ishibashi N
Laser fluorimetry of polynuclear aromatic hydrocarbons based on time-resolved fluorescence detection
Anal Chim Acta Vol 173 (1985) pp 367-372

*Kawabata Y , Imasaka T and Ishibashi N
Fibre optic pH sensor based on laser fluorimetry
OFS'86 Tokyo Vol (1986) pp 139-142

*Kawachi, Edahiro and Toba
Micro-lens formation on VAD single-mode fibre ends
Elect Lett Vol 18 No 2 (Jan 1982) pp 71

*Kayoun, Peuch, Papuchon and Arditty
Improved coupling between laser diode and single-mode fibre tipped with a chemically etched self-centered diff element
Elect Lett Vol 17 No 12 (11 Jun 1981) pp 400

*Kelly J M
Electronic spectra and photophysical properties of ions as probes for the properties and structure of perfluorinated ionomer membranes
Structure and properties of Ionomers Eds M Pineri & A Eisenberg (1987) p127-140

*Kelly J M , Meunier H M , McCormack D E and Michas A
Uranyl ions in perfluormated (Nafion and Flemion) membranes Spectroscopic and photophysical properties and reactions with potassium hydroxide
Polymer Vol (1989) pp 23

Kim J Y and Lee Y H
An improvement in stability of oxygen microbe
Biotech Bioeng Vol 35 (1990) pp 850-851

*Kirkbright G F , Narayanaswarmy R and Welti N A
Fibre-optic pH probe based on the use of an imobilised colorimetric indicator
Analyst Vol 109 (Aug 1984) pp 1025

Klassen D M
Synthesis and spectroscopic characterisation of Ru and Os complexes with sterically hindered ligands
Inorg Chem Vol 15 No 12 (1976) pp 3166

*Knopp J A and Longmuir I S
Intracellular measurment of oxygen by quenching of fluorescence of pyrene butyric acid (PBA)
Biochim Biophys Acta Vol 279 (1972) pp 393

*Kober E M , Marshall J L , Dressick W J , Sullivan B P, *et al*
Synthetic control of excited states Non-chromophoric ligand variations in polypyridyl complexes of Osmium (II)
Inorg Chem Vol 24 (1985) pp 2755-2763

*Kober E M and Meyer T J
An electronic stuctural model for the emitting MLCT excited states of Ru $(bpy)_3^{2+}$ and Os $(bpy)_3^{2+}$
Inorg Chem Vol 23 (1984) pp 3877-3886

*Kober E M , Sullivan B P and Meyer T J
Solvent dependence of metal to ligand charge transfer transitions Evidence for initial electron localisation in MLCT excited states of 2,2'-bipyridine complexes of Ruthenium(II) and Osmium(II)
Inorg Chem Vol 23 (1984) pp 2098-3204

*Kohen E , Salmon J M , Kohen C and Bengtsson G
Mirospectrofluorometric evaluation of the oxygen probe 1-pyrenebutyric acid in single living cells
Exp Cell Res Vol 89 (1974) pp 105-110

*Krishnan M , Zhang X and Bard A J
Polymer films on electrodes Spectral sensitisation of n-type SnO_2 and voltametry at electrodes modified with
J Am Chem Soc Vol 106 (1984) pp 7371-7380

*Kroneis H W and Marsoner H J
A fluorescence-based sterilisable oxygen probe for use in bioreactors
Sensors and Actuators Vol 4 (1983) pp 587-592

Kurimura Y , Yokota H , Shigehara K and Tsuchida E
The interaction of the tris(2,2'-bipyridine)ruthemum(II) ion with poly(p-styrenesulfonate)
Bull Chem Soc Jpn Vol 55 (1982) pp 55-58

*Lakowicz J R
Principles of Fluorescence Spectroscopy
Plenum Press (1983) pp 51-59

Lakowicz J R and Cherek H
Phase-sensative fluorescence spectroscopy a new method to resolve fluorescence lifetimes or emission spectra of components in a mixture of fluorophore
J Biochem Biophys Meth Vol 5 (1981) pp 19-35

*Lawson D R , Whiteley L D , Martin C R and Szentirmay M N
Transport and Kinetics
J Electrochem Soc Vol 135 No 9 (Sept 1988) pp 2247-2253

Lee E D , Werner T C and Seitz W R
Luminescence ratio indicators for oxygen
Anal Chem Vol 59 (1987) pp 279

*Lee P C and Meisel D
Luminescence quenching in the cluster network of perfluorosolfonate membrane
J Am Chem Soc Vol 102 (1980) pp 5477-5481

*Lee P C and Meisel D
Photophysical studies of pyrene incorporated in Nafion membranes
Photochem and Photobiol Vol 41 No 1 (1985) pp 21 - 26

*Lee P C and Rodgers M A J
Kinetic properties of singlet oxygen in a polymeric microheterogenous system
J Phys Chem Vol 88 (1984) pp 4385-4389

Leyden D E
Characterisation and analytical applications of chelating silylated surfaces
Midland Macromol Monogr Vol 7 (1978) pp 321-332

Lieberman R A , Blyler L L and Cohen L G
A distributed fibre optic sensor based on cladding fluorescence
J Lightwave Tech Vol 8 No 2 (Feb 1990) pp 212-220

Lieberman S H , Inman S M and Stromvall E J
Fibre optic fluorescence sensors for remote detection of chemical species in seawater
Proc Symp Chem Sens Vol 87-9 (1987) pp 464-475

*Lim S K., Pineri G M and Coey J M D
Microstructure studies of perfluorocarboxylated ionomer membranes
J Membrane Sci Vol 30 (1987) pp 171-189

*Lin C and Sutin N
Quenching of the luminescence of the tris(2,2'-bipyridine) complexes of Ru(II) and Os(II)
J Phys Chem Vol 80 No 2 (1976) pp 97-105

Linden Y , Tenerez L , Tiren J and Hok B
Fabrication of three-dimensional silicon structures by means of doping-selective etching (DSE)
Sensors and Actuators Vol 16 (1989) pp 67-82

*Lippitsch M E , Pusterhoffer J , Leiner M J and Wolfbeis O S
Fibre optic oxygen sensor with fluorescence decay time as the information carrier
Anal Chim Acta Vol 205 (1988) pp 1-6

Louch J and Ingle J D
Experimental comparison of single- and double-fibre configutations for remote fibre-optic fluorescence sensing
Anal Chem Vol 60 (1988) pp 2537-2540

*Lubbers D W and Opitz N
Optical fluorescence sensors for continuous measurement of chemical concentration in biological systems
Sens and Actuators Vol 4 (1983) pp 641-654

Maclay G J , Buttner W J and Stetter J R
Microfabricated amperometric gas sensors
IEEE Electron Devices Vol 35 No 6 (June 1988) pp 793-799

Marhic M E , Ho P S and Epstein M
Nondestructive refractive index profile of clad optical fibres
Appl Phys Lett Vol 26 No 10 (May 1975) pp 574-575

*Martin C R and Dollard K A
Effect of hydrophobic interactions on the rates of ionic diffusion in Nafion films at electrode surfaces
J Electroanal Chem Vol 159 (1983) pp 127-135

*Martin C.R., Rhoades T A and Ferguson J A
Dissolution of perfluormated ion containing polymers
Anal Chem Vol 54 (1982) pp 1639-1641

*Martin C R , Rubinstein I and Bard A
J Polymer films on electrodes Electron and mass transfer in NAFion films containing Ru trisbippy
J Am Chem Soc Vol 104 (1982) pp 4817-4824

*Mauritz K A and Fu Puey-Mei
Dielectric relaxation studies of ion motions in electrolyte- containing perfluorosulphonate ionomers 1) NaOH, NaCl system
Macromolecules Vol 21 (1988) pp 1324-1333

*McFarlane R and Hamilton M C
A fluorescence Based Dissolved Oxygen Sensor
Seastar Instruments Ltd

McGown L B and Bright F V
Comparison of phase-resolved and steady state fluorimetric multicomponent determinations using wavelenght selection
Anal Chem Vol 56 No 12 (1984) pp 2195-2199

McGown L B and Bright F V
Phase-resolved fluorescence spectroscopy
Anal Chem Vol 56 No 13 (Nov 1984) pp 1400A

*Meisel D and Matheson M S
Quenching and quenching reversal of tris(2,2'-bipyridine) ruthenium(II) emission in polyelectrolyte solutions
J Am Chem Soc Vol 99 No 20 (Sept 1977) pp 6577-6581

Meyer G J , Lisensky G C and Ellis A B
A new class of chemical sensors for gases based on photoluminescence from semiconductor based interfaces
Proc Symp Chem Sens Vol 87-9 (1987) pp 439-448

*Meyer T J
Photochemistry of metal coordination complexes metal to ligand charge transfer excited states
Pure & Appl Chem Vol 58 No 9 (1986) pp 1193-1206

Miller C M
Fibre optic array splicing with etched silicon chips
Bell Syst T Vol 57 (1978) pp 75-90

Miller R M
Factors affecting the performance of fibre optic probes
Proc Symp Chem Sens Vol 87-9 (1987) pp 449-455

*Miller W W , Yafuso M , Yan C F , Hui H K and Arick S
Performance of an *in vivo*, continuous blood-gas monitor with disposable probe
Clinical Chemistry Vol 33 No 9 (1987) pp 1538

Mishra M K
Radical photopolymerisation of vinyl monomers
JMS Rev Macromol Chem Phy Vol C22 (3) (1982-83) pp 409-470

*Mitmck M H and Jobsis F F
Pyrenebutyric acid as an optical oxygen probe in the intact cerebral cortex
J Appl Physiol Vol 41 No 4 (1976) pp 593-597

*Moore R B and Martin C R
Procedure for preparing solution cast perfluorosulfonate ionomer films and membranes
Anal Chem Vol 58 (1986) pp 2569-2570

*Moore R B and Martin C R
Chemical and morphological properties of solution cast perfluorosulphonate ionomers
Macromolecules Vol 21 (1988) pp 1334-1339

Moore R B , Wilkerson J E and Martin C R
High performance liquid chromatography studies of the ion-exchange selectivity of Nafion
Anal Chem Vol 56 (1984) pp 2572-2575

Munkholm C , Walt D , Milanovich F and Klainer S
Polymer modification of fibre optic chemical sensors as a method of enhancing fluorescence signal for pH measurement
Anal Chem Vol 58 No 24 (1986) pp 1427-1430

Munkholm C , Walt D R and Milanovich F P
A fibre-optic sensor for CO_2 measurement
Talanta Vol 35 No 2 (Feb 1988) pp 109-112

*Nagel S R , MacChesney J B and Walker K L
An overview of the modified chemical vapour deposition (MCVD) process and performance
IEEE J Quant Elect Vol QE-18 No 4 (Apr 1982) pp 459-476

*Narayanaswamy R
Optical fibre sensors in chemical analysis
Anal Proc Vol 22 (Jul 1985) pp 204

Narayanaswamy R
Optical fibre chemical sensors
Proc Symp Chem Sens Vol 87-9 (1987) pp 428-437

Narayanaswarmy R
Sensing chemicals with optical fibres
C & I Vol (Feb 1986) pp 35

Narayanaswarmy R and Sevilla F
Flow cell studies with immobilised reagents for the development of an optical fibre sulphide sensor
Analyst Vol 111 (Sept 1986) pp 1085

Netzer L , Iscovici R and Sagiv J
Adsorbed monolayers versus Langmuir-Blodgett monolayers - why and how? 1 From monolayer to multilayer by absorption
Thin Solid Films Vol 99 (1983) pp 235-241

*Noda, Shibata, Edahiro and Sasaki
Splicing of single fibres
J of Lightwave Tech Vol Lt-1 No 1 (March 1983) pp 63

Nutt A , Bristow J , McDonach A and Laybourn P
Fibre-to-waveguide coupling using ion-milled grooves in lithium niobate at 1.3μm wavelenght
Optics Letters Vol 9 No 10 (Oct 1984) pp 463

*O'Connell C
Towards redox catalysis using N-donor complexes of Ruthenium(II)
Ph D Thesis, Trinity College, Dublin (1983)

Omann G M and Glaser M
Dynamic quenchers in fluorescently labelled membranes Theory for quenching in a three phase system
Biophys J Vol 47 (May 1985) pp 623-627

*Opitz N , Graf H.J and Lubbers D W
Oxygen sensor for the temperature range 300 to 500 K based on fluorescence quenching of indicator-treated silicone
Sensors and Actuators Vol 13 (1988) pp 159-163

Opitz N and Lubbers D W
Electrochromic dyes, enzyme reactions and hormone-protein interactions in fluorescence optic sensor (optrode) tech
Talanta Vol 35 No 2 (Feb 1988) pp 123-127

Park H G and Kim B Y
Intermodal coupler using permantly photoinduced grating in two-mode opical fibre
Elect Lett Vol 25 No 12 (1989) pp 797-780

Parker D
Sensors for momtormg blood gases in intensive care
J Phys E Sci Instrum Vol 20 (1987) pp 1103

*Parker J W and Cox M E
Glucose/oxygen sensor
SPIE Vol 713 (1986) pp 113

Penzkofer A and Leupacher W
Fluorescence behaviour of highly concentrated Rhodamine 6G solutions
J Luminescence Vol 37 (1987) pp 61

*Peterson J I , Fitzgerald R and Buckhold D
Fibre-optic probe for in vivo measurement of oxygen partial pressure
Anal Chem Vol 56 (1984) pp 62-67

*Peterson J I , Goldstein S R , Fitzgerald R V and D K Buckhold
Fibre optic probe for *in vivo* measurements of oxygen partial pressure
Anal Chem Vol 52 (1980) pp 864-869

*Peterson J I and Vurek G
Fibre-optic sensors for biomedical applications
Science Vol 224 (13 APR 1984) pp 123

Plaza P , Dao N Q , Jouan M , Fevrier H and Saisse H
Simulation et optimisation des capteurs a fibre optiques adjacents
Applied Optics Vol 25 No 19 (Oct 1986) pp 3448-3454

*Plueddemann E P
Chemistry of silane coupling agents
Midland Macromol Monogr Vol 7 (1978) pp 31-53

*Podgorski G T , Longmuir I S , Knopp J A and Benson D M
Use of an encapsulated fluorescent probe to measure intracellular $P(O_2)$
J Cell Physiol Vol 107 (1981) pp 329-334

Polanyi M L and Hugenholtz P G
Recent developments in dye dilution measurements with fibre optics
Int Conf Med Bio Eng Vol 7th (1967) pp 18-11

Pollack V
Fluorescence photometry of thin layer chromatograms and electropherograms
J Chromatography Vol 133 (1977) pp 49-57

Posch H E , Wolfbeis O S and Pusterhoffer J
Optical and fibre-optic sensors for vapours of polar solvents
Talanta Vol 35 No 2 (Feb 1988) pp 89-94

*Presby H M , Standly R D , MacChesney J B , and O'Connor P B
Material Structure of Germanium-Doped Optical Fibres and Preforms
Bell System Technical Journal (Dec 1975) pp 1681-92

*Prieto N E and Martin C R
Luminescence probe studies of Nafion polyelectrolytes
J Electrochem Soc Electrochemical Science and Tech Vol 131 No 4 (Mar 1984) pp 751-755

Robinson P.J , P Dunnill and Lilly M D
Porous glass as a solid support for immobilisation or affinity chromatography of enzymes
Biochim Biophys Acta Vol 242 (1971) pp 659-661

Royer G P and Liberatore F A
The use of silylated derivatives of porous glass as enzyme supports Stability of the silylated surface
Midland Macromol Monogr Vol 7 (1978) pp 189-199

*Rubinstein I and Bard A J
Polymer films on electrodes 4 Nafion coated electrodes and electrogenerated chemiluminescence of surface attached Ru $(bpy)_3^{2+}$
J Am Chem Soc Vol 102 (1980) pp 6641-6642

*Rubinstein I and Bard A J
Polymer films 5 Electrochemistry and chemiluminescence at Nafion-coated electrodes
J Am Chem Soc Vol 103 (1981) pp 5007-5013

*Saari L A and Seitz W R
pH sensor based on immobilised fluoresceinamine
Anal Chem Vol 54 (1982) pp 821

Sakaguchi M , Seki N and Yamamoto S
Power coupling from laser diodes into single-mode fibres with quadrangular pyramid-shaped hemiellipsoidal ends
Elect Lett Vol 17 No 12 (June 1981) pp 425-426

Sakai J and Kimura T
Design of a miniature lens for semiconductor laser to single-mode fibre coupling
IEEE J Quant Elect Vol QE-16 No 10 (Oct 1980) pp 1059

Sakai Y , Sadaoka Y and Fukumoto H
Humidity-sensative and water-resistive polymeric materials
Sensors and Actuators Vol 13 (1988) pp 243-250

*Sasso M G , Quina F H and Bechara E J H
Ruthenium(II) Tris(bipyridyl) ion as a luminescent probe for oxygen uptake
Anal Biochem Vol 156 (1986) pp 239-243

*Saxena A N and Wolf H F
Optical detectors
Handbook of fibre optics pp 203

Scheggi A M and Baldini F
pH sensing by fibre optics
Optia Acta Vol 33 No 12 (1986) pp 1587

Schulman E M and Parker R T
Room temperature phosphorescence of organic compounds The effects of moisture, oxygen and the nature of the support-matrix
J Phys Chem Vol 81 No 20 (1977) pp 1932

Schwab S D and McCreery R L
Versatile, efficient raman sampling with fibre optics
Anal Chem Vol 56 (1984) pp 2199-2204

*Seitz R
Chemical sensors based on fibre optics
Anal Chem Vol 56 No 1 (Jan 1984) pp 16 A

Seitz W R , Zhujun Z and Mullin J L
Reversible indicators for alkali metal ion optical sensors
SPIE Vol 713 (1986) pp 126

Shaw D W
Localised GaAs etching with acidic hydrogen peroxide solutions
J Electrochem Soc Vol 128 No 4 (Apr 1981) pp 874-880

*Skoog D A and West D M
Determination of dissolved oxygen by the Winkler method
Fundamentals of anal chem Vol Fourth Ed pp 772-773

Slovacek P , Bluestein B , Craig M , Urcioli C and Stundter L L
Proc Symp Chem Sens Vol 87-9 (1987) pp 456-463

Smardzewski R R
Multielement optical waveguide sensor General concept and design
Talanta Vol 35 No 2 (Feb 1988) pp 95-101

Smith A M
Optical fibre sensors - new opportunities for chemical sensing?
Electronics & Power Vol (Nov/Dec 1986) pp 811

*Smith A M
Biomedical Sensing Using Optical Fibres
Analytical Proceedings Vol 22 (July 1985) pp 212

Somogyı B , Papp S , Rosenberg A , Seres I and Matko J
A double-quenchıng method for studyıng protein dynamıcs seperatıon of the fluorescence quenchıng parameters
Bıochem Vol 24 (1985) pp 6674-6679

Sportsman J R and Wılson G S
Chromatographıc properties of sılıca ımmobılised antıbodıes
Anal Chem Vol 52 (1980) pp 2013-2-18

*Sprmtschmk G , Sprmtschnık H W , Kırsch P P and Whıtten D
Photo cleavage of water a system for solar energy conversıon usıng monolayer bound transıtıon metal complexes
J Am Chem Soc Vol 98 No 8 (Apr 1976) pp 2337-2338

Stınson S
Dynamıc fluorescence spectroscopy gams attentıon of more chemısts
Chem Eng News Vol (Mar 1989) pp 27-29

Suzukı H , Tamıya E and Karube I
Fabrıcaatıon of a mıcro oxygen electrode and ıts applıcatıon
Proc Sym Chem Sens Vol 87-9 (1987) pp 393-400

*Svaasand L O , Hopland S and Grande A P
Splıcıng of optıcal fibres wıth a selectıve etchıng technique
4th Euro Conf Opt Comm , Genoa (Sept 1978) pp 304

*Szentırmay M N , Campbell L F and Martın C R
Sılane couplıng agents for attachıng Nafion to glass and sılıca
Anal Chem Vol 56 (1986) pp 661-662

*Szentırmay M N , Prıeto M E and Martın C R
Lumınescence probe studıes of ıonomers 1 Steady state measurements from Nafion membrane
J Phys Chem Vol 89 (1985) pp 3017-3023

*Szentırmay N E Prıeto M N and Martın C R
Lumınescence probe studıes of ıonomers Steady state measurements from Nafion membrane
J Phys Chem Vol 89 (1985) pp 3017-3023

*Tenney A S and M Ghezzo
Etch rates of doped oxıdes ın solutıons of buffered HF
J Electrochem Soc Vol 120 No 8 (Aug 1973) pp 1091-1095

Tımbrell V
A new rapıd response oxygen analyser
Int Conf Med Bıo Eng Vol 7th (1967) pp 18-7

Tromberg B.J , Sepanıak M J , Vo-Dınh T and Grıffin G D
Fıbre-optıc chemıcal sensors for competıtıve bındıng fluoroımmunoassay
Anal Chem Vol 59 (1987) pp 1226-1230

*Tusa J , Hacker T , Hansmann D R , Kaput T M. and Maxwell T.P.
Fibre optıc mıcrosensor for contınuous measurement of blood gasses
SPIE Vol 713 (1986) pp 137

Twining S
Fluorescein isothiocyanate-labeled caesin assay for proteolytic enzymes
Anal Biochem Vol 143 (1984) pp 30-34

Van de Walle C G , Bar-Yam F R McFeely Y and Pantiehdes S T
Summary abstract Theoretical investigations of fluorine silicon systems
J Vac Sci Technol Vol A6 No 3 (May 1988) pp 1973-1974

*VanHouten J and Watts R.J
Temperature dependance of the photophysical and photochemical properties of Ru trisbippy m water
J Am Chem Soc Vol 98 No 16 (Aug 1976) pp 4853-4858

*VanHouten J and Watts R.J
Photochemistry of tris(2,2'-bipyridyl)ruthenium(II) in aqueous solutions
Inorg Chem Vol 17 No 12 (1978) pp 3381-3385

Vaughan W M and Weber G
Oxygen quenching of pyrene butyric acid fluorescence in water A dynamic probe of the microenvironment
Biochem Vol 9 No 3 (Feb 1970) pp 464-473

Vickers G H , Miller R M and Hieftje G M
Time-resolved fluorescence with an optical-fibre probe
Anal Chim Acta Vol 192 (1987) pp 145-153

Vivilecchia R V , Cotter R L , Limpert R J and Thimot N Z
Considerations of small particles in different modes of liquid chromatography
J Chromatography Vol 99 (1974) pp 407-424

*Wallace W M and Hoggard P E
Ion-multiplet formation and the photoanation of tris(2,2'-bipyridine)ruthenium(II)
Inorg Chem Vol 19 (1980) pp 2141-2145

*Walker G M , O'Neill L and Walsh P K
Cheese whey fermentation by *Kluyvermyces fragilis*, technical constraints abd research needs
Proc on European Workshop on Bioethanol, W Palz Ed Brussels, EEC (1986) pp 185-6

Walt D R , Munkholm C , Jordan D , Milanovich F P and Daley P P
Preparation of small diameter sensors for continuous clinical monitorng
SPIE Vol 713 (1986) pp 144

Watts R.J , Harrington J S and VanHouten J
A stable monodentate 2,2'-bipyridine complex of Iridium
J Am Chem Soc Vol 99 No 7 (Mar 1977) pp 2179-2187

Weetall H H
Storage stability of water-insoluble enzymes covalently coupled to organic and inorganic carriers
Biochim Biophys Acta Vol 212 (1970) pp 1-7

*Wilkinson G , Gillard R D and McCleverty J A
Comprehensive coordination chemistry Vol 4 Middle transition elements pp 327-335

*Wolfbeis O S , Leiner M.J and Posch H E
A new sensing material for optical oxygen measurement with the indicator embedded in an aqueous phase
Mikrochem Acta (Wein) Vol III (1986) pp 359-366

*Wolfbeis O S , Posch H E and Kroneis H W
Fibre optical fluorosensor for determination of Halothane and/or oxygen
Anal Chem Vol 57 (1985) pp 2556-2561

Xu J , Driver R D , Gams J and Maack D R
Direct bonding yields low-cost plastic star-couplers
Laser focus/electro-optic Vol (Apr 1988) pp 180

Yamada J , Murakami Y , Sakai J and Kimura T
Characteristics of a hemispherical microlens for coupling between a semiconductor laser and single mode fibre
IEEE J Quant Electron Vol QE-16 No 10 (Oct 1980) pp 1067

*Yeo R S
Dual cohesive energy densities of perfluorosulphonic acid (Nafion) membrane
Polymer Vol 21 (1980) pp 432-435

*Yeo S C and Eisenberg A
Physical properties and supermolecular structure of perfluormated ion-containing (Nafion) polymers
J Appl Polym Sci Vol 21 (1977) pp 875-898

Zhu C , Bright F V , Wyatt W A and Hieftje G M
A new fluorescence sensor for quantification of atmospheric humidity
Proc Symp Chem Sens Vol 87-9 (1987) pp 476-483

Zhujun Z and Seitz R
A carbon dioxide sensor based on fluoresence
Anal Chim Acta Vol 160 (1984) pp 305

Zhujun Z and Seitz W R
A fluorescent sensor for aluminium(III), magnesium(II), zinc(II) and cadmium(II) based on Qumohn-8-ol sulphonate
Anal Chim Acta Vol 171 (1985) pp 251

Zhujun Z and Seitz W R
Optical sensor for oxygen based on immobilised haemoglobin
Anal Chem Vol 58 No 1 (Jan 1986) pp 220-222

Zhujun Z and Seitz R
A fluorescence sensor for quantifying pH in the range from 6 5 to 8 5
Anal Chim Acta Vol 160 (1984) pp 47

*E I duPont deNemours
Nafion resins Versatile heterogenous catylists
Aldrichimica Acta Vol 19 No 3 (1986) pp 76

Acknowledgements

Firstly, I would like to thank my supervisor, Dr Brian Lawless, for his contributions to the project over the years

My thanks to Dr Han Vos for his assistance during this work and also to Boris Fennema for discussing some of the chemical aspects of the research Thank you also to Dr Danny Heffernan and Dr John Costello for the use of their machines during the writing up period I would also like to thank Al Devine for the photographs used in this thesis Regards also to Alan Hughes and the rest of the technical staff for their contributions to this work

I would like to mention my lab mates Cohn Potter, Simon McCabe , Gerry Shaw , Joe Maxwell, Brian Cummins, Kieran Higgins, Dave Connolly as well as Dr Brian MacCraith and Dr Vince Ruddy of course

I would also like to show my appreciation to John O'Dwyer, Charles Markham and Neil O'Hare for the many interesting "experiments" which were conducted during the lunch hour Then there are the Physics department's postgraduate population, who have made my stay in DCU most memorable, including Kevin McGuigan, Kieran McCarthy, Kevin Devlin, Jim Campion, Siobhain Daly, Liam Roberts, Brian Hurley, Ciaran O'Morán Ger Ennis, Pauline Marron, Brian Finnegan, John Scanlon, James Molloy, Kevin Mellon, Paul Jenkins, Mark Daly, Jim Brilly, Richie Corcoran, Dave Evans, Lar Kiernan, as well as all the rest of the staff

Appendix A: PMT Characteristics

The Photo Multiplier Tube used in the work described in this thesis was a side-on, nine stage Hamamatsu R928 tube used with an EMI PMT power supply unit (PM28B) The PMT was operated at -900Vdc The base was configured as shown in Figure A 1 which is simply a resistor divider network using 100kΩ resistors between dynodes The output was taken across a 1MΩ resistor and passed to a Lock-in amp or directly to the chart recorder The following characteristics of the PMT are of interest especially to the section on calculating the efficiencies of the systems in Chapter II B(5)

Characteristic:

Spectral response range	185 - 930 nm
Peak wavelength	400nm
Photochathode material	Multialkali
Window material	UV glass
Number of dynode stages (n)	9
Anode sensitivity S_A @ -1kV (A/W)	$6\,8 \times 10^5$
Current amplification	$1\,0 \times 10^7$
Rise time (typ)	2 2ns
dynode material and structure coeffifient (α)	0 75
Anode sensitivity @ -900V $S_A(900/1000)^{\alpha_n}$	$2\,1 \times 10^5$ A/W

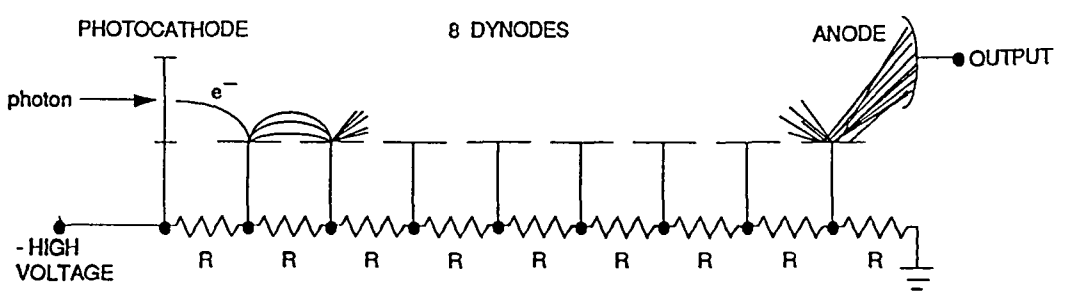

Figure A.1 Resistive divider PMT base

Appendix B Best fit program

The following program was used in the calculation for best fit line using a set of data input by the user

```
#include<stdlib.h>
#include<stdio.h>
#include<math.h>
#include<float.h>

int main()
{
 double n,tx,txx,ty,tyy,txy,
 double t,tp,r,m,em,c,ec,
 double datax[100],datay[100],
 int ct,nd,
 printf("How many data points   "),
 scanf("%i",&nd);
 printf("Enter x y \n"),
 for(ct=1,ct<=nd,ct++)
 {
  scanf("%lf %lf",&datax[ct],&datay[ct]),
 }
 n=(double)nd,
 tx=ty=txx=tyy=txy=0,
 for(ct=1,ct<=nd,ct++)
 {
  tx+=datax[ct],
 txx+=datax[ct]*datax[ct],
  ty+=datay[ct],
 tyy+=datay[ct]*datay[ct],
 txy+=datax[ct]*datay[ct],
 }
 m=((n*txy)-(tx*ty))/((n*txx)-(tx*tx)),
 c=((txx*ty)-(tx*txy))/((n*txx)-(tx*tx)),
tp=(n*tyy)-(ty*ty)-(((n*txy)-(tx*ty))*((n*txy)-(tx*ty)))/((n*txx)-(tx*tx)),
 t=sqrt(fabs(tp)),

em=t/sqrt((n-2)*((n*txx)-(tx*tx))),
ec=(t*sqrt(txx))/sqrt(n*(n-2)*((n*txx)-(tx*tx))),
printf("Slope     = %lf  +- = %lf\n\n",m,em),
printf("Intercept = %lf  +- = %lf\n",c,ec),
}
```

Appendix C Lifetime based quenching measurements

This appendix is concerned with describing changes to the existing experimental set-up so that changes in lifetimes can be used for determining the oxygen concetrations The theory for this is discussed in the Introduction (Chapter I E) and the Stern - Volmer relation holds for the excited state lifetime also Lippitsch *et al* (1988) described a system based on the lifetime quenching of Ru $(bpy)_3^{2+}$ immobilised on Kiesel gel They used a blue emitting LED modulated at 455kHz as light source and the lifetime was deduced from the phase shift between the excitation and emission signals It is proposed that a similar system could be applied to the present system as follows

A blue SiC LED was used in conjunction with Ru $(bpy)_3^{2+}$ fluorescence (Chapter II I) This LED can be modulated at rates upto 500kHz which allow it to be used as an excitation source for the proposed system The PMT base would have to be modified to that shown in Figure C 1 below This base has been modified for use with photon counting and it is designed for use with the Stanford Research Systems Gated Photon Counter (Model SR400) The fibre should be changed to 100μm core multimode fibre, as in the Canstar PC-4-C-100 fibre used in some of the work Because of the low light levels emitted by the LED, this light would have to be focussed into the fibre for best results The lifetimes of the Ru $(phen)_3^{2+}$ is given at 850ns and should be within range of the photon counter which has a lag time of 10ns Thus by monitoring the excited state lifetime of the dye at various oxygen concentrations, a Stern - Volmer plot can be drawn which can later be used for the measurement of disolved oxygen concetrations

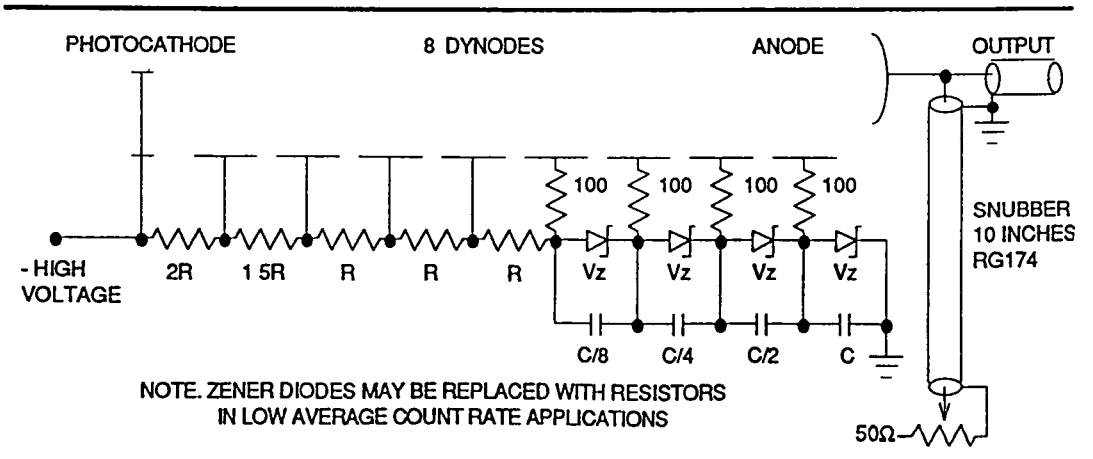

Figure C 1 PMT base for photon counting

Appendix D· Data display software

Program listing of the software used to display the data aquired during experimental work The data initially collected on a BBC microcomputer, was transfered to an IBM PC compatible using Kermit communicator The format of the data file was converted to ASCII standard which could then be read by the following program The program was written in TurboC version 2 0 and requires a Hercules Graphics adapter card, although with minor modifications, the program will run on other systems

```
#include <stdio.h>
#include <stdlib.h>
#include <conio.h>
#include <ctype.h>
#include <string.h>
#include <graphics.h>
#include <dos.h>
#include <alloc.h>
#include <plot.h>
#include <bios.h>
#include <lx800.h>

#define ARRAYSIZE  7000

int main(int argc, char *argv[])
{
struct bit_field        {
                                        unsigned        Filelist        1,
                                        unsigned        SetmaxX         1,
                                        unsigned        SetmaxY         1,
                                        unsigned        Smooth          1,

                                        unsigned        Titles          1,
                                        unsigned        Markers         1,
                                        unsigned        Period          1,
                                        unsigned        Print           1,

                                        unsigned        Offset          1,
                                        unsigned        Region          1,
                                        unsigned        Temper          1,
                                        unsigned        Drift           1,

                                        unsigned        Plotter         1,
                                        unsigned        Poff            1,
                                        unsigned        Float           .1,
                                        }       flags = {0,0,0,0,0,0,0,0,0,0,0,0,0,0,0,0},
register int loop,
int row=1, row1=1,
unsigned long temp, temp2, period=0, offset=100;
unsigned int gtemp, gtemp1,
unsigned long *buffer, *mem, *swop,
unsigned long npoints, memsize, maxy=0, maxyo=0, fscale=1000,
```

```
unsigned long r_st=0, r_end=0,
unsigned long d_st=0, d_end=0,
long ltemp,
float xscale, yscale, ftemp,
float tscale, pscale, slope=0.0, drift=0.0,
FILE *fh, *fl=NULL, *gfh,
char filename[80], filelist[80],
char titles[80], markers[80], temper[80], plotfile[80],
char tmp[50], tmp2[20], *ptr,

mem = (unsigned long *)calloc(ARRAYSIZE,sizeof(unsigned long)),
if(mem==NULL)
        {
        printf("Error - memory allocation'\n"),
        exit(1),
        }

if(argc==1)
        {
        puts("    AGSCAN - Data File Presentation Utility!   (c) A  Geissel 1990"),
        puts("       Usage   AGSCAN <filename>[.<ext>] [options] [...]"),
        puts("\n    Options."),
        puts("      /C[<filename>[.<ext>]] - Display second data file."),
        puts("      /D[<filename>[.<ext>]] - Calculate and remove drift for given region."),
        puts("      /F[<scalar>]           - Read and scale floating point data from file."),
        puts("      /G[<filename>[ <ext>]] - Create HPGL output from data file."),
        puts("      /H                     - Print screen contents to LX800 dot matrix."),
        puts("      /M[<filename>[.<ext>]] - Read marker file contents and display."),
        puts("      /N                     - No horizontal guides in HPGL output."),
        puts("      /O<value>              - Remove offset from data "),
        puts("      /P<value>              - Set scan duration."),
        puts("      /R<st>,[<end>]         - Display only selected region."),
        puts("      /S                     - Smooth data (7-point floating average "),
        puts("      /T<filename[.<ext>]    - Read title and axis labels from file."),
        puts("      /X<value>              - Set X-axis scale."),
        puts("      /Y<value>              - Set Y-axis scale."),
        exit(0),
        }

for(loop=2,loop<argc,loop++)
        {
        if(argv[loop][0]!='/')
                continue,
        switch((int)_toupper((int)argv[loop][1]))
                {
                case 'X'
                                flags.SetmaxX = 1;
                                memsize = atol(argv[loop]+2),
                                break,
                case 'Y'.
                                flags.SetmaxY = 1,
                                maxy = atol(argv[loop]+2),
                                break,
                case 'S'
                                flags.Smooth = 1;
                                break,
                case 'O'.
                                flags Offset = 1;
                                offset = atol(argv[loop]+2),
                                break,
                case 'P'.
                                flags.Period = 1,
```

```
                period = atol(argv[loop]+2),
                break,
case 'T'
                strcpy(titles,argv[loop]+2),
                if(strchr(titles,' ')==NULL)    strcat(titles,".lst"),
                flags Titles = 1,
                break,
case 'N'
                flags.Poff=1,
                break,
case 'M'
                if(strlen(argv[loop]+2)==0)
                        {
                        strcpy(markers,argv[1]),
                        if((ptr=strchr(markers,'.'))'=NULL)
                                *ptr=0x00,
                        }
                else
                        strcpy(markers,argv[loop]+2),
                if(strchr(markers,'.')==NULL)   strcat(markers,".lst"),
                flags.Markers = 1,
                break,
case 'H'
                flags.Print = 1,
                break,
case 'G'
                flags.Plotter = 1,
                if(strlen(argv[loop]+2)==0)
                        {
    strcpy(plotfile,argv[1]),
                        if((ptr=strchr(plotfile,'.'))!=NULL)
                                *ptr=0x00,
                        }
                else
                        strcpy(plotfile,argv[loop]+2),
                if(strchr(plotfile,'.')==NULL&&strstr(plotfile,"COM")==NULL)
                        strcat(plotfile,".HPG"),
break,

case 'R'
                ptr = strchr(argv[loop]+2,','),
                if(ptr>argv[loop]+2)
                        {
                        flags.Region = 1,
                        *ptr=0x00,
                        r_st = atol(argv[loop]+2),
                        r_end = atol(ptr+1),
                        }
                break,
case 'C'
                if(strlen(argv[loop]+2)==0)
                        {
                        strcpy(temper,argv[1]),
                        if((ptr=strchr(temper,'.'))!=NULL)
                                *ptr=0x00,
                        }
                else
                        strcpy(temper,argv[loop]+2);
                if(strchr(temper,'.')==NULL)    strcat(temper,".tem"),
                flags.Temper = 1,
                break,
```

```
                case 'D'
                                ptr = strchr(argv[loop]+2,','),
                                if(ptr>argv[loop]+2)
                                        {
                                        flags Drift = 1,
                                        *ptr=0x00,
                                        d_st = atol(argv[loop]+2),
                                        d_end = atol(ptr+1),
                                        }
                                break,
                case 'F'
                                if(atoi(argv[loop]+2)!=0)
                                        fscale =atof(argv[loop]+2),
                                flags Float = 1,
                                break,
                }
        }



if(argc>1)
        strcpy(filelist,argv[1]),
else
        {
        printf("Enter file list name "),
        scanf(" %s",filelist),
        }

if(strchr(filelist,'.')==NULL)  strcat(filelist,".lst"),

if(strchr(argv[1],'@')!=NULL)
        {
        flags.Filelist = 1,
        fl = fopen(filelist,"r"),
        if(fl==NULL)
                {
                printf("Error - Invalid file list name'"),
                exit(1),
                }
        }

if(flags.Filelist)
        fscanf(fl,"  %s", filename),
else
        strcpy(filename,argv[1]),

if(flags.Filelist)
        flags Offset=0,

if(flags.Plotter)
        {
        gfh = fopen(plotfile,"wt"),
        if(gfh==NULL)
                {
                printf("Error - Opening plotter output file!");
                exit(1);
                }
        fprintf(gfh,"IN,IP0,0,7300,4200,SC0,7300,0,4300;PU,PA;"),
        fprintf(gfh,"PU200,100;PD200,4150,7200,4150,7200,100,200,100,"),
        fprintf(gfh,"PT 1;LT1,4;");
        if(!flags.Poff)
```

```
        for(loop=0,loop<10,loop++)
                        {
                        gtemp = 100+405*loop,
                        gtemp1 = gtemp,
                        fprintf(gfh,"PU200,%d,PD7100,%d,PU,",gtemp, gtemp1),
                        }
        fprintf(gfh,"PT 3,LT,"),
    }

initialise(),
rectangle(20,50,710,320),
settextstyle(SMALL_FONT, HORIZ_DIR, USER_CHAR_SIZE),
setusercharsize(1,1,1,1),

if(flags.Offset)
        {
        sprintf(tmp,"Offset  %li%",offset),
        outtextxy(20,row1,tmp),
        row1+=textheight("H")+1,
        }

if(flags.Smooth)
        {
        outtextxy(20,row1,"Smoothed"),
        row1+=textheight("H")+1,
        }

if(flags.SetmaxX)
        {
        sprintf(tmp,"Max X  %li",memsize),
        outtextxy(20,row1,tmp),
        row1+=textheight("H")+1,
        }

if(flags.SetmaxY)
        {
        sprintf(tmp,"Max Y  %li",maxy),
        outtextxy(20,row1,tmp),
        row1+=textheight("H")+1,
        }

setlinestyle(USERBIT_LINE,0x4040,NORM_WIDTH),
for(loop=77,loop<320,loop+=27)
        line(20,loop,710,loop),

if(flags.Titles)
        {
        setusercharsize(2,1,2,1),
        fh = fopen(titles,"r"),
        if(fh!=NULL)
                {
                fgets(tmp,50,fh);
                outtextxy(350-textwidth(tmp)/2,15,tmp),
                fgets(tmp,50,fh),
                outtextxy(350-textwidth(tmp)/2,331,tmp);
                fgets(tmp,50,fh);
                settextstyle(SMALL_FONT,VERT_DIR,USER_CHAR_SIZE);
                setusercharsize(3,2,3,2);
                outtextxy(0,100,tmp),
                fclose(fh),
                }
```

```
        settextstyle(SMALL_FONT,HORIZ_DIR,USER_CHAR_SIZE),
        setusercharsize(1,1,1,1),
        }

if(flags.Markers)
        {
        setusercharsize(1,1,1,1),
        setlinestyle(CENTER_LINE, 0, NORM_WIDTH),
        fh = fopen(markers,"r"),
        if(fh!=NULL)
                {
                if(!flags.Period)
                        {
                        fscanf(fh," %li",&period),
                        flags.Period=1,
                        if(r_end==0)    r_end=period,
                        }
                sprintf(tmp,"Period  %i",period),
                outtextxy(20,row1,tmp),
                row1+=textheight("H")+1,
                if(flags.Region)
                        pscale = 690/(float)(r_end-r_st),
                else
                        pscale=690/(float)period,
                if(flags.Plotter)
                        fprintf(gfh,"PU,LT2,3,PT 1,"),
                while(!feof(fh))
                        {
                        fscanf(fh," %li ",&temp),
                        fgets(tmp,20,fh),
                        if(tmp!=NULL&&temp<=r_end&&temp>r_st)
                                {
                                sprintf(tmp2,"%i",temp),
                                temp2 = 20+(temp-r_st)*pscale,
                                if(tmp[0]!='.')
                                        {
                                        outtextxy(temp2-textwidth(tmp)/2,37,tmp),
                                        outtextxy(temp2-textwidth(tmp2)/2,322,tmp2),
                                        }
                                line(temp2,50,temp2,320),
                                if(flags.Plotter)
                                        {
                                        gtemp = temp2*10,
                                        gtemp1 = gtemp,
                                        fprintf(gfh,"PU%d,100,PD%d,4150,PU,",gtemp,gtemp1),
                                        }
                                }
                        }
                if(flags.Plotter)
                        fprintf(gfh,"PU,LT,PT.3,"),
                fclose(fh);
                }
        }
setusercharsize(1,1,1,1);

if(flags.Drift&&!flags Filelist&&!flags.Region)
        {
        if(flags.Plotter)
                fprintf(gfh,"PU;LT4,3;PT 2;");
        pscale = 690/(float)period;
        setlinestyle(DOTTED_LINE,0,1),
```

```
        temp2=20+d_st*pscale,
        line(temp2,50,temp2,320),
        if(flags.Plotter)
                {
                gtemp = temp2*10,
                gtemp1 = gtemp,
                fprintf(gfh,"PU%d,100,PD%d,4150,PU,",gtemp,gtemp1),
                }
        outtextxy(temp2-textwidth("Drift")/2,322,"Drift"),
        temp2=20+d_end*pscale,
        line(temp2,50,temp2,320),
        if(flags.Plotter)
                {
                gtemp = temp2*10,
                gtemp1 = gtemp,
                fprintf(gfh,"PU%d,100,PD%d,4150,PU,LT,PT.3,",gtemp,gtemp1),
                }
        }

if('flags.Period)
        {
        period=120,
        flags.Period=1;
        }

if('flags.Markers&&flags.Period)
        {
        sprintf(tmp,"Period  %li",period);
        outtextxy(20,row1,tmp),
        row1+=textheight("H")+1,
        }

if(r_end==0)    r_end=period,
if(r_st>r_end)  r_st=0,

{
sprintf(tmp,"%li",r_st),
outtextxy(20,322,tmp),
sprintf(tmp,"%li",r_end),
outtextxy(710-textwidth(tmp),322,tmp),
}


if(flags.Temper)
        {
        outtextxy(20,row1,"Temp  Correl"),
        row1+=textheight("H")+1;
        }

if(flags.Region)
        {
        sprintf(tmp,"Region  %li-%li",r_st,r_end),
        outtextxy(20,row1,tmp),
        sprintf(tmp,"%li",r_st);
        outtextxy(20,322,tmp);
        sprintf(tmp,"%li",r_end);
        outtextxy(710-textwidth(tmp),322,tmp),
        }
```

```
row1 = 1,

do
        {
        if(strchr(filename,' ')==NULL)  strcat(filename," dat"),
        fh = fopen(filename,"r"),
        if(fh==NULL)
                {
                end(),
                printf("Error - opening file %s'\n",filename),
                exit(1),
                }

        rewind(fh),
        loop=0,

        outtextxy(710-textwidth(filename),row,filename),
        row+=textheight("H")+1,

        while('feof(fh)&&loop<ARRAYSIZE)
                {
                if(flags.Float)
                        {
                        fscanf(fh," %f", &ftemp),
                        mem[loop] = (int)((float)fscale*ftemp),
                        }
                else
                        fscanf(fh," %li",&mem[loop]),
                if('flags.SetmaxY)
                        if(mem[loop]>maxy)      maxy = mem[loop],
                loop++,
                }


        npoints = loop,
        if('flags.SetmaxX)
                {
                sprintf(tmp,"Max X  %li",npoints),
                outtextxy(220,row1,tmp),
                }

        if(!flags.SetmaxY)
                {
                sprintf(tmp,"Max Y  %li",maxy),
                outtextxy(120,row1,tmp),
                row1+=textheight("H")+1,
                }

        if(!flags.SetmaxX)
                memsize=loop-1;
        fclose(fh),

        if(flags.Offset)
                {
                maxyo = maxy - (unsigned long)(((float)maxy/100)*(float)offset);
                maxy  = (unsigned long)(((float)maxy/100)*(float)(offset)),
                }

        if(flags.Region&&flags.Period)
                {
                if((buffer=(unsigned long *)calloc(ARRAYSIZE,sizeof(unsigned long)))!=NULL)
```

```
                {
                memcpy(buffer,mem,npoints*sizeof(unsigned long)),
                if(r_st>=0&&r_end<=period)
                        {
                        pscale=(float)npoints/(float)period,
                        temp = pscale*r_st,
                        for(loop=pscale*r_st,loop<pscale*r_end,loop++)
                                mem[loop-temp] = buffer[loop],
                        memsize = (int)(pscale*(float)(r_end-r_st));
                        }
                free(buffer),
                }
        }

xscale = (float)(690/(float)memsize),
yscale = (float)(270/(float)maxy),

if(flags Smooth)
        {
        if((buffer=(unsigned long *)calloc(ARRAYSIZE,sizeof(unsigned long)))!=NULL)
                {
                memcpy(buffer,mem,npoints*sizeof(unsigned long)),
                for(loop=3,loop<npoints-3,loop++)
                        {
                        ltemp = (long)(buffer[loop-3]+buffer[loop-2]+3*buffer[loop-1] +
                                        3*buffer[loop]+3*buffer[loop+1]+buffer[loop+2] +
                                        buffer[loop+3]) /13,
                        mem[loop] = (int)ltemp;
                        }
                free(buffer),
                }
        }

if(flags.Drift&&'flags.Filelist&&'flags.Region)
        {
        if(d_end==0)
                d_end=period,
        if(d_st>d_end)
                d_st=0,
        sprintf(tmp,"Drift  %li,%li",d_st,d_end),
        outtextxy(120,row1,tmp),
        row1+=textheight("H")+1,
        pscale = (float)(npoints-2)/(float)(period),
        slope = ((float)mem[d_end*pscale]-(float)mem[d_st*pscale])/(pscale*(float)(d_end-d_st)),
        drift=0.0,
        }

for(loop=0,loop<memsize&&loop<npoints,loop++)
        {
        if(flags.Drift&&!flags.Filelist&&!flags.Region)
                if(loop/pscale>d_st && loop/pscale<d_end)
                        drift+=slope,
        putpixel(20+loop*xscale,320-(int)(yscale*((float)(mem[loop]-maxyo)-drift)),1),
        if(flags Plotter)
                {
                gtemp =(loop*xscale)*10+200,
                gtemp1=(int)(yscale*((float)(mem[loop]-maxyo)-drift))*15+100;
                fprintf(gfh,"PU%d,%d,CI5,45;",gtemp,gtemp1),
                }
        }
```

```
        if(flags.Filelist)
                fscanf(fl," %s", filename),
        if('flags SetmaxY)
                maxy=0,
        }
        while(fl'=NULL&&'feof(fl)),

if(flags.Filelist)
        fclose(fl),
free(mem),

if(flags Temper&&!flags.Filelist)
        {
        if((buffer=(unsigned long *)calloc(ARRAYSIZE,sizeof(unsigned long)))!=NULL)
                {
                if((fh=fopen(temper,"r"))!=NULL)
                        {
                        loop=0,
                        while(!feof(fh)&&loop<ARRAYSIZE)
                                {
                                fscanf(fh," %li ",&buffer[loop]),
                                loop++;
                                }

                        if(flags.Region&&flags.Period)
                                {
                                if((mem=(unsigned long *)calloc(ARRAYSIZE,sizeof(unsigned long)))!=NULL)
                                        {
                                        memcpy(mem,buffer,npoints*sizeof(unsigned long)),
                                        if(r_st>=0&&r_end<=period)
                                                {
                                                pscale=(float)npoints/(float)period,
                                                temp = pscale*r_st,
                                                for(loop=pscale*r_st,loop<pscale*r_end,loop++)
                                                        buffer[loop-temp] = mem[loop],
                                                npoints = (int)(pscale*(float)(r_end-r_st)),
                                                }
                                        free(mem),
                                        }
                                }

                                if((mem=(unsigned long *)calloc(ARRAYSIZE,sizeof(unsigned long)))'=NULL)
                                        {
                                        memcpy(mem,buffer,npoints*sizeof(unsigned long)),
                                        for(loop=3,loop<npoints-3;loop++)
                                        buffer[loop]=(mem[loop-3]+mem[loop-2]+3*mem[loop-1] +
                                                        3*mem[loop]+3*mem[loop+1]+mem[loop+2] +
                                                        mem[loop+3]) /13,
                                        free(mem),
                                        }
                                for(loop=0,loop<npoints,loop++)
                                        {
                                        putpixel(20+loop*xscale,320-buffer[loop],1),
                                        if(flags.Plotter)
                                        {
                                        gtemp =(loop*xscale)*10+200;
                                        gtempl=buffer[loop]*15+100;
                                        fprintf(gfh,"PU%d,%d;CI5,45;",gtemp,gtempl);
                                        }
                                        }
```

```
                        fclose(fh),
                        }
                free(buffer),
                }
        }

if(flags.Print)         lx800dmp(1,1,719,347,'A'),
else                            getch(),
if(flags.Plotter)
        fclose(gfh),
end(),
exit(0),
}
```

Appendix E. Etch simulation program

This appendix contains a listing of the program used in the computer simulation of optical fibre etching in HF The program was written in TurboC version 2 0 and requires the use of a Hercules Graphics adapter, although with minor modifications will run on other graphics systems

```
#include <math.h>
#include <mathsupl.h>
#include <plot h>
#include <stats.h>

int x,
int etchtime, maxetchtime,
double etchprofile[102],
double etchrate[102],
double base_etchrate = 1,
double dopant_etchrate = 0.04,
double a, b, c;
double sigma, top,
int profile,

main()
{

printf("1... Step profile\n"),
printf("2... Parabolic profile\n"),
printf("3... Gaussian profile\n\n"),
printf("Enter profile  "),  profile = getch(),

switch(profile)  {
        case '3'   printf("\nEnter sigma  "),
                   scanf("%G",&sigma),
                   break,
        }

printf("\n\nEnter duration of etch  "),
scanf("%d",&maxetchtime),

initialise(),
box(),
outtextxy(30,60,"Dopant profile "),
outtextxy(430,15,"Etched profile "),
/*
    define the etch rate profile  stored in etchrate[]
*/

for(x=0, x<100, x++)
{
switch(profile)  {
        case '1'   a = stepindex(x,100),                break,
        case '2'   a = parabolic(x,100),
                   if(x>97) a=0,
```

```
                else if(x>92) a*=((x-93)/4 0+1 0),
                break,
        case '3'    a = normal(x,sigma,100),              break,
        default     end(),
                printf("Incorrect value for profile  %d",profile),
                exit(0),
        }
etchrate[x] = base_etchrate + a*dopant_etchrate,
putpixel(x+30,(etchrate[x]-etchrate[0])*400+100,1),
putpixel(227-x,(etchrate[x]-etchrate[0])*400+100,1),
}
moveto(430,240),
lineto(430,40),
moveto(625,40),
lineto(625,240),


for(etchtime=0, etchtime<maxetchtime, etchtime++)
{

/*
    Calculate the etch depth profile  Stored in etchprofile[]
*/

for(x=1; x<98, x++)
{
if(etchrate[x+1]>etchrate[x])
etchrate[x] = (etchrate[x+1]+etchrate[x])/2,
else if(etchrate[x-1]>etchrate[x]) {
etchrate[x] = (etchrate[x-1]+etchrate[x])/2,
}
etchprofile[x] += etchrate[x],

putpixel(x+430,(etchprofile[x]-etchprofile[1])*10+40,1),
putpixel(625-x,(etchprofile[x]-etchprofile[1])*10+40,1),
}
}
pause(),
end(),
}
```

Appendix F: Program for determining oxygen concentrations

This program was used to calculate calibrated dissolved oxygen concentrations from the intensity observed from the fibre optic probe knowing the temperature, exposure time and various probe parameters The zero intensity and offset are calculated from the calibration data points entered at the beginning of the program

```
#include <stdlib.h>
#include <stdarg.h>
#include <stdio.h>
#include <math.h>

void main(void)
{
int loop,

double I[30], time[30], temp[30], Qo2[30], f[30],
double cd, pex, tempdecayconst,
double n, d,
double iz, c,
double x, y, z,
double ttime, ttemp, tint, tqo2,

clrscr();
printf("Program for calculating the signal at arbitrary times(min), \n"),
printf("temperature(oC), oxygen partial pressure(bar)\n\n"),
printf("This program allows for possible light leakage giving a DC offset\n"),
printf("by requiring two calibration points at the start of the run.\n\n"),

printf("\tTime    \tTemp    \tIntensity\tOxygen\n"),
printf("CALIBRATION POINTS \n\n"),

cd = 0.5,
pex = 0.05,
tempdecayconst = 0.004,

printf("Enter calibration points  (I[j], time[j], temp[j], Qo2[j])\n"),
for(loop=0,loop<2,loop++)
      {
      printf("J = %i    ",loop+1),
      scanf(" %lf %lf %lf %lf", &I[loop],&time[loop], &temp[loop],
                                    &Qo2[loop]),
      n = ((100.0-(cd*pex*time[loop]))/100),
      d = ((1+0.5*Qo2[loop])*pow(10.0,(tempdecayconst*temp[loop]))),

      f[loop] = n/d,
      }
iz = fabs((I[0] - I[1])/(f[0]-f[1])),
c = fabs(I[0] - iz*f[0]),

printf("\n Iz  = %lf,  C = %lf\n\n",iz,c);

printf("Enter values for experimental points.\n");
```

```
do
        {
        printf("Intensity ,time, temp  ->"),
        scanf(" %lf %lf %lf", &tint, &ttime, &ttemp),

        x = 100 - cd*pex*ttime,
        y = 100 * pow(10,0.004*ttemp),
        z = 2*iz/(tint-c),

        tqo2 = z*x/y -2,
        printf("\t\t%lf\n",tqo2),

        } while (ttime!=999),
exit(0),
}
```